

**Molecular and cellular mechanisms of axonal pathology in
Theiler's murine encephalomyelitis virus-induced demyelination**

Thesis

Submitted in partial fulfilment of the requirements for the degree

Doctor of Philosophy

- Ph.D.-

at the

Department of Pathology

University of Veterinary Medicine Hannover

and

the Center for Systems Neuroscience Hannover

awarded by the University of Veterinary Medicine Hannover

by

Mihaela Kreutzer

born in

Târgu-Cărbunești / Romania

Hannover, Germany 2011

Supervisor: Prof. Dr. Wolfgang Baumgärtner, Ph.D.

Tutorial group: Prof. Dr. Wolfgang Baumgärtner, Ph.D.

Prof. Dr. Claudia Grothe

Prof. Dr. Karin Weißenborn

First evaluation:

Prof. Dr. Wolfgang Baumgärtner, Ph.D. - Department of Pathology, University of Veterinary Medicine Hannover, Germany

Prof. Dr. Claudia Grothe - Department of Neuroanatomy, Hannover Medical School, Germany

Prof. Dr. Karin Weißenborn – Department of Neurometabolics, Center for Neurological Medicine, Clinic for Neurology, Hannover Medical School, Germany

Second evaluation:

Prof. Dr. Andrea Gröne – Pathology Division, Department of Pathobiology, Faculty of Veterinary Medicine, Utrecht University, the Netherlands

Date of final examination:

08.04.2011

The present work was supported by a grant provided by the Ministry for Science and Culture of Lower Saxony.

Parts of this thesis have already been published:

Ulrich R, Seeliger F, **Kreutzer M**, Germann PG, Baumgärtner W. Limited remyelination in Theiler's murine encephalomyelitis due to insufficient oligodendroglial differentiation of nerve/glial antigen 2 (NG2)-positive putative oligodendroglial progenitor cells. Neuropathol. Appl. Neurobiol. 34:603-620, 2008.

TABLE OF CONTENT

Chapter 1	Introduction	1
1.1.	Theiler's murine encephalomyelitis virus-induced demyelination	2
1.1.1.	Animal models for multiple sclerosis	2
1.1.2.	Theiler's murine encephalomyelitis virus (TMEV)	2
1.1.3.	Clinical and pathological characteristics of Theiler's murine encephalomyelitis virus-induced demyelination	4
1.1.4.	Host immune response and virus tropism in Theiler's murine encephalomyelitis virus-induced demyelination	
1.1.5.	Axonal pathology in Theiler's murine encephalomyelitis virus-induced demyelination	9
1.1.5.1.	Primary/secondary axonal pathology	9
1.1.5.2.	Triggers of axonal pathology with special emphasis on TMEV	10
1.2.	Axon and axonopathies	13
1.2.1.	Axonal structure and transport	13
1.2.2.	Axonopathies	20
1.3.	References	27
Chapter 2	Limited remyelination in Theiler's murine encephalomyelitis due to insufficient oligodendroglial differentiation of nerve/glial antigen 2 (NG2)-positive putative oligodendroglial progenitor cells	52
Chapter 3	Axonopathy due to axonal transport defects in a model of multiple sclerosis	53
Chapter 4	General discussions	87
4.1.	Hypothesis and aims	88
4.2.	Myelin pathology	89
4.3.	Axonal pathology	91
4.4.	Glial-axon interaction	93
4.5.	References	95
SUMMARY		101
ZUSAMMENFASSUNG		103
ACKNOWLEDGEMENTS		105

Chapter 1: Introduction

1.1 Theiler's murine encephalomyelitis virus-induced demyelination

1.1.1 Animal models for multiple sclerosis

Multiple sclerosis (MS) is a human immune-mediated demyelinating disease of the central nervous system (CNS). Its precise etiology is unknown, but it occurs most likely as a result of a combination of genetic and environmental (infectious and non-infectious) factors. Until now, the neurological decline observed in most MS patients remains irreversible. Animal models simulating features of MS provide a powerful tool to investigate the pathogenesis of the disease. Thus, to analyze possible autoimmune mechanisms in MS, experimental autoimmune (allergic) encephalomyelitis (EAE) is most frequently used. EAE is produced by either subcutaneous injection of various myelin antigens emulsified with complete Freund's adjuvant or transfer of CNS antigen-specific CD4⁺ T cells (Olitsky *et al.*, 1949; Gold *et al.*, 2006). To investigate the relevance of infectious factors for MS, the chronic virus-induced demyelination triggered either by Theiler's virus, mouse hepatitis virus, canine distemper virus or Visna virus were used as suitable models (table 1.1; Baumgärtner and Alldinger, 2005; Lipton *et al.*, 2007; Beineke, 2009).

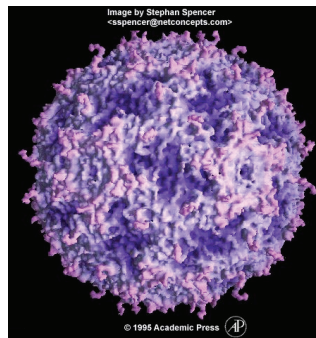
Table 1.1 Animal models of chronic virus-induced demyelination (Lipton *et al.*, 2007)

Virus	Virus Family	Host
Theiler's virus	Picornaviridae	Mouse
Mouse hepatitis virus	Coronaviridae	Mouse
Canine distemper virus	Paramyxoviridae	Carnivore
Visna virus	Retroviridae	Sheep

Among these, the most common animal model used to investigate the consequences of an infectious trigger for MS is Theiler's murine encephalomyelitis virus-induced demyelination (TMEV-ID). TMEV-ID is produced by infection of mice with specific TMEV strains (Theiler, 1934; Lehrich *et al.*, 1976; Lipton and Dal Canto, 1976).

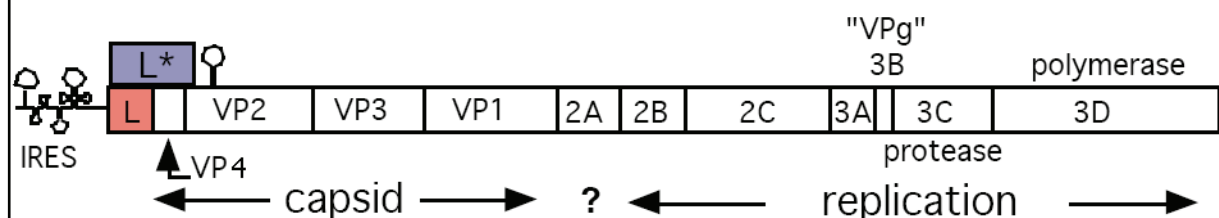
1.1.2 Theiler's murine encephalomyelitis virus

Theiler's murine encephalomyelitis virus (TMEV), a member of the Picornaviridae family, genus *Cardiovirus*, is a positive single-stranded RNA virus whose genome is surrounded by a 60 capsomers icosahedral capsid (figure 1.1; Luo *et al.*, 1992).

Figure 1.1 Three-dimensional structure of Theiler's murine encephalomyelitis virus (BeAn strain).

The virion consists of a spherical protein shell that encapsidates the genome. The capsid presents an icosahedral symmetry and contains 60 copies of each of the four capsidal polypeptide species termed viral proteins (VP1, VP2, VP3 and VP4; Luo *et al.*, 1992).

The 8105 nucleotide long RNA genome (GenBank Acc No: M20562) contains a large open reading frame which encodes a 2000 amino acid-long polyprotein that is cleaved by autoproteolytic activity into 12 mature proteins (figure 1.2; Pevear *et al.*, 1987; Ohara *et al.*, 1988).

Figure 1.2 Schematic view of Theiler's murine encephalomyelitis virus genome.

Theiler's virus genome encodes for capsidal proteins VP1-VP4, L proteins L and L* and proteins involved in viral replication termed 2B, 2C, 3A, 3B, 3C and 3D. Responsible for translation initiation of all viral proteins is an internal ribosome entry site (IRES) located in the 5'-region. VP = viral protein; ? = unknown function.

An additional protein (L*) is encoded by an alternative open reading frame, overlapping regions of L, VP4 and VP2 (Chen *et al.*, 1995). The translation of both open reading frames (ORFs) is driven by an internal ribosome entry site (IRES) present in a large 5' non-coding region of the genome. Protein L* was shown to facilitate TMEV infection of macrophages and viral persistence (Shaw-Jackson and Michiels, 1999). Protein L inhibits the immediate-early type-I interferon (van Eyll and Michiels, 2002). The role of protein 2A is unknown, protein 2B, 2C and 3A participate in the replication complex, 3B (also termed VPg) is covalently linked to the 5' end of the RNA molecule during encapsidation and replication. 3C is the protease responsible for most of the cleavages occurring during polyprotein processing

and 3D is the RNA-dependent RNA polymerase. Each of the 60 capsomers contains a single copy of the four capsid proteins designated VP1-4. A replication signal has been discovered in the VP2 coding sequence and is denoted CRE for “cis-acting replication element”.

TMEV is a ubiquitous pathogen of **wild and laboratory mice** as well as water, bank and meadow voles. All strains are of the same serotype and cross-neutralize with polyclonal antisera (Rozhon *et al.*, 1982). The clinical outcome depends on the mouse and virus strains. Thus, SJL/J, DBA/1, DBA/2, SWR, PL/J and NZW mouse strains are highly susceptible, C3H, CBA, AKR, C57BR have intermediate susceptibility, while BALB/c, C57BL/6, C57BL/10, C57/L, 129/Jm and H-2D(b) are resistant to experimental intracerebral TMEV inoculation (Lipton and Dal Canto, 1979; Dal Canto *et al.*, 1995).

Regarding the virus strains, **two TMEV subgroups** were described. The GDVII subgroup (FA, GDVII) includes the high-neurovirulent strains which grow to high titers and produce large plaques *in vitro*. Experimental infection with members of the GDVII subgroup resulted in an acute fatal polioencephalomyelitis with the following clinical manifestations: excitability, circling, rolling, tremor and flaccid paralysis leading to the death of the animals within 1-2 weeks. The acute polioencephalomyelitis is characterized by necrosis of ganglion cells in cortex, hippocampus and the anterior horn of the spinal cord, non-suppurative inflammation, a high apoptosis rate of neurons and lack of viral persistence in the CNS (Lipton, 1975).

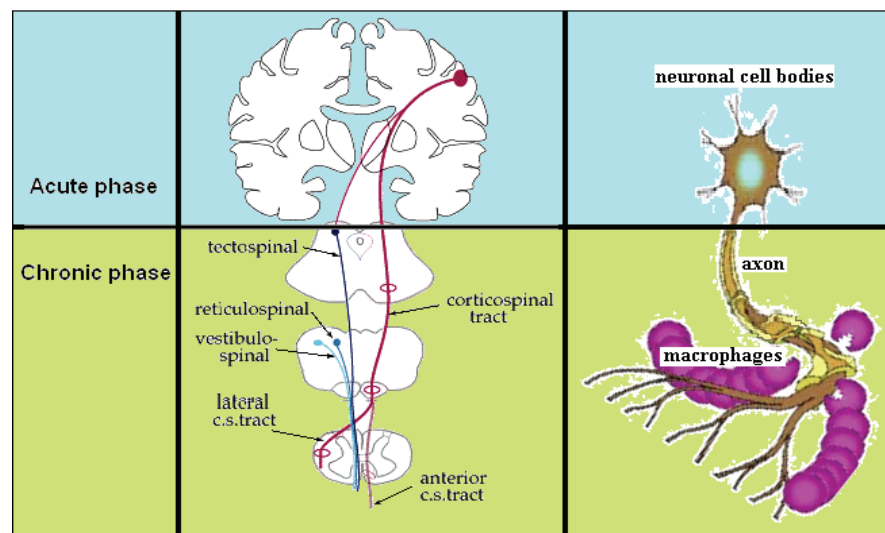
The Daniels (DA) / Theiler's original (TO) subgroup contains low-neurovirulent strains such as BeAn 8386, DA, WW, TO, Yale, which grow to relatively low titers and produce small plaques *in vitro*. Infection with DA/TO viruses is responsible for an asymptomatic intestinal infection after virus replication in the gastrointestinal mucosa or a biphasic disease with persistent CNS infection after intracerebral inoculation (Lipton, 1975; Rodriguez *et al.*, 1987). Sequencing of the entire RNA genome of GDVII and TO (BeAn 8386) viruses revealed a 90.4% homology at the nucleotide level and a 95.7% similarity at the amino acids level (Pevear *et al.*, 1987). Almost half of the differences in amino acid sequence were found in the three surface-coat proteins VP1, VP2 and VP3, suggesting that these mutations may represent the neutralizing immunogenic epitopes of TMEV.

1.1.3 Clinical and pathological characteristics of Theiler's murine encephalomyelitis virus-induced demyelination

Studies on TMEV-induced demyelinating disease have utilized TO strains such as the Daniel's (DA) or the BeAn 8386 strain. Another tissue culture adapted strain, designated

WW, has also been utilized to produce a relapsing model of TMEV infection (Wroblewska *et al.*, 1979). One week after intracerebral infection with one of the DA/TO subgroup viruses, SJL/J mice develop an acute polioencephalomyelitis characterized by gray matter involvement and clinically by flaccid paralysis (figure 1.3).

Figure 1.3 Evolution of Theiler's murine encephalomyelitis virus-induced demyelination (TMEV-ID).



TMEV-ID has an acute and a chronic phase. During the acute phase TMEV is present in the neuronal cell bodies of the brain, while in the chronic phase the virus seems to migrate along the axons through the corticospinal tracts into the spinal cord.

While recovering from the acute phase, the SJL/J enter the chronic phase characterized by an inflammatory demyelinating disease with the following clinical hallmarks: wobbling gait, weakness of posterior limbs and spastic paralysis. The pathological features of the chronic phase of mice inoculated with TO subgroup strains are acute neuronal degenerative changes and microglial proliferation primarily in brain stem and thalamus, perivascular inflammation in the spinal cord white matter and leptomeninges and varying degrees of chronic progressive demyelination (Lipton, 1975; Rodriguez, 1987). Although TMEV-induced demyelination due to infection with DA/TO strains revealed similar lesions, there are particularities described for each strain. Thus, for the BeAn strain the disease starts with minimal early gray matter involvement and the chronic inflammatory demyelinating phase differs depending on the susceptibility of the mouse strain. In SJL/J mice, BeAn produces a severe inflammatory disease of the white matter characterized by macrophage infiltration and destruction of axons and the glia-limiting membrane (GLM). Remyelination is minimal and mainly accomplished by Schwann cells migrating through the damaged GLM in these mice (Dal Canto *et al.*, 1995; Ulrich *et al.*, 2008). In other mice strains, including the SWR/J, NZW and DBA2 strain,

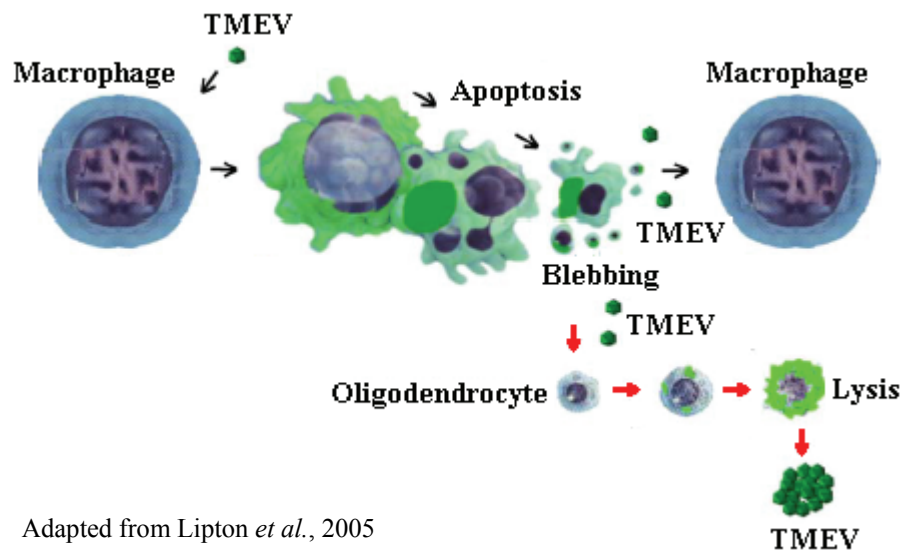
demyelination is accompanied by a moderate inflammation with lower number of macrophages, well preserved axons and minimally affected GLM. Consequently, in these mice there is considerable remyelination, which is mainly carried out by oligodendrocytes with a minor Schwann cell component. A similar situation has been described in hybrids between resistant C57BL/J and susceptible SJL/J animals (Dal Canto *et al.*, 1995). These studies demonstrated the genetic regulation of susceptibility/resistance to disease development in terms of de- and re-myelination.

1.1.4 Host immune response and virus tropism in Theiler's murine encephalomyelitis virus-induced demyelination

An essential difference in the pathogenesis between susceptible and resistant mice represents virus persistence in SJL/J versus virus clearance in C56BL/6 mice (Gerhauser *et al.*, 2007). Virus persistence during the chronic stage of TMEV-ID is partially explained by a limited viral protein synthesis which induces only a mild cytopathic effect, and therefore allows the virus to bypass immunological clearance in highly susceptible mice (Obuchi and Ohara, 1999). In addition, it was shown that the L* protein plays a role in virus persistence due to its antiapoptotic activity that prolongs viral replication in macrophages and interferes with virus clearance in these cells (Ghadge *et al.*, 1998). Another element important for CNS persistence represents the virus- cell receptor interaction. Although the entry receptor for TMEV has not yet been identified, it was observed that sialic acid reacts as a co-receptor by making contact with four conserved and tightly clustered amino acids, three from the VP2 and the fourth at the VP3 C-terminus (Zhou *et al.*, 2000). Site-specific mutations result in a dramatically reduction of virus persistence in mice (Kumar *et al.*, 2004). Moreover, TMEV persistence in the CNS of SJL/J mice was associated with continuous viral replication (Trottier *et al.*, 2001; Lipton *et al.*, 2005) and progression of the demyelinating disease (Lipton *et al.*, 1991; Pullen and Friesen, 1995). It was therefore important to identify those cells responsible for virus production. Although limited by host anti-viral immune responses, TMEV is able to spread to and infect astrocytes, microglia/macrophages, oligodendrocytes and neurons. Viral tropism differs between the acute and chronic phase of TMEV-ID (Lipton *et al.*, 2005). Thus, during the acute phase of TMEV-ID viral antigen was predominantly found in neurons and astrocytes. In the chronic phase, macrophages, astrocytes and oligodendrocytes showed the highest levels of viral antigen (Rodriguez *et al.*, 1983). However, cell tropism in the chronic phase is still discussed controversially. Dal Canto *et al.* (Dal Canto *et al.*, 1995) consider

astrocyte as being the main cell for TMEV BeAn replication (Zheng *et al.*, 2001), whereas others (Lipton *et al.*, 2005) proposed TMEV persistence primarily in macrophages (figure 1.4).

Figure 1.4 Macrophage-based model of TMEV persistence in the mouse CNS.



Adapted from Lipton *et al.*, 2005

Infected macrophages restrict TMEV replication and undergo apoptosis, whereas oligodendrocytes are productively infected cells that undergo lysis. → = TMEV in macrophages; → = TMEV in oligodendrocytes.

However, both cell types (astrocytes and macrophages) are potential or professional capable antigen-presenting cells (APCs) which may play an important role in antigen presentation at the onset of clinical disease contributing to the myelin destruction (Palma *et al.*, 1999; Mack *et al.*, 2003). After infection, TMEV-infected astrocytes increase the expression of pro-inflammatory cytokines by activation of the NFκB pathway. This elevated astrocytic pro-inflammatory reaction was closely correlated to viral clearance and strain-dependent protection (Molina-Holgado *et al.*, 2002; Palma, 2003; Palma and Kim 2004; Rubio *et al.*, 2006, Rubio and Sanz-Rodriguez 2007; Gerhauser *et al.*, 2007; Carpentier *et al.*, 2008). Beside this direct effect on the CNS immune response, astrocytes might trigger a proteolysis cascade initiated by matrix metalloproteinases (MMPs) and tissue inhibitors of matrix metalloproteinases (TIMPs) that could be responsible for opening of the blood -brain barrier during TMEV-ID progression (Ulrich *et al.*, 2008).

Alike astrocytes, CNS resident microglia/macrophages from susceptible mice showed higher levels of pro-inflammatory cytokines compared to cells from resistant mice (Clatch *et al.*, 1990; Rubio and Capa, 1993; Jin *et al.*, 2007). Thus, after TMEV infection, microglia/macrophages activate innate immune functions and/or serve as APCs to elevate the T-cell response (Pope *et al.*, 1998; Katz-Levy *et al.*, 1999; Olson *et al.*, 2001; Mack *et al.*,

2003). After TMEV infection of CD8⁺ T cells deficient mice, the motor functions and axonal integrity were preserved, indicating a role of CD8⁺ T cells in virus clearance (Murray *et al.*, 1998; Johnson *et al.*, 2001, 2007). Furthermore, TMEV-infected mice treated with either anti-thymocyte, anti-Ia or anti-CD4 antibodies showed a delayed onset of the disease suggesting that CD4⁺ T cells are also involved in TMEV-ID pathogenesis. Among CD4⁺ T cells, in particular T helper type 1 (Th1) cells were found preferentially within demyelinating lesions of the CNS in TMEV infected mice (Kim *et al.*, 2005). Upon infection, TMEV-specific CD4⁺ T cells target persistent viral antigens in the CNS and initiate myelin damage. The activation of naïve T cells occurs directly in the CNS by local APCs, possibly dendritic cells (DC) and not in the cervical lymph nodes or other peripheral lymphoid organs (McMahon *et al.*, 2005). The activated T cells are reactive against a variety of myelin antigens including myelin basic protein (MBP), myelin oligodendrocyte glycoprotein (MOG) and proteolipid protein (PLP; de Rosbo and Ben-Nun, 1998). Later in the disease, these autoimmune myelin-specific CD4⁺ T cells are primed by epitope spreading and resistant to apoptosis mediated by β -arrestin 1 overexpression (Tompkins *et al.*, 2002; Shi *et al.*, 2007). Recently, it was shown that inflammation is driven by a newly-designated T-lymphocyte subtype that secretes interleukin-17, responsible for blood-brain barrier disruption (Langrish *et al.*, 2005).

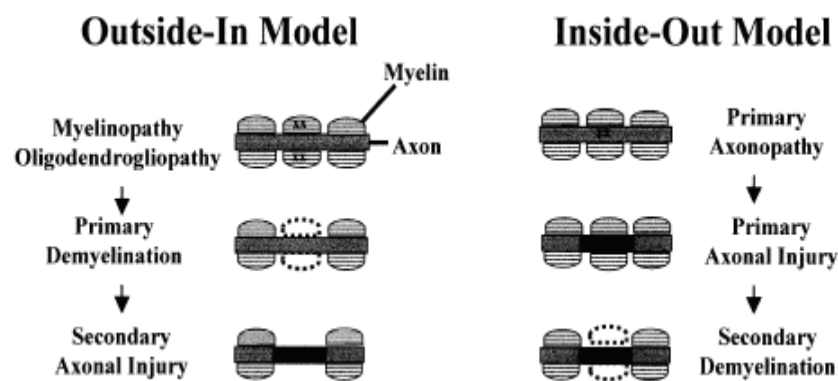
This immune response has a direct and an indirect influence on the myelin-producing cells. Thus, the oligodendrocytes undergo cellular lysis under the direct attack of the activated T cells (Selmaj and Raine, 1988) and/or under the influence of pro-inflammatory cytokines (Molina-Holgado, 2002). Moreover, oligodendrocytes yield a heavy viral load. Thus, while TMEV-infected macrophages produce 1 plaque-forming unit (pfu) of infectious virus per cell (Jelachich, 1995), the oligodendrocytes yield 500 times more virus (500pfu/cell; Trottier *et al.*, 2001). Due to these high levels of virus replication, the oligodendrocytes undergo cytopathic death after infection with TMEV (Carlson *et al.*, 2006). In the mature nervous system the loss of oligodendrocytes can be compensated by a pool of oligodendrocyte precursors which are able to migrate in response to semaphorin 3A and 3F (Williams *et al.*, 2007). In multiple sclerosis, undifferentiated oligodendrocyte precursors surround the lesions and remyelinate naked axons (Chandran *et al.*, 2008). However, repeated cycles of demyelination/remyelination apparently are reducing the capacity for tissue regeneration (Compston and Coles, 2008). In addition, there is evidence that an impaired oligodendrocyte precursor cell (OPC) maturation contributes to the oligodendrocytes loss and finally to inflammatory demyelination (Ulrich *et al.*, 2008).

1.1.5 Axonal pathology in Theiler's murine encephalomyelitis virus-induced demyelination

1.1.5.1 Primary/secondary axonal pathology

Although myelin loss represents a main feature of MS and TMEV-ID, observed neurological deficits like weakness of the posterior limbs and spastic paralysis correlate better with axonal loss and dysfunction than with the demyelination process (Filippi and Rocca, 2005; Neumann *et al.*, 2003; Herrero-Herranz *et al.*, 2008). Pathological studies indicate that as many as 70% of axons are lost from the lateral corticospinal tracts in patients with advanced paraparesis (Bjartmar *et al.*, 2000). Therefore, the focus of interest has shifted in the past decade from multiple sclerosis as a demyelinating disease to a broader perspective in which the relative contribution of axonal loss represents a major pathogenetic factor. Though axonal damage was firstly described by Charcot already over a century ago (Charcot, 1868), it is still unknown whether axonal pathology in TMEV-ID as well as in MS is the primary or secondary lesion and its evolution follows the “outside-in” or “inside-out” model (figure 1.5). Similarly, axonal damage precedes myelin loss in canine distemper, a naturally occurring animal model of MS (Seehusen and Baumgärtner, 2009).

Figure 1.5 Outside-In and Inside-Out models for TMEV-ID/MS.



In the “outside-out” model the axonopathies are secondary to myelinopathies/oligodendrogliaopathies. In the “inside-out” model the axonopathies precede demyelination (Tsunoda and Fujinami, 2002).

In the “outside-in” scenario, axonal lesions develop secondary to myelin loss or damage to myelin forming cell (outside), therefore demyelination is considered as primary lesion (Tsunoda and Fujinami, 2002). Historically, this has been termed primary demyelination. The observation that most axons survived the demyelinating process (McGavern *et al.*, 2000) seems to substantiate this hypothesis, although axonal degeneration alone may be responsible

for similar effects (Grigoriadis *et al.*, 2004). However, presence of injured axons in the normal appearing white matter (NAWM; Tsunoda *et al.*, 2005), progressive axonal loss (Trapp *et al.*, 1998), reduction of the neuronal specific marker N-acetyl-aspartic acid (Bjartmar, 2000) and brain atrophy in MS (Simon *et al.*, 1999) underlined the “inside-out” model. In this model, the primary target is the axon or its cell body. Such primary axonal injuries lead to so-called secondary demyelination (Ferguson *et al.*, 1997; Trapp *et al.*, 1998; Bitsch *et al.*, 2000; Tsunoda *et al.*, 2002).

1.1.5.2 Triggers of axonal pathology with special emphasis on TMEV

Factors like

- a) toxic chemicals;
- b) physical injuries;
- c) viral replication in the cell body and neuronal apoptosis;
- d) axonal transport of the virus;
- e) direct/indirect inflammatory attack of the axons as well as
- f) demyelination can result in axonal injuries.

a) Toxic chemicals like acrylamide, hexacarbons, carbon disulfide and organophosphorus (OP) compounds are used as experimental probes to induce axonopathies in laboratory animals. OP inhibition of the neurotoxic esterase (NTE) is correlated with an irreversible and progressive decrease of the retrograde transport that culminates in axonal degeneration. Exposure to neurotoxic heavy metals such as lead and mercury also lead to permanent damages, with clinical manifestations which often intensify with age. Other axonal toxins (2,5 hexanedione, acrylamide) that require repeated dosing to induce axonopathy, produced a similar decrease in the retrograde transport, however these changes are reversible if treatment is decreased. Clinically, toxic axonopathies are associated with muscular weakness of extremities and uncoordinated gait causing ataxia.

b) Although the spatiotemporal evolution of axonal degeneration caused by physical factors like mechanical injury, temperature and ischemic insults, varies with the experimental procedure (axotomy, crush, chronic ligature) and depends on the factors including the used laboratory animals, their age, site of lesion and assessment method, there are convergent mechanisms involved in a wide of range of axonal insults. These include disruption of axonal transport in the distal stump, mitochondrial swelling, ATP deficiency, impaired $\text{Na}^+\text{-K}^+\text{-ATP-ase}$ activity and reversion of $\text{Na}^+\text{-Ca}^{2+}\text{-exchanger}$ which cause a rise in free intracellular Ca^{2+} which activates calpain-inducing degradation of cytoskeleton and membrane proteins (Coleman, 2005).

c) TMEV viral antigens were found in the neuronal cytoplasm between 4 and 11 days post-infection (Rodriguez *et al.*, 1983). In this acute phase of infection, it was shown that TMEV induces neuronal apoptosis followed by its dissemination along the axons without disrupting the myelin (Anderson *et al.*, 2000; Tsunoda *et al.*, 2007a, b). Afterwards, between the second and third week post-infection, virus replication shifts from neurons to oligodendrocytes and macrophages located in the white matter (Sethi and Lipton, 1983).

d) The CNS distribution of the virus appears to be facilitated by both neuronal axoplasmic and dendritic flow (Dal Canto and Lipton, 1982; Tsunoda *et al.*, 2007). In an experimental model using TMEV injection in the retina, the virus was transported along the axons from the optic nerve and infected the retinal ganglion neurons and the optic nerve oligodendrocytes through their myelin sheaths (Roussarie *et al.*, 2007). This intra-axonal transport of the virus could prevent an effective anti-virus immune response (Tsunoda *et al.*, 2008).

e) There is no clear proof *in vivo* that the inflammatory reaction of TMEV-ID/MS is a prerequisite for the initiation of axonal injury although there is evidence that axonal injury may coexist with inflammation (Lassmann, 2003a, b). *In vitro*, the CD8⁺ T cells were capable of damaging neurons and axons which are expressing MHC class I molecules (Höftberger *et al.*, 2004; McDole *et al.*, 2006; Johnson *et al.*, 2007). Moreover, it was shown that an interaction between neurons and T-cells results in the differentiation of CD15+TGFβ1+CTLA-4+Foxp3+ T cells that suppresses both proliferation of encephalogenic CD4⁺ T cells and progression of myelin loss in the EAE model (Liu *et al.*, 2006).

Macrophages and activated microglia have been reported to be in close proximity to degenerating axons. These cells produce inflammatory mediators such as nitric oxide (NO) and nitric oxide synthase (NOS) which damage mainly the small diameter electrically active axons *in vitro* and oligodendrocytes (Smith *et al.*, 2001; Garthwaite *et al.*, 2002; Acar *et al.*, 2003). Demyelinated axons exposed *in vitro* to NO showed a significant conduction block, whereas the myelinated axons were affected only at higher concentrations (Redford *et al.*, 1997). Therefore, a link between NO and subsequent molecular events causing irreversible axonal injury was proposed (Kapoor *et al.*, 2003). Thus, it was suggested that NO injures axons by inhibiting mitochondrial metabolism, which in turn results in an energy failure and an intra-axonal increase in Na⁺ concentration. Consequently, a Na⁺ influx via sodium channels may lead to a deleterious concentrations of Ca²⁺ within axons via a reverse mode of action of the Na⁺/Ca²⁺ exchanger. The excess of the intra-axonal Ca²⁺ activates deleterious enzymes like Ca²⁺-dependent proteases and causes axonal injury and a conduction block (Stys *et al.*, 1992). In addition, NO mediates the excitatory effect of glutamate. The excess of glutamate

released by microglia and macrophages accompanied by a decrease in glutamate intake and metabolism, activates α -amino-3-hydroxy-5-methyl-4-isoxazolepropionic acid (AMPA). This is highly toxic to oligodendroglial cells and neurons. Blockage of AMPA-responsive glutamate receptors ameliorates the neurological sequel in EAE, increases oligodendrocytes survival and reduces dephosphorylation of neurofilament H, an indicator of axonal damage (Platten, 2005).

In contrast, Bitsch *et al.* (2000) reported that in MS plaques, neither inducible NOS (iNOS) nor TNF- α mRNA expression were correlated to axonal loss or acute axonal damage. Moreover, it was shown that TMEV can cause demyelination in organotypic culture in the absence of immune cells and that immune-deficient mice, including nude mice and MHC class I or II deficient mice, also develop demyelination (Rosenthal *et al.*, 1986; Tsunoda *et al.*, 1999).

Antibodies to neuronal components represent another compartment of the inflammatory reaction which is thought to play a causative role in axonal pathology. It was shown that antibodies to specific axonal structures like neurofilaments and tubulins may mediate axonal injury in MS patients (Newcombe *et al.*, 1985; Tsunoda and Fujinami, 2002; Zhang *et al.*, 2005).

f) Whether demyelination is a prerequisite for axonal injury in MS is unclear. Contradictory results were obtained from knock-out mice experiments. Thus, mice lacking the glial cyclic nucleotide phosphodiesterase (Cnp1) gene developed axonal swellings and neurodegeneration throughout the brain, leading to hydrocephalus and premature death. However, the ultrastructure, periodicity and physical stability of the myelin sheaths were apparently not altered (Lappe-Siefke *et al.*, 2003). On the other hand, mice deficient for myelin associated glycoprotein (MAG) showed late-onset axonal disease preceded by paranodal axon atrophy with reduced neurofilament spacing, suggesting that an underlying disruption of the myelin can lead to a delayed and progressive axonal loss (Li, 1994). Late-onset, degeneration and disability also occurred in proteolipid protein (PLP) null mice (Griffiths *et al.*, 1998). This also may be the case in human MS (Garbern *et al.*, 2002).

In addition, it has been shown that the CNS myelin sheaths contains growth inhibitors like NogoA, myelin-associated glycoprotein (MAG) and myelin-oligodendrocyte glycoprotein (MOG) that are responsible for the inability of mature axons to regenerate after injury (Cajal, 1928; Mukhopadhyay *et al.*, 1994; Chen *et al.*, 2000; GrandPre *et al.*, 2000; Prinjha *et al.*, 2000). Thus, one could conclude that naked axons are more vulnerable to damage and the

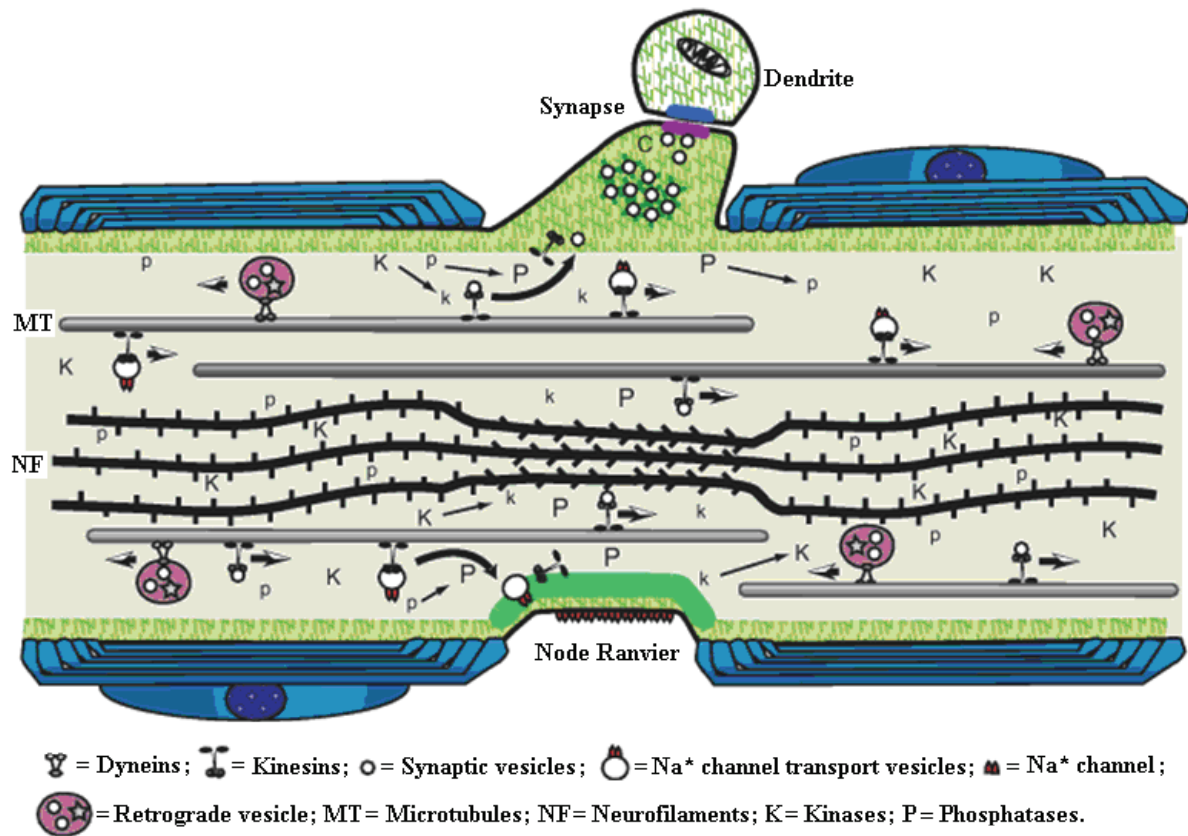
failure of remyelination in chronic MS lesions may promote axonal degeneration (Chang *et al.*, 2002).

However, demyelination has also functional consequences and is not a simple lack of myelin sheaths around the axons. Demyelination is responsible for a reduced support of axons, reorganization of ion channels and destabilization of axonal membrane potentials which result in reduced excitability and conduction block. During remission, axons can adapt and restore conduction (Hauser and Oksenberg, 2006). The extensive interneuron sprouting and connectivity associated with neurological recovery observed in a modified EAE model revealed that axons have a strong remodelling potential (Kerschensteiner *et al.*, 2004). However, in cases of severe injuries, distal and retrograde degeneration is triggered and ion fluxes, mitochondrial dysfunction and activation of proteases culminate in a degradation of cytoskeletal proteins and axonal disintegration (Dutta *et al.*, 2006). The early influx of Na^+ and Ca^{2+} ions into the axoplasm as a result of channel exposure or their upregulation is highly excitotoxic and leads to interrupted axonal transport and accumulation of proteins, such as the amyloid precursor protein, N-type voltage-gated Ca^{2+} channels, nonphosphorylated neurofilament proteins, and metabotropic glutamate receptors (Peterson *et al.*, 2005).

1.2 Axon and axonopathies

1.2.1 Axonal structure and transport

Neurons are specialized cells, responsible for the transmission of electrical impulses to and from the central nervous system. The main structures of the neuron are the cell body, the axon, and the dendrites. Each neuron is equipped with hundreds of dendrites, but only one axon. To summarize the function of these components George Spelvin (1995) said that in neurons “the cell body proposes and the axon disposes”. To achieve this disposable function, axons need a well-structured axonal cytoskeleton, generated in the neuronal stroma, composed of three main components: microtubules, neurofilaments and the actin network (figure 1.6).

Figure 1.6 Axonal cytoskeleton.

Modified from Vale, 2005

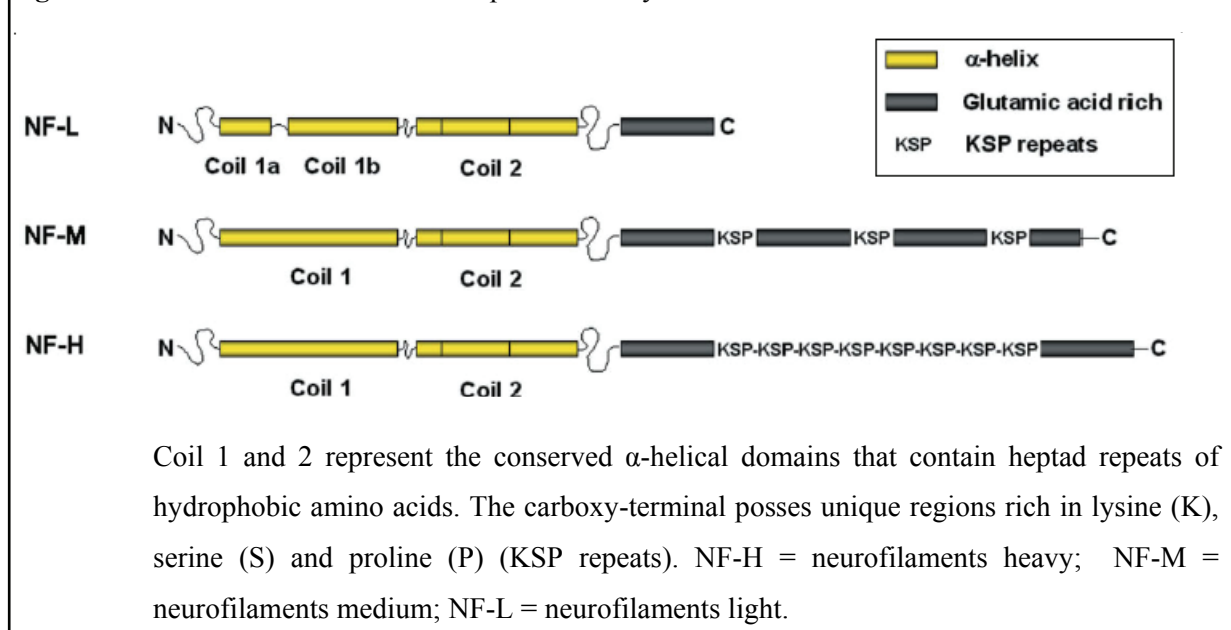
The main components of the axonal cytoskeleton are the microtubules (MTs) and neurofilaments (NFs). MTs facilitate the axonal transport in the anterograde direction by kinesins and in the retrograde direction by dyneins. NFs are phosphorylated by kinases and dephosphorylated by phosphatases. Their phosphorylated/dephosphorylated status is responsible for variations in the axonal diameter and velocity of conduction.

Microtubules (MTs) are assembled from tubulin heterodimers consisting of α - and β -tubulin and comprises 15 - 20% of the cellular protein content in the brain (Laferriere *et al.*, 1997). MTs are polarized structures with a faster growing end referred as the plus end and a slower growing end called the minus end. They promote the extension of the axonal growth cone and are thus responsible for axonal migration and longitudinal growth, as well as for providing the conduit of the fast axonal transport (figure 1.6). MTs are linked to their neighbours (other MTs, neurofilaments and actin network) by cross-bridges composed of microtubule-associated proteins (MAP) like MAP1, MAP2 or tau (Vickers *et al.*, 1994). MAPs are able to organize microtubules and affect their stability. They can prevent or promote microtubule depolymerisation and induce microtubule bundling.

Neurofilaments (NF's) are 10-nm class IV intermediate filaments which consist of the 200-kD heavy (NF-H), 150-kD medium (NF-M) and 68-kD light (NF-L) subunits (Hirokawa and

Takeda, 1982; Hoffman and Lasek, 1975). All three share a conserved central rod (yellow), but they differ in their carboxy-terminal (figure 1.7).

Figure 1.7 Schematic illustration of the protein family of neurofilaments.



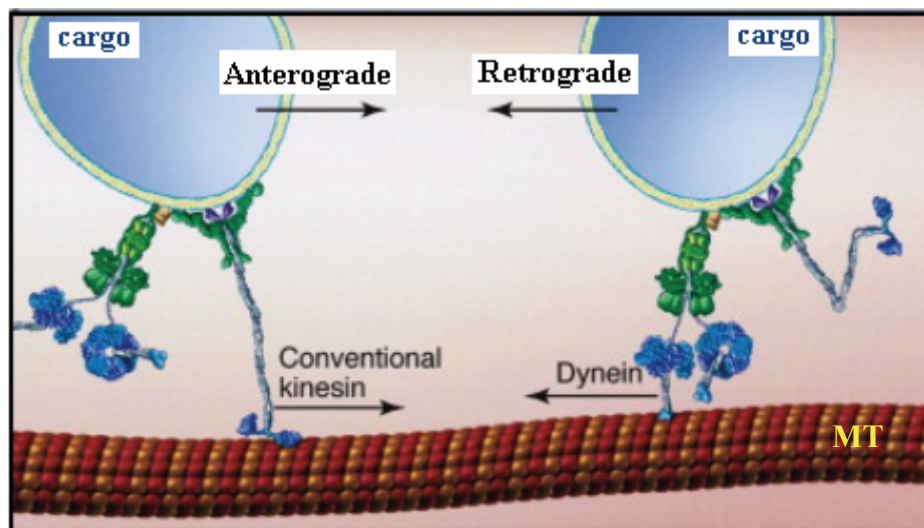
In NF-H, the c-region contains over 40 lysine-serine-proline (KSP) repeats (Julien and Mushynski, 1982; 1983), which provide potential phosphorylation sites (Black and Lee, 1988; Lee *et al.*, 1987; 1988). Thus, under physiological conditions, NFs are synthesized in the neuronal cell body as non-phosphorylated proteins which, subsequently, undergo a gradual and complex pattern of phosphorylation along the axon (Nixon *et al.*, 1994; Perrot *et al.*, 2008).

Using immune-electron microscopy Mata et al. (1992) analyzed the distribution of the phosphorylated neurofilaments inside of one or more types of nerve fibers. It was observed that the non-myelinated regions and the nodes of Ranvier contain a much lower proportion of phosphorylated epitopes than the myelinated regions of the same axon and that, neurofilament spacing and phosphorylation are reduced in demyelinated fibers and are largely restored after remyelination (de Waegh *et al.*, 1992; Fuchs and Cleveland, 1998). Because the spacing between neurofilaments is substantially greater in settings in which highly phosphorylated NF-H are found, it seems likely, that the number and extent of neurofilament phosphorylation could increase with the axonal diameter, and thus the speed of conduction (de Waegh *et al.*, 1992; Mata *et al.*, 1992; Hsieh *et al.*, 1994). In addition, it was shown that NF-M and NF-H side arm phosphorylation is able to alter the physical and biological properties of neurofilaments. Under physiological conditions, neurofilament polymers are conveyed from the cell body to the axon by a slow axonal transport. This movement occurs in both antero-

and retrograde directions, requires microtubules and is characterized by relatively rapid brief movements of neurofilaments, interrupted by prolonged pauses (Francis *et al.*, 2005, Trivedi *et al.*, 2007). Heavily phosphorylated side arm domains can induce bundling of filaments that coincides with a reduction in motility (Yabe *et al.*, 2001; Leterrier *et al.*, 1996) due to increased pausing in neurofilament movement (Ackerley *et al.*, 2003). Deletion of the NF-H sidearm accelerates transport of the slow-moving neurofilaments (Zhu *et al.*, 1998).

In conjunction with its activator, p35, cyclin-dependent kinase 5 (CDK5), a kinase highly expressed in the nervous system, it was proposed that it plays a critical role in NF-H phosphorylation along with extracellular signalling-regulated kinases 1/2 (ERK1/2) (Hellmich *et al.*, 1992; Shetty *et al.*, 1995; Sun *et al.*, 1996; Veeranna *et al.*, 2000; Kesavapany *et al.*, 2003, 2004). The CDK5 has a direct and an indirect effect on NF phosphorylation. Thus, the direct impact consists in phosphorylation of the KSPXK repeats from the carboxy-terminal, while the indirect influence depends on CDK5-dependent MEK1 phosphorylation which, in consequence, down-regulates ERK1/2 activity. Due to these properties, CDK5 can inhibit the anterograde transport of the neurofilaments (Moran *et al.*, 2005). However, neurofilament phosphorylation is a dynamic process and CDK5 action can be reversed by the activity of protein phosphatase 2A (PP2A), which dephosphorylated the CDK5 phosphorylated sites from NF-H (Veeranna *et al.*, 1995). The catalytic subunits of PP2A, as well as the A and B alpha regulatory subunits of PP2A were detected in the neurofilament fraction by immunoblotting. Inhibition with okadaic acid results in accumulation of hyperphosphorylated neurofilaments (Strack *et al.*, 1997).

While most of the neuronal proteins are synthesized in the cell body (Mohr and Richter, 2000, Campenot and Eng, 2000), the components of the entire axonal cytoskeleton presented above are highly specialized for the intracellular transport of proteins and organelle cargoes. Thus, neurons rely on their transport machinery for growth, differentiation and survival. The main mechanism to deliver cellular components to their site of action is the long-range microtubule-based transport. As already mentioned, the axonal microtubules are orientated with the plus ends pointing towards the synapse and the minus ends facing the cell body. The molecular motors are moving the cargoes along the microtubule tracks in an ATP-dependent manner. There are three main classes of motor proteins: kinesins, dyneins and myosins. As most molecular motors of the kinesin family unidirectionally move towards the microtubule plus end, they mostly mediate the anterograde transport. In contrast, the molecular motor cytoplasmic dynein moves towards the microtubule minus end and, accordingly, mediates the retrograde transport (figure 1.8).

Figure 1.8 Axonal dynamics in a myelinated axon.

Adapted from Vale, 2003

Kinesins transport cargoes towards the synapse (anterograde) while dyneins move mostly toward the cell body (retrograde). MT = microtubule.

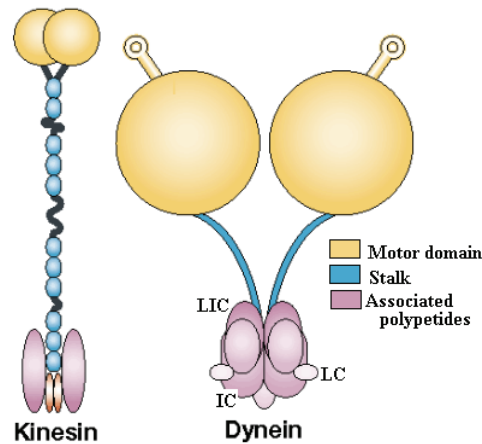
Vesicles and organelles are moved by the fast axonal transport $\sim 1\mu\text{m/s}$, whereas cytoskeleton components (like microtubules, neurofilaments) are transported by the slow axonal transport $\sim 1\text{mm/day}$ along the axons. Fast or slow, the axonal transport is mediated by the same molecular motors: kinesins and dyneins (Roy *et al.*, 2000; Wang *et al.*, 2000). The molecular motors are proteins that are able to move along the surface of a suitable substrate. They are powered by ATP hydrolysis and convert chemical energy into mechanical work. There are more than 10 different families of kinesins and 2 groups of dyneins, each with up to several dozen members. Although these numbers may easily be tripled as a result of post-translational modifications or various combinations of associated proteins, clear functions are assigned to only a small subset of molecular motors.

Kinesin-I was the first identified member of the kinesin superfamily (Brady, 1985; Vale, 1985). Native kinesin-I is a heterotetramer composed of two kinesin heavy chain (KHC) subunits (110–130 kD) and two kinesin light chain (KLC) subunits (60–70 kD; Bloom *et al.*, 1988). KHC has a motor domain that interacts with the microtubule track and hydrolyzes ATP. KLC subunits are involved in cargo binding or modulation of KHC activity (Bloom and Endow, 1995; Goldstein and Philp, 1999; Rahman *et al.*, 1999; Kamal and Goldstein, 2000; figure 1.9).

Although only one conventional KHC gene is found in many species, including *Drosophila melanogaster* and *Caenorhabditis elegans*, mammals have three KHC genes (KIF5A, KIF5B, and KIF5C). KIF5B appears to be ubiquitously expressed, whereas both KIF5A and KIF5C appear to be expressed only in neuronal tissues (Navone *et al.*, 1992; Niclas *et al.*, 1994; Xia

et al., 1998). KIF5C has been suggested to be important for the viability of motor neurons (Kanai, 2000), and KIF5A plays a role in the slow axonal transport of NFs (Koehnle and Brown, 1999; Xia *et al.*, 2003).

Figure 1.9 Structure of the motor proteins kinesin and dynein.



Adapted from Woehlke and Schliwa, 2000

Kinesins and dyneins have a unitary structure. Both contain a motor domain responsible for microtubules binding, a stalk which stabilizes the whole structure and associated polypeptides which bind and modulate the interaction with cargo (LIC = light intermediate chains; IC = intermediate chains; LC = light chains).

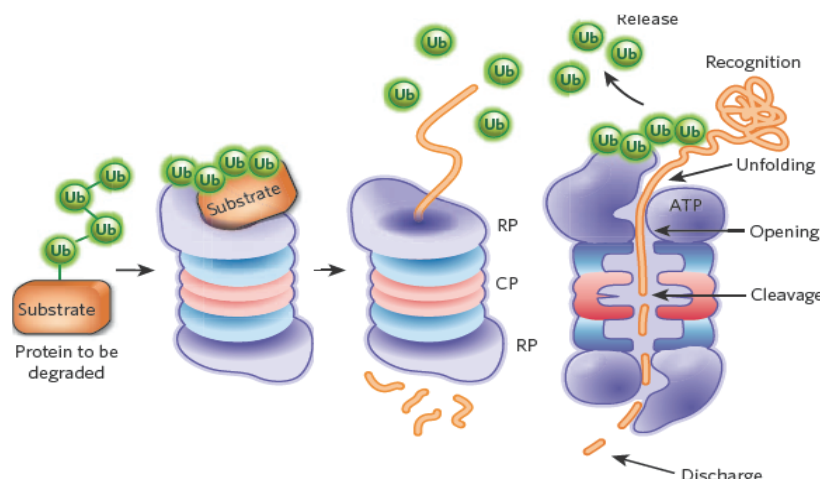
The association among NFs and KIF5A is regulated by NF phosphorylation, thus, highly phosphorylated NFs dissociate from kinesin, associate with other NFs and therefore slow down the anterograde transport rate (Yabe *et al.*, 1999, Jung *et al.*, 2005). In addition, kinesins have been reported to transport numerous membrane cargoes including mitochondria, lysosomes, endoplasmic reticulum, and a subset of anterograde-moving vesicles in axons (Hirokawa and Takeda, 1998) and nonmembranous cargoes, such as mRNAs (Brendza *et al.*, 2000).

Dyneins can be divided into cytoplasmic dyneins which carry organelles and microtubule fragments along the axons and axonemal dyneins which cause sliding of microtubules in the axonemes of cilia and flagella (Karp, 2005). Cytoplasmic dynein contains two identical heavy chains (HC) which are responsible for generating the movement along the microtubule including two intermediate chains (IC), four light intermediate chains (LIC) and several light chains (LC) which are believed to anchor dynein to dynactin, a linker between dynein and its cargoes (Susalka and Pfister, 2000; figure 1.9). There is a large and growing list of activities attributed to cytoplasmic dynein including mRNA localization, nuclear envelope breakdown, apoptosis, transport of centrosomal proteins, mitotic spindle assembly, virus transport, kinetochore functions and movement of signaling and spindle checkpoint proteins (Vale,

2003). In addition, similar to KIF5A, dynein is involved in the transport of the intermediate filaments. Thus, dynein mediates the retrograde transport of NFs within axons and the anterograde delivery of NFs from perikarya into axons. Dynein-NFs association is regulated by multiple phosphorylation events (Motil *et al.*, 2006).

In conclusion, the cytoskeleton consisting of neurofilaments and microtubules is generated in the neuronal soma and transported along the axons. This is an active process, which occurs throughout the whole life of the neuron, so an active degradation process has to exist too. However, less information about axonal cytoskeleton degradation is available. It was shown that leupeptin injection in the optic tectum of goldfish induces the synaptic degradation of neurofilaments, arguing for their synaptic degradation by a calcium-activated protease (Roots, 1983; Fasani *et al.*, 2004). Similar proteases are found in human tissues that degrade neurofilaments from squids and rats (Paggi and Lasek, 1984; Schlaepfer *et al.*, 1985; Gallant *et al.*, 1986; Vitto and Nixon, 1986). At micromolar calcium concentrations a limited proteolysis of NF occurs during the axonal transport. At higher concentrations (i.e. following axonal transections), a pronounced degradation of NF occurs (Nixon *et al.*, 1986; Banik *et al.*, 1997). Neurofilaments are also proteolyzed by the lysosomal cathepsin D (Nixon and Marotta, 1984; Banay-Schwartz *et al.*, 1987; Suzuki *et al.*, 1988), trypsin and chymotrypsin (Chin *et al.*, 1983; 1989). Moreover, the ubiquitin-proteasome system (UPS) was involved in neurofilament degradation according to a mechanism similar to that described in figure 1.10.

Figure 1.10 Protein ubiquitin-mediated degradation.



Adapted from Hochstrasser, 2009

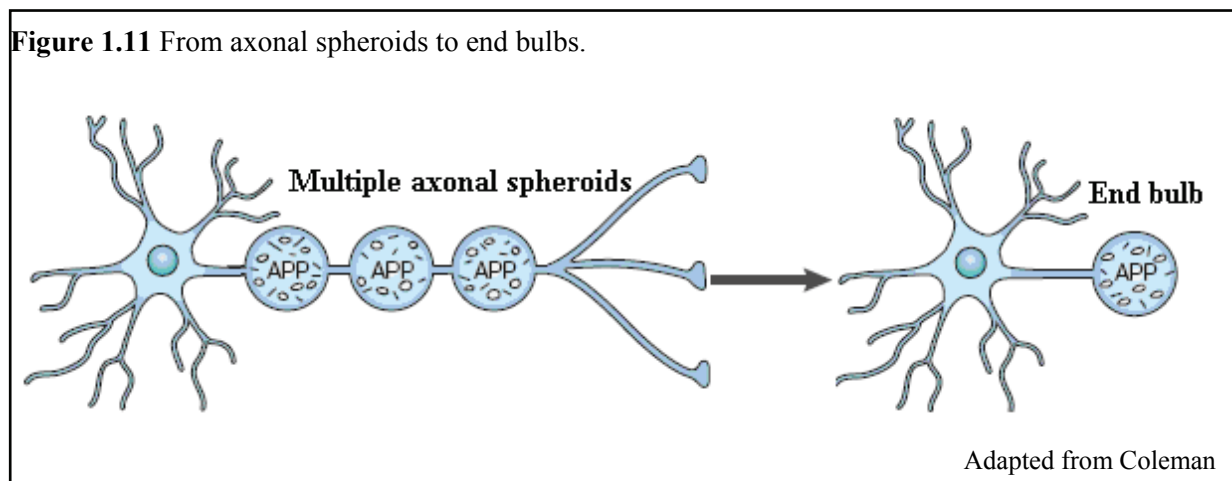
A polyubiquitin-modified protein is targeted to the proteasome. Ubiquitin receptors or adaptor proteins allow binding of the proteolytic substrate to the proteasome. Thus, the substrate is cleaved to small peptides. Ub= ubiquitin, RP= regulatory particles, CP= core particle (blue and red rings).

Thus, using proteasome inhibitors, like lactacystin, a perikaryal accumulation of phosphorylated neurofilaments was observed (Masaki *et al.*, 2000). Furthermore, deficiency in an ubiquitin ligase tripartite RING finger protein 2 (TRIM2) increased NF-L levels and determined neurodegeneration (Balastik *et al.*, 2008). Another ubiquitin ligase, termed PAM, Highwire and RPM-1 (Phr1) is tightly associated with the microtubule cytoskeleton and modulates microtubule dynamics in axons (Lewcock *et al.*, 2007).

New functions were discovered for ubiquitin (Ub) carboxy-terminal hydrolase L1 (UCH-L1, PGP9-5), one of the most abundant proteins in the brain (1-2% of the total soluble protein). Thus, originally characterized as a deubiquitinating enzyme (Wilkinson *et al.*, 1989), UCH-L1 showed ubiquitin ligase characteristics (Liu *et al.*, 2002). Moreover, UCH-L1 seems to function as a mono-Ub-stabilizer (Osaka *et al.*, 2003). Abnormal brain expression of UCH-L1 was associated with Alzheimer and Parkinson diseases (Castegna *et al.*, 2002; Choi *et al.*, 2004; Butterfield *et al.*, 2006; Das *et al.*, 2006).

1.2.2 Axonopathies

The majority of axonal proteins presented above are involved in different neurodegenerative disorders characterized by axonal degeneration. Axonal dystrophies are the manifestations of axonal degeneration. Frequent morphological manifestations of axonal pathology are focal swellings named axonal spheroids. Spheroids appear, frequently, as tandem-repeated swellings (figure 1.11). When the axons are completely transected the spheroids are called end bulbs.



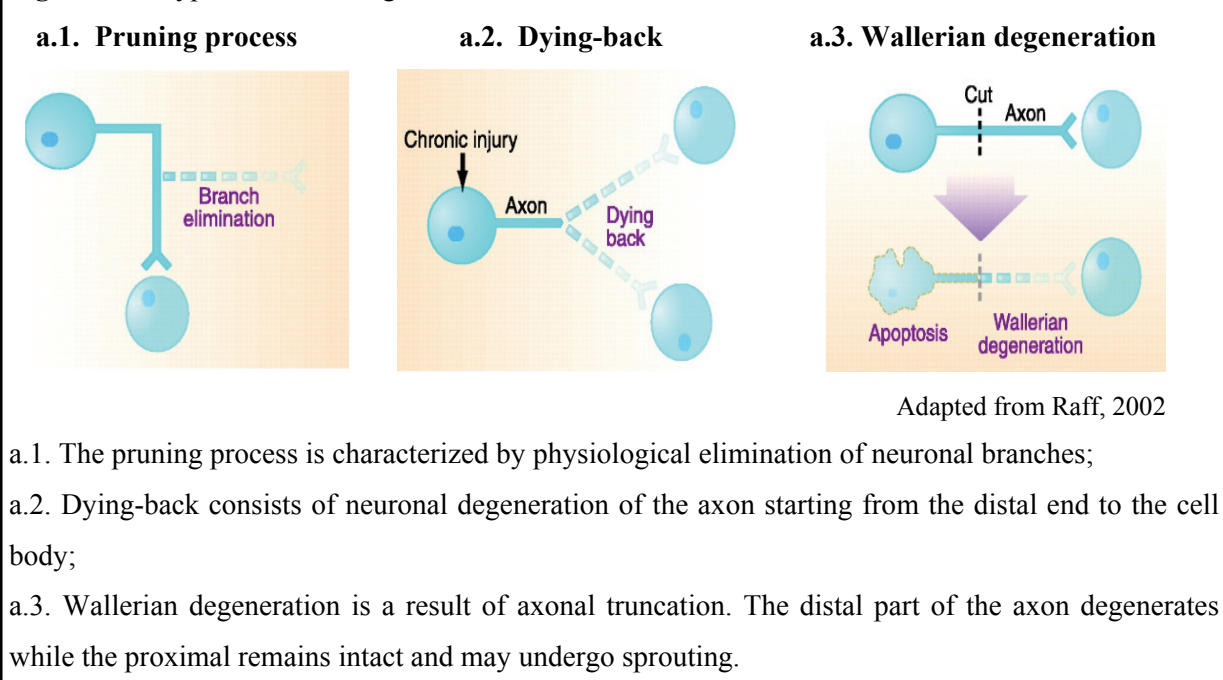
Focal blockages of axonal transport leads to accumulation of organelles and disorganized cytoskeleton in axonal spheroids. Amyloid precursor protein (APP) also accumulates in these swellings. As the spheroids grow, axonal transport may become increasingly impaired. At the end an end bulb remains on the proximal axon stump.

1.2.2.1 Types of axonal degeneration

Axonal degeneration can be observed under physiological or pathological conditions (figure 1.12).

Physiological axonal degeneration occurs during normal nervous system development when inappropriate neuronal branches are deleted through a so called ***branch elimination or pruning process*** (O’Leary and Koester, 1993; Lee, 1999; Raff, 2002; figure 1.12). Pruning occurs either by axonal retraction or degeneration and is involved in generation of precise neural circuits (Kage, 2005; Luo and O’Leary, 2005).

Figure 1.12 Types of axonal degeneration.



Pathological axonal degeneration occurs in conditions like: nerve trauma, toxic insults and neurodegenerative diseases (Hilliard, 2009). Two main types of pathological axonal degeneration were described: distal axonopathy and Wallerian degeneration.

Distal axonopathy or “Dying-back” is a common term for generalized axonal neuropathies with many underlying etiologies like mechanical injury, several chemical and toxic insults (acrylamide, vincristine, nitrofurantoin and heavy metals) and inherited diseases (Prineas, 1969; Schlaepfer, 1971; Spencer and Schaumburg 1974; 1980; Wang *et al.*, 2000; Rubens *et al.*, 2001; Silva *et al.*, 2006). In ‘dying back’ degeneration, the axon of a chronically injured neuron slowly degenerates from the distal end to the cell body (Cavanagh, 1964; figure 1.12). When both the central and the peripheral nervous systems are involved (motor fibers of sciatic nerve), the condition is referred to as central-peripheral distal axonopathy. If the involvement is only confined to the central nervous system, this process may be referred to as central distal axonopathy.

The nature and the site of initial injury to the neuron are unknown; in particular, it is unclear if the process starts in the axons itself or in the neuronal cell body. In a scenario proposed by Raff et al. (2002) ‘dying back’ degeneration is a stereotyped response of axons, which under some circumstances activate a self-destruct program, similar to what happens in the cell body during apoptosis. However, genetic evidences indicate that axonal degeneration and neuronal cell death are two distinct events. Thus, in a mouse model of progressive motor neuropathy (*pnn* mice), the mutant animals develop a neuropathy in which the axons of motor neurons are dying back and the neurons undergo apoptosis (Sagot *et al.*, 1995). The cardinal features of dying-back axonal degeneration are summarized in table 1.2.

Table 1.2 Distinguishing characteristics between dying-back and Wallerian degeneration (adapted from Oh, 2002).

Characteristics	Type of axonal degeneration	
	Dying back	Wallerian degeneration
Metabolism	- aggregates of tau, NFs and α -synuclein	- no aggregates
Conduction	- slow or midly	- failure - paralysis and anaesthesia
Distal muscles	- denervation atrophy - prominent fibrillation or positive sharp waves	- denervation atrophy - prominent fibrillation and positive sharp waves
Chromatolysis	- sometimes	- sometimes
Schwann cell proliferation	- indolent	- burst of proliferation distal to transection
Recovery	- slow by axonal sprouting	- is variable and depends upon: (a) intactness of the neural tube, (b) the proximo-distal site of injury; (c) the age of the individual and (d) the closeness of the severed ends and the degree of adjacent soft-tissue injury

Axonal truncation as a result of injury causes degeneration of the distal part of the axon, while the proximal axon remains intact (figure 1.12). This process, in which the axon beads forming the so-called axonal spheroids or swellings, is commonly referred as **Wallerian degeneration** (Waller, 1850). Wallerian degeneration was initially described in experimental axotomy and later in neuropathies of the peripheral nerve caused by trauma, infarction of peripheral nerve (diabetic mononeuropathy, vasculitis) and neoplastic infiltration. The main characteristics of Wallerian degeneration are summarized in table 1.2.

Histologically, Wallerian degeneration is characterized by swollen neuronal bodies, disaggregated ER, central chromatolysed nuclei, degraded neurofilaments, swallowed mitochondria and fragmented axons (Griffin *et al.*, 1996).

Initially, Wallerian degeneration was considered a passive process. Subsequently, by identification of *Wld^S* mouse strain, which displays a much slower rate of axonal degeneration than the wild-type mice, Lunn *et al.* (1989) showed that Wallerian degeneration implies an active program (Lunn *et al.*, 1989) which not always ended with axonal lost. Therefore, Wallerian degeneration triggered by focal lesions which do not complete section the axon seems to be reversible, at least, in Alzheimer disease models after A β -immunotherapy (Tsai *et al.*, 2004; Brendza *et al.*, 2005).

1.2.2.2 Molecular mechanisms of axonal degeneration

Studies regarding the axonal degeneration pathways revealed an overlap among the mechanisms underlying different axonal degeneration events but also suggest the existence of alternative, as yet uncovered, axonal degeneration pathways.

Thus, though different in directionality, the “dying back” and Wallerian degeneration are difficult to distinguish when they are analyzed at single sites. Therefore, a common mechanism was proposed (Bouldin and Cavanagh, 1979; Spencer and Schaumburg, 1977). Common characteristics among the “dying back” and Wallerian degeneration were also revealed by morphological studies. Thus, although at the PNS level, Wallerian degeneration involves only slight axonal swellings, the same process at the CNS revealed prominent axon swellings. These results indicated the possibility that axonal swelling in many CNS disorders (traumatic brain injury, Alzheimer’s disease, Parkinson’s disease, HIV dementia, multiple sclerosis) reflects a Wallerian-related mechanism (Cheng and Povlishock, 1988; Tsai *et al.*, 2004; Galvin *et al.*, 1999; Adle-Biassette *et al.*, 1999; Ferguson *et al.*, 1997; Trapp *et al.*, 1998).

More details about these related pathways were obtained after discovery of the *Wld^S* mice. Thus, a protective effect of *Wld^S* was observed in mouse models of progressive motor neuropathy (pmn mice), Charcot-Marie-Tooth disease (myelin protein zero null mutants) and gracile axonal dystrophy (gad mutant mice; Ferri *et al.*, 2003; Samsam *et al.*, 2003; Mi *et al.*, 2005) as well as in axonal degeneration initiated by physical and toxic insults (Wang *et al.*, 2001; Sajadi *et al.*, 2004; Adalbert *et al.*, 2005; MacDonald *et al.*, 2006).

In contrast, not all forms of axonal degeneration are delayed in *Wld^S*. *Wld^S* cannot prevent the developmentally regulated axonal pruning (Hoopfer *et al.*, 2006) and degeneration in the

SOD1 transgenic mouse model of amyotrophic lateral sclerosis (ALS; Vande Velde *et al.*, 2004; Fischer *et al.*, 2005) or in the proteolipid protein (plp) null animal model of hereditary spastic paraplegia (Edgar *et al.*, 2004).

To investigate the molecular mechanisms involved in initiation, promotion and evolution of axonal degeneration, *Wld^S* mice were further investigated. Positioning cloning has revealed that the dominant *Wld^S* mutation is an 85kb tandem triplication that results in the production of a chimeric protein (*Wld^S*). The *Wld^S* protein includes the N-terminal 70 amino acids of the ubiquitin fusion degradation protein 2a (Ufd2a), the complete sequence of the NAD⁺ synthetizing enzyme NMN adenylyltransferase 1 (Nmnat1) and a linker region of 18 amino acids (Lyon *et al.*, 1993; Coleman *et al.*, 1998; Conforti *et al.*, 2000; Mack *et al.*, 2001). Considerable experimental evidence suggests an important role of Nmnat1 and the NAD⁺ pathway in protecting axons from degeneration (Araki *et al.*, 2004; Wang *et al.*, 2005; Sasaki *et al.*, 2006). In *Wld^S* mice part of the protective effect could arise from the over-expression of Nmnat1 with a consequent increase in NAD⁺ levels (Araki *et al.*, 2004). Araki *et al.* (2004) have also shown that sirtuin silent mating type information regulation 1 (SIRT1), a NAD⁺-dependent histone deacetylase (the mammalian ortholog of Sir2), is a downstream effector of Nmnat1 activation that leads to axonal protection. A particularly interesting and relevant finding is that resveratrol, a polyphenol found in red grapes and an enhancer of silent mating type information regulation 2 activity, is able to mimic the axonal protective effect of NAD⁺ (Araki *et al.*, 2004). However, in different conditions Nmnat1 alone cannot fully recapitulate the effect of the *Wld^S* mutation, suggesting the involvement of other components of the chimeric protein (Conforti *et al.*, 2007; Watanabe *et al.*, 2007).

Several studies indicate that the ubiquitin proteasome system (UPS) is a critical player in axonal degeneration, although its role appears more complex (Saigoh *et al.*, 1999; Zhai *et al.*, 2003; Watts *et al.*, 2003). In *Drosophila*, axonal pruning and axonal degeneration following injury depend on a functional UPS (Watts, 2003). Similarly in rats, axonal degeneration following injury is delayed by inhibition of the UPS (Zhai *et al.*, 2003). In the *Wld^S* mutation, the truncated UPS molecule (Ufd2a) might function as a dominant negative protein and provide some axonal protection. However, different mutations reducing the function of the UPS molecules can also be the cause of neurodegenerative diseases and axonal degeneration, as observed in Parkinson's disease patients carrying mutations in the parkin gene (ubiquitin-protein ligase; Kitada *et al.*, 1998; Shimura *et al.*, 2000) and in *gad* mice (ubiquitin carboxy-terminal hydrolase-L1; Saigoh *et al.*, 1999). This apparent paradoxal role of UPS functioning in both processes (degeneration–protection) could be explained by different levels of UPS

triggering diverse responses, by having alternative effects in different neuronal compartments (cell body, axon, or synapse) or by mutation in different UPS components. Recent findings revealed that the N-terminal 70 amino acids of Wld^S binds directly to the vasolin-containing protein (VCP/p97), a protein with a key role in the ubiquitin proteasome system (Laser *et al.*, 2006). Interaction with Wld^S targets VCP in discrete intranuclear foci where other UPS components can also accumulate (Laser *et al.*, 2006). Thus, the N-terminal domain of Wld^S influences the intranuclear location of the ubiquitin proteasome as well as its intrinsic NAD⁺ synthesis activity, although VCP itself can also regulate Wld^S intracellular distribution (Wilbrey *et al.*, 2008). Differential proteomic analysis of isolated synaptic preparations from the striatum in mice revealed 16 proteins with modified expression levels in Wld^S synapses (Wishart, 2007). Interestingly, downstream protein changes were found in pathways corresponding to both Ufd2a (including ubiquitin-activating enzyme 1) and Nmnat1 (including voltage-dependent anion-selective channel protein and aralar1, calcium-binding mitochondrial carrier protein; Wishart *et al.*, 2007). Furthermore, increased expression of a broad spectrum of cell cycle-related genes was found in the cerebellum of Wld^S mice and in Wld^S-expressing human embryonic kidney 293 cells (Wishart *et al.*, 2008), suggesting a correlation between modified cell cycle pathways and altered vulnerability of axons.

Recently, axonal pruning and axonal degeneration following injury have been shown to have other common effectors. Cell death abnormality (CED)-1/DRAPER and CED-6 are scavenger receptor-like molecules essential for the clearance of apoptotic cells in *C. elegans* and *Drosophila* (Liu *et al.*, 1998; Zhou *et al.*, 2001; Freeman *et al.*, 2003). In worms they are expressed in the phagocytic cell, whereas in flies they are expressed in the glia. Mutations in CED-1/DRAPER inhibit clearance of the distal fragment of severed axons in *Drosophila* olfactory receptor neurons (MacDonald *et al.*, 2006). Similarly, in axons of the *Drosophila* mushroom body, ced-1/draper and ced-6 are necessary for the clearance of axonal fragments undergoing pruning (Awasaki *et al.*, 2006). The finding that cell death genes such as ced-1 and ced-6 are involved in the axonal degeneration process suggests a partial commonality in the mechanisms, at least in the later stages of these events, such as the removal of axonal fragments or cell bodies after damage. The activation of the glia and the function of these receptor molecules indicate the existence of specific signals coming from the damaged axon to which the glia are responding. Discovering these cues is a key step towards understanding further how axonal degeneration is triggered and achieved.

The axonal transport failure is another mechanism suspected to underly axonal degeneration pathology (Griffin *et al.*, 1988). Mutations in many proteins involved in axonal transport were observed in different neurodegenerative diseases (Salinas *et al.*, 2008; table 1.3).

Table 1.3 Molecular motors, adaptors and regulators of axonal transport and associated neurological diseases.

Protein	Function	Molecular defect	Disease (spontaneous)
p150^{Glued}	Motor associated protein	Point mutation/transcriptional repression	Amyotrophic lateral sclerosis; spinal bulbar muscular atrophy
KIF1Bβ	Motor protein	Point mutation	Charcot-Marie-Tooth disease type 2A
KIF5A	Motor protein	Point mutation	Hereditary spastic paraplegia 10
Tau	Microtubule associated protein	Overexpression, Point mutation, Altered splicing	Alzheimer's disease, Taupathies, Fronto-temporal dementia and Parkinsonism linked to chromosome 17
Alsln	Rab5 guanine-nucleotide exchange factor	Downregulation	Motor neuron disease
Rab7	Small GTP-ase	Point mutation	Charcot-Marie-Tooth disease type 2B
APP	Kinesin-1 adaptor	Overexpression	Alzheimer's disease, Down's syndrome
Htt	Dynein/dynactin adaptor	Poly Q repeats	Hungtinton's disease
SOD1	Free radical scavenging enzyme	Missense mutation	Amyotrophic lateral sclerosis
MFN2	Mitochondrial outer membrane protein	Missense mutation	Charcot-Marie-Tooth disease type 2A
KBP	Kif1B adaptor	Nonsense mutation	Goldberg-Shprintzen syndrome

p150^{Glued}= dynactin 1; KIF1B β = kinesin family member 1B beta; KIF5A= kinesin family member 5A; Rab5, 7= Ras- associated protein 5, 7; APP= amyloid precursor protein; Htt= huntingtin; SOD1= superoxide dismutase 1; MFN2= mitofusin 2; KBP= Kif1B binding protein. (Salinas *et al.*, 2008).

Moreover, the most obvious common feature of models in which *Wld^S* delays axon degeneration is a blockade of axonal transport from the cell body. Normal microtubule functioning, which is essential for axonal transport, is prevented by mutation in the *tubulin-specific chaperone e* (TBCE) gene in *pmn* mice (Martin *et al.*, 2002) and by the microtubule-stabilizing action of Taxol. Dysmyelination in P0 null mice may prevent axons to impair transport (Martini, 2001). In addition, accumulation of APP is evidence of a defective axonal transport in the axons of *gad* mice, however the precise mechanism remains unknown (Ichihara *et al.*, 1995). Nerve transection is the ultimate block of axonal transport from the

cell body. Interestingly, when axonal transport is severely blocked in *pmn* mice (Martin *et al.*, 2002), *Wld^S* causes a 2–3 week delay in axon degeneration that is strikingly similar to that observed after transection. Wallerian-like degeneration also results when axonal transport is disrupted in other ways, such as by colchicine treatment or mutation of neurofilament proteins (Singer *et al.*, 1956; Julien, 1999). The fact that a Wallerian-related mechanism can be triggered without physical axonal injury rules out calcium influx at the transection site as the initiating event. An interruption of axonal transport from the cell body seems to be a likely alternative trigger for Wallerian degeneration. Genetic defects in the kinesin family proteins often specifically cause axon degeneration (Zhao *et al.*, 2001; Reid *et al.*, 2002), whereas defects in retrograde transport also cause cell body death (Hafezparast *et al.*, 2003), which suggests that anterograde transport might be particularly important for preventing axon degeneration.

APP which is normally transported through axons by fast axonal transport without reaching detectable levels can accumulate in axonal spheroids, providing an immunohistochemical marker for blockages of axonal transport (Seehusen and Baumgärtner, 2009).

The actual view upon the pathological mechanisms in multiple sclerosis, is that axons become injured by inflammatory events and the severed ends then swell to form end bulbs (Ferguson *et al.*, 1997; Trapp *et al.*, 1998). However, there is little evidence for a transection event *in vivo*, and observations of spheroids and varicosities of continuous axons in multiple sclerosis and EAE (Kornek *et al.*, 2001) suggest a different sequence of events. A working model for spheroid pathology involves localized failure of axonal transport, particularly at nodes of Ranvier, which causes an excessive build-up in the axoplasm, including rapidly transported proteins such as APP. Failure of axonal transport from cell bodies eventually triggers Wallerian degeneration of distal axons, leaving proximal axons with large end bulbs.

1.3 References

1. Acar G, Idiman F, Idiman E, Kirkali G, Cakmakçi H, Ozakbaş S. Nitric oxide as an activity marker in multiple sclerosis. *J. Neurol.* 250:588-592, 2003.
2. Ackerley S, Thornhill P, Grierson AJ, Brownlees J, Anderton BH, Leigh PN, Shaw CE, Miller CC. Neurofilament heavy chain side arm phosphorylation regulates axonal transport of neurofilaments. *J. Cell. Biol.* 161:489-495, 2003.
3. Adalbert R, Gillingwater TH, Haley JE. A rat model of slow Wallerian degeneration (*Wld^S*) with improved preservation of neuromuscular synapses. *Eur. J. Neurosci.* 21: 271–277, 2005.

4. Adle-Biassette H, Chrétien F, Wingertsman L, Héry C, Ereau T, Scaravilli F, Tardieu M, Gray F. Neuronal apoptosis does not correlate with dementia in HIV infection but is related to microglial activation and axonal damage. *Neuropathol. Appl. Neurobiol.* 25:123-133, 1999.
5. Anderson R, Harting E, Frey MS, Leibowitz JL, Miranda RC. Theiler's murine encephalomyelitis virus induces rapid necrosis and delayed apoptosis in myelinated mouse cerebellar explant cultures. *Brain Res.* 868:259-267, 2000.
6. Araki T, Sasaki Y, Milbrandt J. Increased nuclear NAD biosynthesis and SIRT1 activation prevent axonal degeneration. *Science.* 305:1010-1013, 2004.
7. Awasaki T, Tatsumi R, Takahashi K, Arai K, Nakanishi Y, Ueda R, Ito K. Essential role of the apoptotic cell engulfment genes draper and ced-6 in programmed axon pruning during *Drosophila* metamorphosis. *Neuron.* 50: 855–867, 2006.
8. Balastik M, Ferraguti F, Pires-da Silva A, Lee TH, Alvarez-Bolado G, Lu KP, Gruss P. Deficiency in ubiquitin ligase TRIM2 causes accumulation of neurofilament light chain and neurodegeneration. *Proc. Natl. Acad. Sci. U S A.* 105:12016-12021, 2008.
9. Banay-Schwartz M, Dahl D, Hui KS, Lajtha A. The breakdown of the individual neurofilament proteins by cathepsin D. *Neurochem. Res.* 12:361-367, 1987.
10. Banik NL, Matzelle DC, Gantt-Wilford G, Osborne A, Hogan EL. Increased calpain content and progressive degradation of neurofilament protein in spinal cord injury. *Brain Res.* 752:301-306, 1997.
11. Baumgärtner W, Alldinger S. The pathogenesis of canine distemper virus induced demyelination: a biphasic process. In: Lavi, E.; Constantinescu, C. S. (Hrsg.): *Experimental models of multiple sclerosis.* New York: Springer, S. 871-887, 2005, ISBN 0-387-25517-6.
12. Bitsch A, Schuchardt J, Bunkowski S, Kuhlmann T, Brück W. Acute axonal injury in multiple sclerosis. Correlation with demyelination and inflammation. *Brain.* 123:1174-1183, 2000.
13. Bjartmar C, Kidd G, Mörk S, Rudick R, Trapp BD. Neurological disability correlates with spinal cord axonal loss and reduced N-acetyl aspartate in chronic multiple sclerosis patients. *Ann. Neurol.* 48:893-901, 2000.
14. Black MM, Lee VM. Phosphorylation of neurofilament proteins in intact neurons: demonstration of phosphorylation in cell bodies and axons. *J. Neurosci.* 8:3296-3305, 1988.
15. Bloom GS, Endow SA. Motor proteins 1: kinesins. *Protein Profile.* 2:1105-1171, 1995.

16. Bloom GS, Wagner MC, Pfister KK, Brady ST. Native structure and physical properties of bovine brain kinesin and identification of the ATP-binding subunit polypeptide. *Biochemistry*. 27:3409-3416, 1988.
17. Bouldin TW, Cavanagh JB. Organophosphorous neuropathy. II. A fine-structural study of the early stages of axonal degeneration. *Am. J. Pathol.* 94:253-270, 1979.
18. Brady ST. A novel brain ATPase with properties expected for the fast axonal transport motor. *Nature*. 317:73-75, 1985.
19. Brendza RP, Bacsikai BJ, Cirrito JR, Simmons KA, Skoch JM, Klunk WE, Mathis CA, Bales KR, Paul SM, Hyman BT, Holtzman DM. Anti-Abeta antibody treatment promotes the rapid recovery of amyloid-associated neuritic dystrophy in PDAPP transgenic mice. *J. Clin. Invest.* 115:428-433, 2005.
20. Brendza RP, Serbus LR, Duffy JB, Saxton WM. A function for kinesin I in the posterior transport of oskar mRNA and Staufen protein. *Science*. 289:2120-2122, 2000.
21. Butterfield DA, Gnjec A, Poon HF, Castegna A, Pierce WM, Klein JB, Martins RN. Redox proteomics identification of oxidatively modified brain proteins in inherited Alzheimer's disease: an initial assessment. *J. Alzheimers Dis.* 10:391-397, 2006.
22. Campenot RB, Eng H. Protein synthesis in axons and its possible functions. *J. Neurocytol.* 29:793-798, 2000.
23. Carpentier PA, Getts MT, Miller SD. Pro-inflammatory functions of astrocytes correlate with viral clearance and strain-dependent protection from TMEV-induced demyelinating disease. *Virology*. 375:24-36, 2008.
24. Castegna A, Aksenov M, Thongboonkerd V, Klein JB, Pierce WM, Booze R, Markesbery WR, Butterfield DA. Proteomic identification of oxidatively modified proteins in Alzheimer's disease brain. Part II: dihydropyrimidinase-related protein 2, alpha-enolase and heatshock cognate 71. *J. Neurochem.* 82:1524-1532, 2002.
25. Cavanagh JB. The significance of the "dying back" process in experimental and human neurological disease. *Int. Rev. Exp. Pathol.* 3:219-267, 1964.
26. Chandran S, Hunt D, Joannides A, Zhao C, Compston A, Franklin RJ. Myelin repair: the role of stem and precursor cells in multiple sclerosis. *Philos. Trans. R. Soc. Lond. B Biol. Sci.* 363:171-178, 2008.
27. Chang A, Tourtellotte WW, Rudick R, Trapp BD. Premyelinating oligodendrocytes in chronic lesions of multiple sclerosis. *N. Engl. J. Med.* 346:165-173, 2002.

28. Chen HH, Kong WP, Zhang L, Ward PL, Roos RP. A picornaviral protein synthesized out of frame with the polyprotein plays a key role in a virus-induced immune-mediated demyelinating disease. *Nat. Med.* 1:927-931, 1995.
29. Chen MS, Huber AB, van der Haar ME, Frank M, Schnell L, Spillmann AA, Christ F, Schwab ME. Nogo-A is a myelin-associated neurite outgrowth inhibitor and an antigen for monoclonal antibody IN-1. *Nature.* 403:434-439, 2000.
30. Cheng CL, Povlishock JT. The effect of traumatic brain injury on the visual system: a morphologic characterization of reactive axonal change. *J Neurotrauma.* 5:47-60, 1988.
31. Chin TK, Eagles PA, Maggs A. The proteolytic digestion of ox neurofilaments with trypsin and alpha-chymotrypsin. *Biochem. J.* 215:239-252, 1983.
32. Chin TK, Harding SE, Eagles PA. Characterization of two proteolytically derived soluble polypeptides from the neurofilament triplet components NFM and NFH. *Biochem. J.* 264:53-60, 1989.
33. Choi J, Levey AI, Weintraub ST, Rees HD, Gearing M, Chin LS, Li L. Oxidative modifications and down-regulation of ubiquitin carboxyl-terminal hydrolase L1 associated with idiopathic Parkinson's and Alzheimer's diseases. *J. Biol. Chem.* 279:13256-13264, 2004.
34. Clatch RJ, Miller SD, Metzner R, Dal Canto MC, Lipton HL. Monocytes/macrophages isolated from the mouse central nervous system contain infectious Theiler's murine encephalomyelitis virus (TMEV). *Virology.* 176:244-254, 1990.
35. Coleman MP, Conforti L, Buckmaster EA, Tarlton A, Ewing RM, Brown MC, Lyon MF, Perry VH. An 85-kb tandem triplication in the slow Wallerian degeneration (Wlds) mouse. *Proc. Natl. Acad. Sci. U S A.* 95:9985-9990, 1998.
36. Coleman M. Axon degeneration mechanisms: commonality amid diversity. *Nat. Rev. Neurosci.* 6:889-898, 2005.
37. Conforti L, Fang G, Beirowski B, Wang MS, Sorci L, Asress S, Adalbert R, Silva A, Bridge K, Huang XP, Magni G, Glass JD, Coleman MP. NAD(+) and axon degeneration revisited: Nmnat1 cannot substitute for Wld(S) to delay Wallerian degeneration. *Cell Death Differ.* 14:116-127, 2007.
38. Conforti L, Tarlton A, Mack TG, Mi W, Buckmaster EA, Wagner D, Perry VH, Coleman MP. A Ufd2/D4Cole1e chimeric protein and overexpression of Rbp7 in the slow Wallerian degeneration (WldS) mouse. *Proc. Natl. Acad. Sci. U S A.* 97:11377-11382, 2000.

39. Dal Canto MC, Melvold RW, Kim BS. A hybrid between a resistant and a susceptible strain of mouse alters the pattern of Theiler's murine encephalomyelitis virus-induced white matter disease and favors oligodendrocyte-mediated remyelination. *Mult. Scler.* 1:95-103, 1995.
40. Dal Canto MC, Lipton HL. Ultrastructural immunohistochemical localization of virus in acute and chronic demyelinating Theiler's virus infection. *Am. J. Pathol.* 106:20-29, 1982.
41. Das C, Hoang QQ, Kreinbring CA, Luchansky SJ, Meray RK, Ray SS, Lansbury PT, Ringe D, Petsko GA. Structural basis for conformational plasticity of the Parkinson's disease-associated ubiquitin hydrolase UCH-L1. *Proc. Natl. Acad. Sci. U S A.* 103: 4675-4680, 2006.
42. de Rosbo NK, Ben-Nun A. T-cell responses to myelin antigens in multiple sclerosis; relevance of the predominant autoimmune reactivity to myelin oligodendrocyte glycoprotein. *J. Autoimmun.* 11:287-299, 1998.
43. de Waegh SM, Lee VM, Brady ST. Local modulation of neurofilament phosphorylation, axonal caliber, and slow axonal transport by myelinating Schwann cells. *Cell.* 68:451-463, 1992.
44. Dutta R, McDonough J, Yin X, Peterson J, Chang A, Torres T, Gudz T, Macklin WB, Lewis DA, Fox RJ, Rudick R, Mirnics K, Trapp BD. Mitochondrial dysfunction as a cause of axonal degeneration in multiple sclerosis patients. *Ann. Neurol.* 59:478-489, 2006.
45. Edgar JM, McLaughlin M, Yool D, Zhang SC, Fowler JH, Montague P, Barrie JA, McCulloch MC, Duncan ID, Garbern J, Nave KA, Griffiths IR. Oligodendroglial modulation of fast axonal transport in a mouse model of hereditary spastic paraplegia. *J. Cell. Biol.* 166:121-131, 2004.
46. Fasani F, Bocquet A, Robert P, Peterson A, Eyer J. The amount of neurofilaments aggregated in the cell body is controlled by their increased sensitivity to trypsin-like proteases. *J. Cell. Sci.* 117: 861-869, 2004.
47. Ferri A, Sanes JR, Coleman MP, Cunningham JM, Kato AC. Inhibiting axon degeneration and synapse loss attenuates apoptosis and disease progression in a mouse model of motoneuron disease. *Curr. Biol.* 13:669-673, 2003.
48. Ferguson B, Matyszak MK, Esiri MM, Perry VH. Axonal damage in acute multiple sclerosis lesions. *Brain.* 120:393-399, 1997.

49. Filippi M, Rocca MA. MRI evidence for multiple sclerosis as a diffuse disease of the central nervous system. *J. Neurol.* 252:16-24, 2005.
50. Fischer LR, Culver DG, Davis AA, Tennant P, Wang M, Coleman M, Asress S, Adalbert R, Alexander GM, Glass JD. The WldS gene modestly prolongs survival in the SOD1G93A fALS mouse. *Neurobiol. Dis.* 19:293-300, 2005.
51. Francis F, Roy S, Brady ST, Black MM. Transport of neurofilaments in growing axons requires microtubules but not actin filaments. *J. Neurosci. Res.* 79:442-450, 2005.
52. Freeman MR, Delrow J, Kim J, Johnson E, Doe CQ. Unwrapping glial biology: Gcm target genes regulating glial development, diversification, and function. *Neuron.* 38: 567–580, 2003.
53. Fuchs E, Cleveland DW. A structural scaffolding of intermediate filaments in health and disease. *Science.* 279:514-519, 1998.
54. Gallant PE, Pant HC, Pruss RM, Gainer H. Calcium-activated proteolysis of neurofilament proteins in the squid giant neuron. *J Neurochem.* 46:1573-1581, 1986.
55. Galvin JE, Uryu K, Lee VM, Trojanowski JQ. Axon pathology in Parkinson's disease and Lewy body dementia hippocampus contains alpha-, beta-, and gamma-synuclein. *Proc. Natl. Acad. Sci. U S A.* 96:13450-13455, 1999.
56. Garbern JY, Yool DA, Moore GJ, Wilds IB, Faulk MW, Klugmann M, Nave KA, Garthwaite G, Goodwin DA, Batchelor AM, Leeming K, Garthwaite J. Nitric oxide toxicity in CNS white matter: an in vitro study using rat optic nerve. *Neuroscience.* 109:145-155, 2002.
57. Gerhauser I, Alldinger S, Baumgärtner W. Ets-1 represents a pivotal transcription factor for viral clearance, inflammation, and demyelination in a mouse model of multiple sclerosis. *J. Neuroimmunol.* 188:86-94, 2007.
58. Ghadge GD, Ma L, Sato S, Kim J, Roos RP. A protein critical for a Theiler's virus-induced immune system-mediated demyelinating disease has a cell type-specific antiapoptotic effect and a key role in virus persistence. *J. Virol.* 72:8605-8612, 1998.
59. Gold R, Linington C, Lassmann H. Understanding pathogenesis and therapy of multiple sclerosis via animal models: 70 years of merits and culprits in experimental autoimmune encephalomyelitis research. *Brain.* 129:1953-71, 2006.
60. Goldstein LS, Philp AV. The road less traveled: emerging principles of kinesin motor utilization. *Annu. Rev. Cell. Dev. Biol.* 15:141-183, 1999.

61. GrandPré T, Nakamura F, Vartanian T, Strittmatter SM. Identification of the Nogo inhibitor of axon regeneration as a Reticulon protein. *Nature*. 403:439-444, 2000.
62. Griffin JW, George EB, Chaudhry V. Wallerian degeneration in peripheral nerve disease. *Baillieres Clin. Neurol.* 5:65-75, 1996.
63. Griffin JW, Watson DF. Axonal transport in neurological disease. *Ann. Neurol.* 23:3-13, 1988.
64. Griffiths I, Klugmann M, Anderson T, Yool D, Thomson C, Schwab MH, Schneider A, Zimmermann F, McCulloch M, Nadon N, Nave KA. Axonal swellings and degeneration in mice lacking the major proteolipid of myelin. *Science*. 280:1610-1613, 1998.
65. Grigoriadis N, Ben-Hur T, Karussis D, Milonas I. Axonal damage in multiple sclerosis: a complex issue in a complex disease. *Clin. Neurol. Neurosurg.* 106:211-217, 2004.
66. Hafezparast M, Klocke R, Ruhrberg C, Marquardt A, Ahmad-Annuar A, Bowen S, Lalli G, Witherden AS, Hummerich H, Nicholson S, Morgan PJ, Oozageer R, Priestley JV, Averill S, King VR, Ball S, Peters J, Toda T, Yamamoto A, Hiraoka Y, Augustin M, Korthaus D, Wattler S, Wabnitz P, Dickneite C, Lampel S, Boehme F, Peraus G, Popp A, Rudelius M, Schlegel J, Fuchs H, Hrabe de Angelis M, Schiavo G, Shima DT, Russ AP, Stumm G, Martin JE, Fisher EM. Mutations in dynein link motor neuron degeneration to defects in retrograde transport. *Science*. 300:808-812, 2003.
67. Hauser SL, Oksenberg JR. The neurobiology of multiple sclerosis: genes, inflammation, and neurodegeneration. *Neuron*. 52:61-76, 2006.
68. Hellmich MR, Pant HC, Wada E, Battey JF. Neuronal cdc2-like kinase: a cdc2-related protein kinase with predominantly neuronal expression. *Proc. Natl. Acad. Sci. U S A*. 89:10867-10871, 1992.
69. Herrero-Herranz E, Pardo LA, Gold R, Linker RA. Pattern of axonal injury in murine myelin oligodendrocyte glycoprotein induced experimental autoimmune encephalomyelitis: implications for multiple sclerosis. *Neurobiol. Dis.* 30:162-173, 2008.
70. Hilliard MA. Axonal degeneration and regeneration: a mechanistic tug-of-war. *J. Neurochem.* 108:23-32, 2009.
71. Hirokawa N, Takemura R. Kinesin superfamily proteins and their various functions and dynamics. *Exp. Cell. Res.* 301:50-59, 2004.

72. Hirokawa N, Takeda S. Gene targeting studies begin to reveal the function of neurofilament proteins. *J. Cell. Biol.* 143:1-4, 1998.
73. Hirokawa N. Cross-linker system between neurofilaments, microtubules, and membranous organelles in frog axons revealed by the quick-freeze, deep-etching method. *J. Cell. Biol.* 94:129-142, 1982.
74. Hoffman PN, Lasek RJ. The slow component of axonal transport. Identification of major structural polypeptides of the axon and their generality among mammalian neurons. *J. Cell. Biol.* 66:351-366, 1975.
75. Hochstrasser M, Origin and function of ubiquitin-like proteins. *Nature.* 458:422-429, 2009.
76. Höftberger R, Aboul-Enein F, Brueck W, Lucchinetti C, Rodriguez M, Schmidbauer M, Jellinger K, Lassmann H. Expression of major histocompatibility complex class I molecules on the different cell types in multiple sclerosis lesions. *Brain Pathol.* 14:43-50, 2004.
77. Hooper ED, McLaughlin T, Watts RJ, Schuldiner O, O'Leary DD, Luo L. Wlds protection distinguishes axon degeneration following injury from naturally occurring developmental pruning. *Neuron.* 50:883-895, 2006.
78. Hsieh ST, Kidd GJ, Crawford TO, Xu Z, Lin WM, Trapp BD, Cleveland DW, Griffin JW. Regional modulation of neurofilament organization by myelination in normal axons. *Neurosci.* 14:6392-6401, 1994.
79. Ichihara N, Wu J, Chui DH, Yamazaki K, Wakabayashi T, Kikuchi T. Axonal degeneration promotes abnormal accumulation of amyloid beta-protein in ascending gracile tract of gracile axonal dystrophy (GAD) mouse. *Brain Res.* 695:173-178, 1995.
80. Jin YH, Mohindru M, Kang MH, Fuller AC, Kang B, Gallo D, Kim BS. Differential virus replication, cytokine production, and antigen-presenting function by microglia from susceptible and resistant mice infected with Theiler's virus. *J. Virol.* 81:11690-11702, 2007.
81. Julien JP, Neurofilament functions in health and disease. *Curr. Opin. Neurobiol.* 9:554-560, 1999.
82. Julien JP, Mushynski WE. Multiple phosphorylation sites in mammalian neurofilament polypeptides. *J. Biol. Chem.* 257:10467-10470, 1982.
83. Julien JP, Mushynski WE. The distribution of phosphorylation sites among identified proteolytic fragments of mammalian neurofilaments. *J. Biol. Chem.* 258:4019-4025, 1983.

84. Jung C, Lee S, Ortiz D, Zhu Q, Julien JP, Shea TB. The high and middle molecular weight neurofilament subunits regulate the association of neurofilaments with kinesin: inhibition by phosphorylation of the high molecular weight subunit. *Brain Res. Mol. Brain Res.* 141:151-155, 2005.
85. Kage E, Hayashi Y, Takeuchi H, Hirotsu T, Kunitomo H, Inoue T, Arai H, Iino Y, Kubo T. MBR-1, a novel helix-turn-helix transcription factor, is required for pruning excessive neurites in *Caenorhabditis elegans*. *Curr. Biol.* 15:1554-1559, 2005.
86. Kamal A, Goldstein LS. Connecting vesicle transport to the cytoskeleton. *Curr. Opin. Cell. Biol.* 12:503-508, 2000.
87. Kanai Y, Okada Y, Tanaka Y, Harada A, Terada S, and Hirokawa N. KIF5C, a novel neuronal kinesin enriched in motor neurons. *J. Neurosci.* 20:6374–6384, 2000.
88. Kapoor R, Davies M, Blaker PA, Hall SM, Smith KJ. Blockers of sodium and calcium entry protect axons from nitric oxide-mediated degeneration. *Ann. Neurol.* 53:174-180, 2003.
89. Karp G. *Cell and Molecular Biology: Concepts and Experiments*, Fourth ed, pp. 346-358. John Wiley and Sons, Hoboken, NJ. 2005.
90. Katz-Levy Y, Neville KL, Girvin AM, Vanderlugt CL, Pope JG, Tan LJ, Miller SD. Endogenous presentation of self myelin epitopes by CNS-resident APCs in Theiler's virus-infected mice. *J. Clin. Invest.* 104:599-610, 1999.
91. Kerschensteiner M, Stadelmann C, Buddeberg BS, Merkler D, Bareyre FM, Anthony DC, Linington C, Brück W, Schwab ME. Targeting experimental autoimmune encephalomyelitis lesions to a predetermined axonal tract system allows for refined behavioral testing in an animal model of multiple sclerosis. *Am. J. Pathol.* 164:1455-1469, 2004.
92. Kesavapany S, Li BS, Amin N, Zheng YL, Grant P, Pant HC. Neuronal cyclin-dependent kinase 5: role in nervous system function and its specific inhibition by the Cdk5 inhibitory peptide. *Biochim. Biophys. Acta.* 1697:143-153, 2004.
93. Kesavapany S, Li BS, Pant HC. Cyclin-dependent kinase 5 in neurofilament function and regulation. *Neurosignals.* 12:252-264, 2003.
94. Kim BS, Palma JP, Kwon D, Fuller AC. Innate immune response induced by Theiler's murine encephalomyelitis virus infection. *Immunol. Res.* 31:1-12, 2005.
95. Kitada T, Asakawa S, Hattori N, Matsumine H, Yamamura Y, Minoshima S, Yokochi M, Mizuno Y, Shimizu N. Mutations in the parkin gene cause autosomal recessive juvenile parkinsonism. *Nature.* 392:605-608, 1998.

96. Koehnle TJ, Brown A. Slow axonal transport of neurofilament protein in cultured neurons. *J. Cell. Biol.* 144:447–458, 1999.
97. Kornek B, Storch MK, Bauer J, Djamshidian A, Weissert R, Wallstroem E, Stefflerl A, Zimprich F, Olsson T, Linington C, Schmidbauer M, Lassmann H. Distribution of a calcium channel subunit in dystrophic axons in multiple sclerosis and experimental autoimmune encephalomyelitis. *Brain.* 124:1114-1124, 2001.
98. Kumar AS, Reddi HV, Kung AY, Dal Canto M, Lipton HL. Virus persistence in an animal model of multiple sclerosis requires virion attachment to sialic acid coreceptors. *J. Virol.* 78:8860-8867, 2004.
99. Johnson AJ, Upshaw J, Pavelko KD, Rodriguez M, Pease LR. Preservation of motor function by inhibition of CD8+ virus peptide-specific T cells in Theiler's virus infection. *FASEB J.* 15:2760-2771, 2001.
100. Johnson AJ, Suidan GL, McDole J, Pirko I. The CD8 T cell in multiple sclerosis: suppressor cell or mediator of neuropathology? *Int. Rev. Neurobiol.* 79:73-97, 2007.
101. Laferrière NB, MacRae TH, Brown DL. Tubulin synthesis and assembly in differentiating neurons. *Biochem. Cell. Biol.* 75:103-117, 1997.
102. Langrish CL, Chen Y, Blumenschein WM, Mattson J, Basham B, Sedgwick JD, McClanahan T, Kastelein RA, Cua DJ. IL-23 drives a pathogenic T cell population that induces autoimmune inflammation. *J. Exp. Med.* 201:233-240, 2005.
103. Lappe-Siefke C, Goebbels S, Gravel M, Nicksch E, Lee J, Braun PE, Griffiths IR, Nave KA. Disruption of Cnp1 uncouples oligodendroglial functions in axonal support and myelination. *Nat. Genet.* 33:366-374, 2003.
104. Laser H, Conforti L, Morreale G, Mack TG, Heyer M, Haley JE, Wishart TM, Beirowski B, Walker SA, Haase G, Celik A, Adalbert R, Wagner D, Grumme D, Ribchester RR, Plomann M, Coleman MP. The slow Wallerian degeneration protein, WldS, binds directly to VCP/p97 and partially redistributes it within the nucleus. *Mol. Biol. Cell.* 17:1075-1084, 2006.
105. Lassmann H. The pathology of multiple sclerosis and its evolution. *Philos. Trans. R. Soc. Lond. B Biol. Sci.* 354:1635-1640, 1999.
106. Lassmann H. Brain damage when multiple sclerosis is diagnosed clinically. *Lancet.* 361:1317-1318, 2003.
107. Lassmann H. Axonal injury in multiple sclerosis. *J. Neurol. Neurosurg. Psychiatry.* 74:695-697, 2003.

108. Lee T, Lee A, Luo L. Development of the *Drosophila* mushroom bodies: sequential generation of three distinct types of neurons from a neuroblast. *Development*. 126:4065-76, 1999.
109. Lee VM, Otvos L Jr, Carden MJ, Hollosi M, Dietzschold B, Lazzarini RA. Identification of the major multiphosphorylation site in mammalian neurofilaments. *Proc Natl Acad Sci U S A*. 85:1998-2002, 1988.
110. Lee VM, Carden MJ, Schlaepfer WW, Trojanowski JQ. Monoclonal antibodies distinguish several differentially phosphorylated states of the two largest rat neurofilament subunits (NF-H and NF-M) and demonstrate their existence in the normal nervous system of adult rats. *J. Neurosci*. 7:3474-3488, 1987.
111. Lehrich JR, Arnason BG, Hochberg FH. Demyelinative myelopathy in mice induced by the DA virus. *J. Neurol. Sci*. 29:149-160, 1976.
112. Leterrier JF, Käs J, Hartwig J, Vegners R, Janmey PA. Mechanical effects of neurofilament cross-bridges. Modulation by phosphorylation, lipids, and interactions with F-actin. *J. Biol. Chem*. 271:15687-15694, 1996.
113. Lewcock JW, Genoud N, Lettieri K, Pfaff SL. The ubiquitin ligase Phr1 regulates axon outgrowth through modulation of microtubule dynamics. *Neuron*. 56:604-620, 2007.
114. Li C, Tropak MB, Gerlai R, Clapoff S, Abramow-Newerly W, Trapp B, Peterson A, Roder J. Myelination in the absence of myelin-associated glycoprotein. *Nature*. 369:747-750, 1994.
115. Lipton HL, Dal Canto MC. Chronic neurologic disease in Theiler's virus infection of SJL/J mice. *J. Neurol. Sci*. 30:201-207, 1976.
116. Lipton HL, Dal Canto MC. The TO strains of Theiler's viruses cause "slow virus-like" infections in mice. *Ann. Neurol*. 6:25-28, 1979.
117. Lipton HL, Liang Z, Hertzler S, Son KN. A specific viral cause of multiple sclerosis: one virus, one disease. *Ann. Neurol*. 61:514-523, 2007.
118. Lipton HL, Kumar AS, Trottier M. Theiler's virus persistence in the central nervous system of mice is associated with continuous viral replication and a difference in outcome of infection of infiltrating macrophages versus oligodendrocytes. *Virus Res*. 111:214-223, 2005.
119. Lipton HL. Theiler's virus infection in mice: an unusual biphasic disease process leading to demyelination. *Infect. Immun*. 11:1147-1155, 1975.

120. Liu QA and Hengartner MO Candidate adaptor protein CED-6 promotes the engulfment of apoptotic cells in *C. elegans*. *Cell* 93:961–972, 1998.
121. Liu Y, Teige I, Birnir B, Issazadeh-Navikas S. Neuron-mediated generation of regulatory T cells from encephalitogenic T cells suppresses EAE. *Nat. Med.* 12:518-25, 2006.
122. Lipton HL, Calenoff M, Bandyopadhyay P, Miller SD, Dal Canto MC, Gerety S, Jensen K. The 5' noncoding sequences from a less virulent Theiler's virus dramatically attenuate GDVII neurovirulence. *J Virol.* 65:4370-4377, 1991.
123. Liu Y, Fallon L, Lashuel HA, Liu Z, Lansbury PT Jr. The UCH-L1 gene encodes two opposing enzymatic activities that affect alpha-synuclein degradation and Parkinson's disease susceptibility. *Cell.* 111:209-218, 2002.
124. Lunn ER, Perry VH, Brown MC, Rosen H, Gordon S. Absence of Wallerian Degeneration does not Hinder Regeneration in Peripheral Nerve. *Eur J Neurosci.* 1:27-33, 1989.
125. Luo L, O'Leary DD. Axon retraction and degeneration in development and disease. *Annu. Rev. Neurosci.* 28:127-156, 2005.
126. Luo M, He C, Toth KS, Zhang CX, Lipton HL. Three-dimensional structure of Theiler murine encephalomyelitis virus (BeAn strain). *Proc. Nat. Acad. Sci., USA.* 89: 2409-2413, 1992.
127. Lyon MF, Ogunkolade BW, Brown MC, Atherton DJ, Perry VH. A gene affecting Wallerian nerve degeneration maps distally on mouse chromosome 4. *Proc Natl Acad Sci U S A.* 90:9717-9720, 1993.
128. MacDonald JM, Beach MG, Porpiglia E, Sheehan AE, Watts RJ, Freeman MR. The *Drosophila* cell corpse engulfment receptor Draper mediates glial clearance of severed axons. *Neuron.* 50:869–881, 2006.
129. Mack CL, Vanderlugt-Castaneda CL, Neville KL, Miller SD. Microglia are activated to become competent antigen presenting and effector cells in the inflammatory environment of the Theiler's virus model of multiple sclerosis. *J. Neuroimmunol.* 144:68-79, 2003.
130. Mack TG, Reiner M, Beirowski B, Mi W, Emanuelli M, Wagner D, Thomson D, Gillingwater T, Court F, Conforti L, Fernando FS, Tarlton A, Andressen C, Addicks K, Magni G, Ribchester RR, Perry VH, Coleman MP. Wallerian degeneration of injured axons and synapses is delayed by a Ube4b/Nmnat chimeric gene. *Nat. Neurosci.* 4:1199-1206, 2001.

131. Martin N, Jaubert J, Gounon P, Salido E, Haase G, Szatanik M, Guénet JL. A missense mutation in *Tbce* causes progressive motor neuronopathy in mice. *Nat. Genet.* 32:443-447, 2002.
132. Martini R. The effect of myelinating Schwann cells on axons. *Muscle Nerve.* 24:456-466, 2001.
133. Masaki R, Saito T, Yamada K, Ohtani-Kaneko R. Accumulation of phosphorylated neurofilaments and increase in apoptosis-specific protein and phosphorylated c-Jun induced by proteasome inhibitors. *J. Neurosci. Res.* 62:75-83, 2000.
134. Mata M, Kupina N, Fink DJ. Phosphorylation-dependent neurofilament epitopes are reduced at the node of Ranvier. *J. Neurocytol.* 21:199-210, 1992.
135. Mi W, Beirowski B, Gillingwater TH, Adalbert R, Wagner D, Grumme D, Osaka H, Conforti L, Arnhold S, Addicks K, Wada K, Ribchester RR, Coleman MP. The slow Wallerian degeneration gene, *WldS*, inhibits axonal spheroid pathology in gracile axonal dystrophy mice. *Brain.* 128:405-416, 2005.
136. McDole J, Johnson AJ, Pirko I. The role of CD8+ T-cells in lesion formation and axonal dysfunction in multiple sclerosis. *Neurol. Res.* 28:256-261, 2006.
137. McGavern DB, Murray PD, Rivera-Quiñones C, Schmelzer JD, Low PA, Rodriguez M. Axonal loss results in spinal cord atrophy, electrophysiological abnormalities and neurological deficits following demyelination in a chronic inflammatory model of multiple sclerosis. *Brain.* 3:519-531, 2000.
138. McMahon EJ, Bailey SL, Castenada CV, Waldner H, Miller SD. Epitope spreading initiates in the CNS in two mouse models of multiple sclerosis. *Nat. Med.* 11:335-9, 2005.
139. Mohr E, Richter D. Axonal mRNAs: functional significance in vertebrates and invertebrates. *J. Neurocytol.* 29:783-791, 2000.
140. Molina-Holgado E, Areválo-Martín A, Vela JM, Guaza C. Theiler's virus encephalomyelitis infection as a model for multiple sclerosis: cytokines and pathogenic mechanisms. *Rev. Neurol.* 35:973-978, 2002.
141. Moran CM, Donnelly M, Ortiz D, Pant HC, Mandelkow EM, Shea TB. Cdk5 inhibits anterograde axonal transport of neurofilaments but not that of tau by inhibition of mitogen-activated protein kinase activity. *Brain Res. Mol. Brain Res.* 134:338-344. 2005.
142. Motil J, Chan WK, Dubey M, Chaudhury P, Pimenta A, Chylinski TM, Ortiz DT, Shea TB. Dynein mediates retrograde neurofilament transport within axons and

- anterograde delivery of NFs from perikarya into axons: regulation by multiple phosphorylation events. *Cell. Motil. Cytoskeleton*. 63:266-286, 2006.
143. Mukhopadhyay G, Doherty P, Walsh FS, Crocker PR, Filbin MT. A novel role for myelin-associated glycoprotein as an inhibitor of axonal regeneration. *Neuron*. 13:757-67, 1994.
144. Murray PD, McGavern DB, Lin X, Njenga MK, Leibowitz J, Pease LR, Rodriguez M. Perforin-dependent neurologic injury in a viral model of multiple sclerosis. *J. Neurosci*. 18:7306-7314, 1998.
145. Navone F, Niclas J, Hom-Booher N, Sparks L, Bernstein HD, McCaffrey G, Vale RD. Cloning and expression of a human kinesin heavy chain gene: interaction of the COOH-terminal domain with cytoplasmic microtubules in transfected CV-1 cells. *J. Cell. Biol*. 117:1263-1275, 1992.
146. Niclas J, Navone F, Hom-Booher N, Vale RD. Cloning and localization of a conventional kinesin motor expressed exclusively in neurons. *Neuron*. 12:1059-1072, 1994.
147. Neumann H. Molecular mechanisms of axonal damage in inflammatory central nervous system diseases. *Curr. Opin. Neurol*. 16:267-273, 2003.
148. Newcombe J, Gahan S, Cuzner ML, Connolly AM, Pestronk A, Trotter JL. Serum antibodies against central nervous system proteins in human demyelinating disease. *Clin. Exper. Immunol*. 59:383-390, 1985.
149. Nixon RA, Marotta CA. Degradation of neurofilament proteins by purified human brain cathepsin D. *J. Neurochem*. 43:507-516, 1984.
150. Nixon RA, Quackenbush R, Vitto A. Multiple calcium-activated neutral proteinases (CANP) in mouse retinal ganglion cell neurons: specificities for endogenous neuronal substrates and comparison to purified brain CANP. *J. Neurosci*. 6:1252-1263, 1986.
151. Nixon RA, Paskevich PA, Sihag RK, Thayer CY. Phosphorylation on carboxyl terminus domains of neurofilament proteins in retinal ganglion cell neurons in vivo: influences on regional neurofilament accumulation, interneurofilament spacing, and axon caliber. *J. Cell. Biol*. 126:1031-1046, 1994.
152. Obuchi M, Ohara Y. Theiler's murine encephalomyelitis virus (TMEV): the role of a small out-of-frame protein in viral persistence and demyelination. *Jpn. J. Infect. Dis*. 52:228-233, 1999.

153. Ohara Y, Stein S, Fu JL, Stillman L, Klamann L, Roos RP. Molecular cloning and sequence determination of DA strain of Theiler's murine encephalomyelitis viruses. *Virology*. 164:245-255, 1988.
154. O'Leary DD, Koester SE. Development of projection neuron types, axon pathways, and patterned connections of the mammalian cortex. *Neuron*. 10:991-1006, 1993.
155. Olitsky PK, Yager RH. Experimental disseminated encephalomyelitis in white mice. *J. Exp. Med.* 90:213-224, 1949.
156. Olson JK, Girvin AM, Miller SD. Direct activation of innate and antigen-presenting functions of microglia following infection with Theiler's virus. *J. Virol.* 75:9780-9789, 2001.
157. Osaka H, Wang YL, Takada K, Takizawa S, Setsuie R, Li H, Sato Y, Nishikawa K, Sun YJ, Sakurai M, Harada T, Hara Y, Kimura I, Chiba S, Namikawa K, Kiyama H, Noda M, Aoki S, Wada K. Ubiquitin carboxy-terminal hydrolase L1 binds to and stabilizes monoubiquitin in neuron. *Hum. Mol. Genet.* 12:1945-1958, 2003.
158. Paggi P and Lasek RJ. Degradation of purified neurofilament subunits by calcium-activated neutral protease: characterization of the cleavage products. *Neurochem. Int.* 6: 589-597, 1984.
159. Palma JP, Yauch RL, Lang S, Kim BS. Potential role of CD4+ T cell-mediated apoptosis of activated astrocytes in Theiler's virus-induced demyelination. *J. Immunol.* 162:6543-6451, 1999.
160. Palma JP, Kim BS. The scope and activation mechanisms of chemokine gene expression in primary astrocytes following infection with Theiler's virus. *J. Neuroimmunol.* 149:121-129, 2004.
161. Palma JP, Kwon D, Clipstone NA, Kim BS. Infection with Theiler's murine encephalomyelitis virus directly induces proinflammatory cytokines in primary astrocytes via NF-kappaB activation: potential role for the initiation of demyelinating disease. *J. Virol.* 77:6322-6331, 2003.
162. Perrot R, Berges R, Bocquet A, Eyer J. Review of the multiple aspects of neurofilament functions, and their possible contribution to neurodegeneration. *Mol. Neurobiol.* 38:27-65, 2008.
163. Peterson JW, Kidd GJ, Trapp BD. Axonal degeneration in MS: the histopathological evidence. In: S. Waxman, Editor, *Multiple Sclerosis as a Neuronal Disease*, Elsevier Academic Press, Amsterdam, 165–184, 2005.

164. Pevear DC, Borkowski J, Luo M, Lipton H. Sequence comparison of a highly virulent and a less virulent strain of Theiler's virus. Amino acid differences on a three-dimensional model identify the location of possible immunogenic sites. *Ann. N. Y. Acad. Sci.* 540:652-653, 1988.
165. Pevear DC, Calenoff M, Rozhon E, Lipton HL. Analysis of the complete nucleotide sequence of the picornavirus Theiler's murine encephalomyelitis virus indicates that it is closely related to cardioviruses. *J Virol.* 61:1507-1516, 1987.
166. Platten M, Ho PP, Youssef S, Fontoura P, Garren H, Hur EM, Gupta R, Lee LY, Kidd BA, Robinson WH, Sobel RA, Selley ML, Steinman L. Treatment of autoimmune neuroinflammation with a synthetic tryptophan metabolite. *Science.* 310:850-855, 2005.
167. Pope JG, Vanderlugt CL, Rahbe SM, Lipton HL, Miller SD. Characterization of and functional antigen presentation by central nervous system mononuclear cells from mice infected with Theiler's murine encephalomyelitis virus. *J. Virol.* 72:7762-7771, 1998.
168. Prineas J. The pathogenesis of dying-back polyneuropathies. II. An ultrastructural study of experimental acrylamide intoxication in the cat. *J. Neuropathol. Exp. Neurol.* 28:598-621, 1969.
169. Prinjha R, Moore SE, Vinson M, Blake S, Morrow R, Christie G, Michalovich D, Simmons DL, Walsh FS. Inhibitor of neurite outgrowth in humans. *Nature.* 403:383-384, 2000.
170. Pullen SS, Friesen PD. Early transcription of the ie-1 transregulator gene of *Autographa californica* nuclear polyhedrosis virus is regulated by DNA sequences within its 5' noncoding leader region. *J. Virol.* 69:156-165, 1995.
171. Raff MC, Whitmore AV, Finn JT. Axonal self-destruction and neurodegeneration. *Science.* 296:868-871, 2002.
172. Rahman A, Kamal A, Roberts EA, Goldstein LS. Defective kinesin heavy chain behavior in mouse kinesin light chain mutants. *J. Cell. Biol.* 146:1277-1288, 1999.
173. Ramon y Cajal, In: May RM editor. Degeneration and regeneration of the nervous system. London: Oxford University Press; 1928.
174. Redford EJ, Kapoor R, Smith KJ. Nitric oxide donors reversibly block axonal conduction: demyelinated axons are especially susceptible. *Brain.* 120 :2149-57, 1997.

175. Reid E, Kloos M, Ashley-Koch A, Hughes L, Bevan S, Svenson IK, Graham FL, Gaskell PC, Dearlove A, Pericak-Vance MA, Rubinsztein DC, Marchuk DA. A kinesin heavy chain (KIF5A) mutation in hereditary spastic paraplegia (SPG10). *Am. J. Hum. Genet.* 71:1189-1194, 2002.
176. Rodriguez M, Pierce ML, Howie EA. Immune response gene products (Ia antigens) on glial and endothelial cells in virus-induced demyelination. *J. Immunol.* 138:3438-42, 1987.
177. Rodriguez M, Leibowitz JL, Lampert PW. Persistent infection of oligodendrocytes in Theiler's virus-induced encephalomyelitis. *Ann. Neurol.* 13:426-433, 1983.
178. Roots BI. Neurofilament accumulation induced in synapses by leupeptin. *Science.* 221:971-972, 1983.
179. Roussarie JP, Ruffié C, Brahic M. The role of myelin in Theiler's virus persistence in the central nervous system. *PLoS. Pathog.* 3:23, 2007.
180. Roy S, Coffee P, Smith G, Liem RKH, Brady ST, Black MM. Neurofilaments are transported rapidly but intermittently in axons: implications for slow axonal transport. *J. Neurosci.* 20:6849–6861, 2000.
181. Rosenthal A, Fujinami RS, Lampert PW. Mechanism of Theiler's virus-induced demyelination in nude mice. *Lab. Invest.* 54:515-522, 1986.
182. Rozhon EJ, Lipton HL, Brown F. Characterization of Theiler's murine encephalomyelitis virus RNA. *J. Gen. Virol.* 61:157-165, 1982.
183. Rubens O, Logina I, Kravale I, Eglite M, Donaghy M. Peripheral neuropathy in chronic occupational inorganic lead exposure: a clinical and electrophysiological study. *J. Neurol. Neurosurg. Psychiatry.* 71:200-204, 2001.
184. Rubio N, Sanz-Rodriguez F. Induction of the CXCL1 (KC) chemokine in mouse astrocytes by infection with the murine encephalomyelitis virus of Theiler. *Virology.* 358:98-36108, 2007.
185. Rubio N, Sanz-Rodriguez F, Lipton HL. Theiler's virus induces the MIP-2 chemokine (CXCL2) in astrocytes from genetically susceptible but not from resistant mouse strains. *Cell. Immunol.* 239:31-40, 2006. Epub 2006 May 8.
186. Rubio N, Capa L. Differential IL-1 synthesis by astrocytes from Theiler's murine encephalomyelitis virus-susceptible and -resistant strains of mice. *Cell. Immunol.* 149:237-247, 1993.
187. Sagot Y, Dubois-Dauphin M, Tan SA, de Bilbao F, Aebischer P, Martinou JC, Kato AC. Bcl-2 overexpression prevents motoneuron cell body loss but not axonal

- degeneration in a mouse model of a neurodegenerative disease. *J. Neurosci.* 15:7727-7733, 1995.
188. Saigoh K, Wang YL, Suh JG, Yamanishi T, Sakai Y, Kiyosawa H, Harada T, Ichihara N, Wakana S, Kikuchi T, Wada K. Intragenic deletion in the gene encoding ubiquitin carboxy-terminal hydrolase in gad mice. *Nat. Genet.* 23:47-51, 1999.
189. Salinas S, Bilsland LG, Schiavo G. Molecular landmarks along the axonal route: axonal transport in health and disease. *Curr. Opin. Cell. Biol.* 20:445-453, 2008.
190. Samsam M, Mi W, Wessig C, Zielasek J, Toyka KV, Coleman MP, Martini R. The Wlds mutation delays robust loss of motor and sensory axons in a genetic model for myelin-related axonopathy. *J. Neurosci.* 23:2833-2839, 2003.
191. Sasaki Y, Araki T, Milbrandt J. Stimulation of nicotinamide adenine dinucleotide biosynthetic pathways delays axonal degeneration after axotomy. *J. Neurosci.* 26:8484-8491, 2006.
192. Sajadi A, Schneider BL, Aebischer P. Wlds-mediated protection of dopaminergic fibers in an animal model of Parkinson disease. *Curr. Biol.* 14:326-330, 2004.
193. Schlaepfer WW, Lee C, Lee VM, Zimmerman UJ. An immunoblot study of neurofilament degradation in situ and during calcium-activated proteolysis. *J. Neurochem.* 44:502-509, 1985.
194. Schlaepfer WW. Vincristine-induced axonal alterations in rat peripheral nerve. *J. Neuropathol. Exp. Neurol.* 30:488-505, 1971.
195. Seehusen F, Baumgärtner W. Axonal pathology and loss precede demyelination and accompany chronic lesions in a spontaneously occurring animal model of multiple sclerosis. *Brain Pathol.* Doi:10.1111/j.1750-3639.2009.0032.x
196. Selmaj KW, Raine CS. Tumor necrosis factor mediates myelin and oligodendrocyte damage in vitro. *Ann. Neurol.* 23:339-346, 1988.
197. Sethi P, Lipton HL. Location and distribution of virus antigen in the central nervous system of mice persistently infected with Theiler's virus. *Br. J. Exp. Pathol.* 64:57-65, 1983.
198. Shaw-Jackson C, Michiels T. Absence of internal ribosome entry site-mediated tissue specificity in the translation of a bicistronic transgene. *J. Virol.* 73:2729-2738, 1999.
199. Shetty KT, Kaech S, Link WT, Jaffe H, Flores CM, Wray S, Pant HC, Beushausen S. Molecular characterization of a neuronal-specific protein that stimulates the activity of Cdk5. *J. Neurochem.* 64:1988-1995, 1995.

200. Shi Y, Feng Y, Kang J, Liu C, Li Z, Li D, Cao W, Qiu J, Guo Z, Bi E, Zang L, Lu C, Zhang JZ, Pei G. Critical regulation of CD4⁺ T cell survival and autoimmunity by beta-arrestin 1. *Nat. Immunol.* 8:817-824, 2007.
201. Shimura H, Hattori N, Kubo S, Mizuno Y, Asakawa S, Minoshima S, Shimizu N, Iwai K, Chiba T, Tanaka K, Suzuki T. Familial Parkinson disease gene product, parkin, is a ubiquitin-protein ligase. *Nat. Genet.* 25:302-305, 2000.
202. Oh SJ. *Color Atlas of Nerve Biopsy Pathology*, CRC Press, 2002.
203. Silva A, Wang Q, Wang M, Ravula SK, Glass JD. Evidence for direct axonal toxicity in vincristine neuropathy. *J. Peripher. Nerv. Syst.* 11:211-216, 2006.
204. Simon JH, Jacobs LD, Campion MK, Rudick RA, Cookfair DL, Herndon RM, Richert JR, Salazar AM, Fischer JS, Goodkin DE, Simonian N, Lajaunie M, Miller DE, Wende K, Martens-Davidson A, Kinkel RP, Munschauer FE 3rd, Brownschidle CM. A longitudinal study of brain atrophy in relapsing multiple sclerosis. The Multiple Sclerosis Collaborative Research Group (MSCRG). *Neurology.* 53:139-148, 1999.
205. Singer M, Flinker D, Sidman RL. Nerve destruction by colchicine resulting in suppression of limb regeneration in adult triturus. *J.Exp.Zool.* 131, 267-300, 1956.
206. Sismans EA, van der Knaap MS, Bird TD, Shy ME, Kamholz JA, Griffiths IR. Patients lacking the major CNS myelin protein, proteolipid protein 1, develop length-dependent axonal degeneration in the absence of demyelination and inflammation. *Brain.* 125:551-561, 2002.
207. Smith KJ, Kapoor R, Hall SM, Davies M. Electrically active axons degenerate when exposed to nitric oxide. *Ann. Neurol.* 49:470-476, 2001.
208. Spelvin G. Axonal transport: function and mechanisms. In: S. Waxman, Editor, *The axon: structure, function and pathophysiology*. London: Oxford University Press Inc., 185, 1995.
209. Spencer PS, Schaumburg HH. *Experimental and clinical neurotoxicology*, chapter 7: Classification of neurotoxic disease: a morphological approach, 1980.
210. Spencer PS, Schaumburg HH. A review of acrylamide neurotoxicity. Part II. Experimental animal neurotoxicity and pathologic mechanisms. *Can. J. Neurol. Sci.* 1:152-169, 1974.
211. Spencer PS, Schaumburg HH. Ultrastructural studies of the dying-back process. III. The evolution of experimental peripheral giant axonal degeneration. *J. Neuropathol. Exp. Neurol.* 36:276-299, 1977.

212. Strack S, Westphal RS, Colbran RJ, Ebner FF, Wadzinski BE. Protein serine/threonine phosphatase 1 and 2A associate with and dephosphorylate neurofilaments. *Brain Res. Mol. Brain Res.* 49:15-28, 1997.
213. Stys PK, Waxman SG, Ransom BR. Ionic mechanisms of anoxic injury in mammalian CNS white matter: role of Na⁺ channels and Na(+)-Ca²⁺ exchanger. *Neurosci.* 12:430-439, 1992.
214. Sun D, Leung CL, Liem RK. Phosphorylation of the high molecular weight neurofilament protein (NF-H) by Cdk5 and p35. *J. Biol. Chem.* 271:14245-14251, 1996.
215. Susalka SJ, Pfister KK. Cytoplasmic dynein subunit heterogeneity: implications for axonal transport. *J. Neurocytol.* 29:819-829, 2000.
216. Suzuki H, Takeda M, Nakamura Y, Kato Y, Tada K, Hariguchi S, Nishimura T. Neurofilament degradation by bovine brain cathepsin D. *Neurosci. Lett.* 9:240-245, 1988.
217. Teunissen CE, Dijkstra C, Polman C. Biological markers in CSF and blood for axonal degeneration in multiple sclerosis. *Lancet Neurol.* 4:32-41, 2005.
218. Theiler, M. Spontaneous encephalomyelitis of mice—a new virus. *Science.* 80:122, 1934.
219. Tompkins SM, Fuller KG, Miller SD. Theiler's virus-mediated autoimmunity: local presentation of CNS antigens and epitope spreading. *Ann. N. Y. Acad. Sci.* 958:26-38, 2002.
220. Trapp BD, Peterson J, Ransohoff RM, Rudick R, Mörk S, Bö L. Axonal transection in the lesions of multiple sclerosis. *N. Engl. J. Med.* 338:278-285, 1998.
221. Trivedi N, Jung P, Brown A. Neurofilaments switch between distinct mobile and stationary states during their transport along axons. *J. Neurosci.* 27:507-516, 2007.
222. Trottier M, Kallio P, Wang W, Lipton HL. High numbers of viral RNA copies in the central nervous system of mice during persistent infection with Theiler's virus. *J Virol.* 75:7420-7428, 2001.
223. Tsai J, Grutzendler J, Duff K, Gan WB. Fibrillar amyloid deposition leads to local synaptic abnormalities and breakage of neuronal branches. *Nat. Neurosci.* 7:1181-1183, 2004.
224. Tsunoda I, Fujinami RS. Inside-Out versus Outside- In models for virus induced demyelination: axonal damage triggering demyelination. *Springer Semin. Immunopathol.* 24:105-25, 2002.

225. Tsunoda I. Axonal degeneration as a self-destructive defense mechanism against neurotropic virus infection. *Future Virol.* 3:579-593, 2008.
226. Tsunoda I, Tolley ND, Theil DJ, Whitton JL, Kobayashi H, Fujinami RS. Exacerbation of viral and autoimmune animal models for multiple sclerosis by bacterial DNA. *Brain Pathol.* 9:481-493, 1999.
227. Tsunoda I, Kuang LQ, Kobayashi-Warren M, Fujinami RS. Central nervous system pathology caused by autoreactive CD8⁺ T-cell clones following virus infection. *J. Virol.* 79:14640-14646, 2005.
228. Tsunoda I, Tanaka T, Saijoh Y, Fujinami RS. Targeting inflammatory demyelinating lesions to sites of Wallerian degeneration. *Am. J. Pathol.* 171:1563-1575, 2007.
229. Tsunoda I, Tanaka T, Terry EJ, Fujinami RS. Contrasting roles for axonal degeneration in an autoimmune versus viral model of multiple sclerosis: When can axonal injury be beneficial? *Am. J. Pathol.* 170:214-226, 2007.
230. Ulrich R, Seeliger F, Kreutzer M, Germann PG, Baumgärtner W. Limited remyelination in Theiler's murine encephalomyelitis due to insufficient oligodendroglial differentiation of nerve/glial antigen 2 (NG2)-positive putative oligodendroglial progenitor cells. *Neuropathol. Appl. Neurobiol.* 34:603-620, 2008.
231. Vale RD, Schnapp BJ, Mitchison T, Steuer E, Reese TS, Sheetz MP. Different axoplasmic proteins generate movement in opposite directions along microtubules in vitro. *Cell.* 43:623-632, 1985.
232. Vale RD. The molecular motor toolbox for intracellular transport. *Cell.* 112:467-480, 2003.
233. Vande Velde C, Garcia ML, Yin X, Trapp BD, Cleveland DW. The neuroprotective factor Wlds does not attenuate mutant SOD1-mediated motor neuron disease. *Neuromolecular Med.* 5:193-203, 2004.
234. van Eyll O, Michiels T. Non-AUG-initiated internal translation of the L* protein of Theiler's virus and importance of this protein for viral persistence. *Virol.* 76:10665-10673, 2002.
235. Veeranna, Shetty KT, Link WT, Jaffe H, Wang J, Pant HC. Neuronal cyclin-dependent kinase-5 phosphorylation sites in neurofilament protein (NF-H) are dephosphorylated by protein phosphatase 2A. *J. Neurochem.* 64:2681-2690, 1995.
236. Veeranna, Shetty KT, Takahashi M, Grant P, Pant HC. Cdk5 and MAPK are associated with complexes of cytoskeletal proteins in rat brain. *Brain Res. Mol. Brain Res.* 76:229-236, 2000.

237. Vickers JC, Morrison JH, Friedrich VL Jr, Elder GA, Perl DP, Katz RN, Lazzarini RA. Age-associated and cell-type-specific neurofibrillary pathology in transgenic mice expressing the human mid-sized neurofilament subunit. *J. Neurosci.* 14:5603-5612, 1994.
238. Vitto A, Nixon RA. Calcium-activated neutral proteinase of human brain: subunit structure and enzymatic properties of multiple molecular forms. *J. Neurochem.* 47:1039-1051, 1986.
239. Waller A. Experiments on the section of glossopharyngeal and hypoglossal nerves of the frog and observations of the alternatives produced thereby in the structure of their primitive fibers. *Phil. Trans. R. Soc. Lond.* 140, 423–429, 1850.
240. Wang J, Zhai Q, Chen Y, Lin E, Gu W, McBurney MW, He Z. A local mechanism mediates NAD-dependent protection of axon degeneration. *J. Cell Biol.* 170:349-355, 2005.
241. Wang L, Ho C-L, Sun D, Liem RKH, Brown A. Rapid movement of axonal neurofilaments interrupted by prolonged pauses. *Nat. Cell Biol.* 2:137–141, 2000.
242. Wang MS, Wu Y, Culver DG, Glass JD. Pathogenesis of axonal degeneration: parallels between Wallerian degeneration and vincristine neuropathy. *J. Neuropathol. Exp. Neurol.* 59:599-606, 2000.
243. Wang MS, Fang G, Culver DG, Davis AA, Rich MM, Glass JD. The WldS protein protects against axonal degeneration: a model of gene therapy for peripheral neuropathy. *Ann. Neurol.* 50:773-779, 2001.
244. Watanabe M, Tsukiyama T, Hatakeyama S. Protection of vincristine-induced neuropathy by WldS expression and the independence of the activity of Nmnat1. *Neurosci. Lett.* 411:228-232, 2007.
245. Watts RJ, Hoopfer ED, Luo L. Axon pruning during *Drosophila* metamorphosis: evidence for local degeneration and requirement of the ubiquitin-proteasome system. *Neuron.* 38:871-885, 2003.
246. Wilbrey AL, Haley JE, Wishart TM, Conforti L, Morreale G, Beirowski B, Babetto E, Adalbert R, Gillingwater TH, Smith T, Wyllie DJ, Ribchester RR, Coleman MP. VCP binding influences intracellular distribution of the slow Wallerian degeneration protein, Wld(S). *Mol. Cell. Neurosci.* 38:325-340, 2008.
247. Wilkinson KD, Lee KM, Deshpande S, Duerksen-Hughes P, Boss JM, Pohl J. The neuron-specific protein PGP 9.5 is a ubiquitin carboxyl-terminal hydrolase. *Science.* 246:670-673, 1989.

248. Williams A, Piaton G, Aigrot MS, Belhadi A, Théaudin M, Petermann F, Thomas JL, Zalc B, Lubetzki C. Semaphorin 3A and 3F: key players in myelin repair in multiple sclerosis? *Brain*. 130:2554-2565, 2007.
249. Wishart TM, Paterson JM, Short DM, Meredith S, Robertson KA, Sutherland C, Cousin MA, Dutia MB, Gillingwater H. Differential proteomics analysis of synaptic proteins identifies potential cellular targets and protein mediators of synaptic neuroprotection conferred by the slow Wallerian degeneration (Wld^S) gene. *Mol. Cell. Proteomics* 6:1318–1330, 2007.
250. Wishart TM, Pemberton HN, James SR, McCabe C, Gillingwater H. Modified cell cycle status in a mouse model of altered neuronal vulnerability (slow Wallerian degeneration; Wld^S). *Genome Biol.* 9, R101, 2008.
251. Woehlke G, Schliwa M. Walking on two heads: the many talents of kinesin. *Nat. Rev. Mol. Cell. Biol.* 1:50-58, 2000.
252. Wroblewska Z, Kim SU, Sheffield WD, Gilden DH. Growth of the WW strain of Theiler virus in mouse central nervous system organotypic culture. *Acta Neuropathol.* 47:13-19, 1979.
253. Xia CH, Roberts EA, Her LS, Liu X, Williams DS, Cleveland DW, Goldstein LS. Abnormal neurofilament transport caused by targeted disruption of neuronal kinesin heavy chain KIF5A. *J. Cell. Biol.* 161:55-66, 2003.
254. Xia CH, Rahman A, Yang Z, Goldstein LS. Chromosomal localization reveals three kinesin heavy chain genes in mouse. *Genomics.* 52:209-213, 1998.
255. Yabe JT, Chylinski T, Wang FS, Pimenta A, Kattar SD, Linsley MD, Chan WK, Shea TB. Neurofilaments consist of distinct populations that can be distinguished by C-terminal phosphorylation, bundling, and axonal transport rate in growing axonal neurites. *J. Neurosci.* 21:2195-2205, 2001.
256. Yabe JT, Pimenta A, Shea TB. Kinesin-mediated transport of neurofilament protein oligomers in growing axons. *J. Cell. Sci.* 112:3799–3814, 1999.
257. Yin X, Crawford TO, Griffin JW, Tu PH, Lee VM-Y, Li C, Roder J, Trapp BD. Myelin-associated glycoprotein is a myelin signal that modulates the caliber of myelinated axons. *J. Neurosci.* 18:1953–1962, 1998.
258. Zhai Q, Wang J, Kim A, Liu Q, Watts R, Hoopfer E, Mitchison T, Luo L, He Z. Involvement of the ubiquitin-proteasome system in the early stages of Wallerian degeneration. *Neuron*. 39:217-225, 2003.

259. Zhang Y, Da RR, Hilgenberg LG, Tourtellotte WW, Sobel RA, Smith MA, Olek M, Nagra R, Sudhir G, van den Noort S, Qin Y. Clonal expansion of IgA-positive plasma cells and axon-reactive antibodies in MS lesions. *J. Neuroimmunol.* 167:120-130, 2005.
260. Zheng L, Calenoff MA, Dal Canto MC. Astrocytes, not microglia, are the main cells responsible for viral persistence in Theiler's murine encephalomyelitis virus infection leading to demyelination. *J. Neuroimmunol.* 118:256-267, 2001.
261. Zhao C, Takita J, Tanaka Y, Setou M, Nakagawa T, Takeda S, Yang HW, Terada S, Nakata T, Takei Y, Saito M, Tsuji S, Hayashi Y, Hirokawa N. Charcot-Marie-Tooth disease type 2A caused by mutation in a microtubule motor KIF1Bbeta. *Cell.* 105:587-597, 2001.
262. Zhou L, Luo Y, Wu Y, Tsao J, Luo M. Sialylation of the host receptor may modulate entry of demyelinating persistent Theiler's virus. *J. Virol.* 74:1477-1485, 2000.
263. Zhou Z, Hartweg E, Horvitz HR. CED-1 is a transmembrane receptor that mediates cell corpse engulfment in *C. elegans*. *Cell.* 104:43–56, 2001.
264. Zhu Q, Lindenbaum M, Levavasseur F, Jacomy H, Julien JP. Disruption of the NF-H gene increases axonal microtubule content and velocity of neurofilament transport: relief of axonopathy resulting from the toxin beta,beta'-iminodipropionitrile. *J. Cell. Biol.* 143:183-193, 1998.
265. Charcot JM. Histologie de le sclerose. *Gazette Hopitance.*, 141:554-558, 1868.
266. Compston A, Coles A. Multiple sclerosis. *Lancet.* 372:1502-1517, 2008

Chapter 2: Limited remyelination in Theiler's murine encephalomyelitis due to insufficient oligodendroglial differentiation of nerve/glial antigen 2 (NG2)-positive putative oligodendroglial progenitor cells

R. Ulrich*, F. Seeliger†, M. Kreutzer*, P.G. Germann† and W. Baumgärtner*

* Department of Pathology, University of Veterinary Medicine Hannover, Bünteweg, Hannover

† Institute for Preclinical Safety, Nycomed AG, Haidkrugsweg, Barsbüttel, Germany

Abstract

Limited remyelination is a key feature of demyelinating Theiler's murine encephalomyelitis (TME). It is hypothesized that a dysregulation of differentiation of oligodendroglial progenitor cells (OPCs) represents the main cause of insufficient regeneration in this model of multiple sclerosis. TME virus (TMEV)-infected SJL/J mice were evaluated by footprint analysis, light and electron microscopy, immunohistology, confocal immunofluorescence and RT-qPCR at multiple time points ranging from 1 h to 196 days post infection (dpi). Footprint analysis revealed a significantly decreased stride length at 147 and 196 dpi. Demyelination progressively increased from 14 towards 196 dpi. A mild amount of remyelination was detected at 147 and 196 dpi. Early onset axonal injury was detected from 14 dpi on. TMEV RNA was detectable throughout the observation period and markedly increased between 7 and 28 dpi. Intralesional nerve/glia antigen 2 (NG2)-positive OPCs were temporarily increased between 28 and 98 dpi. Similarly, a transient upregulation of NG2 and platelet-derived growth factor α -receptor mRNA was noticed. In contrast, intralesional 2',3'-cyclic nucleotide 3'-phosphodiesterase (CNPase)-positive oligodendrocytes were decreased between 56 and 196 dpi. Although CNPase mRNA remained unchanged, myelin basic protein mRNA and especially its exon 2 containing splice variants were decreased. Glial fibrillary acidic protein (GFAP)-positive astrocytes and GFAP mRNA were increased in the late phase of TME. A mildly increased colocalization of both NG2/CNPase and NG2/GFAP was revealed at 196 dpi. Summarized, the present results indicated a dysregulation of OPC maturation as the main cause for the delayed and limited remyelination in TME. A shift of OPC differentiation from oligodendroglial towards astrocytic differentiation is postulated.

Published in: Neuropathology and Applied Neurobiology **34**:603-620, 2008

Available at: <http://onlinelibrary.wiley.com/doi/10.1111/j.1365-2990.2008.00956.x/abstract;jsessionid=BA563FCF261B677E06C3A06E90F8A45A.d03t01>

Chapter 3: Axonopathy due to axonal transport defects in a model of multiple sclerosis *

Running title: defects of axonal transport in a multiple sclerosis model

Dr. Mihaela Kreutzer,^{1,4} Dr. Frauke Seehusen,¹ Dr. Reiner Ulrich, PhD,^{1,4}
Dr. Robert Kreutzer, PhD,^{1,4} Kidsadagorn Pringproa, PhD,^{1,4} Maren Kummerfeld,¹ Dr. Peter
Claus,^{2,4} Dr. Ulrich Deschl,³ Dr. Arno Kalkul,³ Dr. Andreas Beineke,¹
Dr. Wolfgang Baumgärtner, PhD,^{1,4}

¹ Department of Pathology, University of Veterinary Medicine, Hannover, Germany

² Department of Neuroanatomy, Hannover Medical School, Germany

³ Boehringer Ingelheim Pharma GmbH&Co KG, Department of Non-Clinical Drug Safety,
Biberach (Riß), Germany

⁴ Centre for Systems Neuroscience, Hannover, Germany

Corresponding author:

Prof. Dr. W. Baumgärtner, Ph.D.

Department of Pathology

University of Veterinary Medicine Hannover

Bünteweg 17, D-30559, Hannover, Germany

wolfgang.baumgaertner@tiho-hannover.de

*** prepared for submission**

Abstract

Objective: Multiple sclerosis is a demyelinating inflammatory neurodegenerative disease characterized by myelin loss and prominent axonal pathology. Though factors triggering axonopathy in multiple sclerosis are unknown, new lines of evidence suggest a prominent role of a disturbed neurofilament homeostasis as a cause for their aggregation. In the present study, molecular processes involved in axonal accumulation of non-phosphorylated neurofilament in Theiler's murine encephalomyelitis (TME), a viral murine model of multiple sclerosis, were analyzed in detail.

Methods: *In vivo* and *in vitro* experiments were done in SJL/J mice and differentiated neuroblastoma N1E-115 cells, respectively, following infection with Theiler's murine encephalomyelitis virus (TMEV). Findings were analyzed by using microarray analysis, histochemistry, immunohistochemistry, immunofluorescence, as well as electron and laser confocal microscopy.

Results: The massive accumulation of non-phosphorylated neurofilaments observed in TME showed a temporal development due to sequential impairments of the bidirectional axonal traffic consisting of the down-regulation of kinesin family member 5A, dynein cytoplasmic heavy chain 1, tau-1 and β -tubulin III expression. In addition, alterations of the neuronal protein metabolism, including down-regulation of ubiquitin-protein conjugates and ubiquitin carboxy-terminal hydrolase L1, causing diminished degradation of non-phosphorylated neurofilament, was noticed.

Interpretation: Data indicate that neurofilament accumulation in TME seems to be the result of specific dysregulations in their axonal transport and also the sequel of non-specific impairments in the neuronal protein metabolism. Findings allow a more precise understanding of the various complex interactions responsible for initiation and development of axonopathies and provide new insights into their pathogenesis and may facilitate the design of new therapy concepts.

Introduction:

Multiple sclerosis (MS) is an inflammatory neurodegenerative disease of the human central nervous system. Its precise etiology is unknown, but most likely MS occurs as a result of a combination of genetic factors such as those responsible for autoimmune conditions and environmental factors like infectious and non-infectious pathogens. The majority of MS patients show a biphasic form of the disease with a relapsing-remitting (RRMS) phase followed by a secondary progressive state (SPMS). Clinic and MRI data suggest that inflammation and the formation of new white matter lesions are the substrate for RRMS, while new inflammatory demyelinating lesions are rare and have a more diffuse distribution in the progressive phase. Until now, the drastic neurological decline observed in MS patients remains irreversible. Animal models simulating immunologic and/or infectious features of MS are powerful tools to investigate the pathogenesis of the disease. Theiler's murine encephalomyelitis virus (TMEV)-induced demyelination (TME) represents a well-characterized and highly suitable virus model for MS with clinical features similar to the progressive forms of MS. Both, the animal model and the human disease, share characteristic pathogenetic and mechanistic features like demyelination, inflammation and axonal injury.^{2,3} Despite decades of intensive research, it is still unknown whether MS and TME pathology follows the model of primary or secondary demyelination. In the primary model, the demyelination caused by myelino- and/or oligodendroglial pathologies is considered to be the primary lesion which predisposes to the secondary lesion, namely the axonal injury. In the secondary scenario, the neuroaxonal damages acts as trigger for the extensive demyelination. In MS and TME it seems both events contribute substantially to disease development and progression.³⁻⁵ Similar mechanisms have been described in other naturally occurring animal models of multiple sclerosis like canine distemper virus.⁶ Either primary or secondary, axonal damages are responsible for the irreversible clinical outcome in MS.

Investigations regarding the axonal pathology were promoted by the identification of amyloid precursor protein (APP) and non-phosphorylated neurofilaments (n-NFs) as early markers for axonal damages.^{7,8} Though these markers allow a precise detection of axonal damage in MS and TME lesions^{3-5,9,10} the molecular mechanisms of APP and n-NF accumulation as well as their role during disease initiation and progression remain to be determined. Under physiological conditions, NFs are synthesized in the neuronal cell body as non-phosphorylated proteins, then they undergo a complex pattern of phosphorylation along the axon forming phosphorylated neurofilaments (p-NFs).¹¹ Phosphorylation and

dephosphorylation of NFs is primarily regulated by the p35 activated cyclin-dependent kinase 5 (Cdk5)¹² and protein phosphatase 2A (Ppp2r2a, Ppp2r2c)¹³ and their activity correlates with the NF dynamics¹⁴. Along the axon, NFs are moved on the microtubular polymers, formed by monomeric α and β - tubulins, in the anterograde direction after association with the kinesin family member 5A (Kif5A)¹⁵ or in the retrograde orientation by coupling with dynein heavy chain (Dync1h1)¹⁶. Microtubule-microtubule (MT) and MT-motor proteins interactions are controlled by Tau-1 protein.^{17,18} Once arrived at the axonal terminus, NFs are degraded either by protease digestion¹⁹ and/or by the ubiquitin-proteasome system.²⁰ In conclusion, NF expression may be modulated at multiple levels and abnormalities in any of these steps could cause NFs accumulation, a feature of many neurodegenerative diseases including MS and TME.

In the present study, different processes which could be responsible for the axonal accumulation of n-NF were investigated *in vivo* and *in vitro* to substantiate the hypothesis that the initiation and development of TMEV-induced axonopathy are based on an impaired axonal transport of NFs. Thus, abnormalities in the NF axonal transport were analyzed by monitoring the expression of cytoskeleton proteins such as β -tubulin III and α -acetylated tubulin as well as cytoskeleton-associated proteins including Tau-1, Kif5A and Dync1h1. Possible deficiencies in NF dephosphorylation followed by the expression of Pp2ac and Pp2aa, subunits of Pp2a, and pathological modifications of the protein degradation pathway of the ubiquitin-protein conjugates and ubiquitin carboxy-terminal hydrolase L1 expression (Uchl-1) were investigated at the transcriptional and translational level.

Materials and Methods

In vivo and in vitro study design

Animal experiments were done as described before.¹⁰ Five-week-old female SJL/JHanHsd mice were purchased from Harlan Winkelmann (Borchen, Germany) and were inoculated under general anaesthesia into the right cerebral hemisphere with 1.63×10^6 plaque-forming units/mouse of BeAn strain of TMEV in 20 μ l Dulbecco's Modified Eagle Medium (PAA Laboratories, Cölbe, Germany) with 2% foetal calf serum and 50 μ g/ml gentamycin. Mock-infected mice received 20 μ l of the diluent only. Placebo and infected groups were killed after 0, 4, 7, 14, 28, 42, 98 and 196 days. Each group consisted of 6 animals. At necropsy, the thoracic segment of the spinal cords was removed from each animal. Subsequently, tissues were fixed in 10% formalin, decalcified in 25% EDTA for 48h and then embedded in paraffin.

For differentiation into neurons, N1E-115 murine neuroblastoma cells (ATCC, CRL-2263) were maintained 14 days in DMEM with 2% FCS. Then, cells were incubated for 1h at a multiplicity of infection of 10 with the BeAn strain of TMEV²¹ and analyzed by immunofluorescence at 1, 3 and 7 days post-infection.

Histochemistry, immunohistochemistry, immunofluorescence, electron and laser confocal microscopy and statistical analysis

To identify demyelination, formalin-fixed, paraffin-embedded thoracic spinal cord sections were stained with Luxol fast blue cresyl-echt violet (LFB).¹⁰ Identification of normal and pathological axonal structures was done by using a modified Bielschowsky silver stain.²² Immunohistochemistry was performed as described previously^{7,10,23} using the primary antibodies mentioned in Table 1. The 2-3 μ m thick paraffin-embedded sections were baked in an oven at 50°C for 30 min. Then, sections were deparaffinized and rehydrated using graded alcohols. The endogenous peroxidase was quenched in 0.5% H₂O₂ prepared in methanol. Antigen retrieval was done by incubation in citrate buffer for 25 min at 800W or 0.25% Triton-X in phosphate buffered saline (PBS) for 15 min at room temperature (RT). To block non-specific binding sites, sections were incubated with normal goat serum for 20 min at RT and then overnight with the primary antibodies (Table 1) at 4°C. For negative controls, the primary antibody was substituted by either rabbit serum or ascites from non-immunized BALB/cJ mice. Subsequently after washing in PBS, sections were incubated with either biotinylated goat anti-mouse or anti-rabbit serum, respectively (Vector Laboratories, Burlingame, CA, USA). Positive antigen-antibody reactions were visualized by incubation with 3,3'-diaminobenzidine-tetrahydrochloride (DAB)- H₂O₂ in 0.1 M imidazole, pH 7.08 for 10 min followed by slight counterstaining with Papanicolaou's hematoxylin. The obtained brown signal was evaluated quantitatively by counting the number of positive axons (number of immunoreactive axons/mm²) in the white matter. The percentage of p-NF and Bielschowsky's silver stain-positive thoracic axons in the ventro-lateral white matter area was evaluated by digitalizing the spinal cord section with a color video camera (Color View II, 3.3 Megapixel CCD; Soft Imaging System, Münster, Germany) mounted on an Axiophot microscope (Zeiss, Oberkochen, Germany) with a 5 \times objective. The positive structures were measured interactively after manually outlining the total white matter area using the analysis 3.1 software package (Soft Imaging System). Data are presented as percentage of labeled axonal profiles in relation to the total white matter area.

Table 1. Antibodies used for immunohistochemistry and immunofluorescence.

Nr	Antibody	Supplier	Catalog number	Source	Dilution		Pre- treatment for IHC
					IHC*	IF**	
1.	Non-phosphorylated neurofilament (n-NF)	Sternberger Monoclonals	SMI311	mouse	1:8000	1:1000	boiled in citrate buffer in the microwave
2.	Phosphorylated neurofilament (p-NF)	Sternberger Monoclonals	SMI312	mouse	1:8000	1:1000	Triton X 0,25% in PBS***
3.	Amyloid precursor protein (APP)	Chemicon	MAB348	mouse	1:2000	n.d.	boiled in citrate buffer in the microwave
4.	Protein phosphatase 2 subunit C (Ppp2r2c)	Cell Signaling Technology	2038	rabbit	1:50	n.d.	boiled in citrate buffer in the microwave
5.	Protein phosphatase 2 subunit A (Ppp2r2a)	Cell Signaling Technology	2041	rabbit	1:50	n.d.	boiled in citrate buffer in the microwave
6.	Kinesin heavy chain isoform 5A (Kif5A)	Sigma Aldrich	MAB161 4	mouse	1:100	1:60	boiled in citrate buffer in the microwave
7.	Dynein heavy chain (Dync1h1)	Santa Cruz Biotechnology	sc-9115	rabbit	1:10	1:10	boiled in citrate buffer in the microwave
8.	β-tubulin III	Sigma Aldrich	T8660	mouse	1:5000	1:2500	boiled in citrate buffer in the microwave
9.	α-acetylated tubulin	Sigma Aldrich	T6793	mouse	1:1000	n.d.	Triton 0,25% in PBS***
10.	Tau-1	Chemicon	MAB 3420	mouse	1:2000	1:200	boiled in citrate buffer in the microwave
11.	Ubiquitin	Chemicon	AB1690	rabbit	1:1000	1:200	boiled in citrate buffer in the microwave
12.	Ubiquitin C-terminal hydrolase (Uchl-1)	Chemicon	AB1761	rabbit	1:1000	n.a.	boiled in citrate buffer in the microwave
13.	VP1- BeAn-TMEV	****	n.a.	rabbit	1:2000	1:200	n.d.

* IHC= immunohistochemistry; ** IF= immunofluorescence; *** PBS= phosphate-buffered saline; ****

Kummerfeld et al., 2009; n.a.= not applicable; n.d.= not done.

For immunostaining, N1E-115 cells were washed with PBS and then fixed with 4% paraformaldehyde for 30 min at RT. After an additional washing step with PBS, cells were permeabilized with 0.25% Triton-X (Sigma-Aldrich, Taufkirchen, Germany) in PBS (PBST) for 15 min. To block unspecific binding sites, cells were kept in 1% bovine serum albumin (BSA) diluted in PBST for 30 min. The cells were then incubated overnight at 4°C with the primary antibody diluted in PBST (Table 1).

After 10 min washing in PBST, cells were incubated for 1h with Cy2/Cy3 conjugated AffiniPure goat anti-rabbit/anti-mouse (Jackson- Immuno Research Laboratoires) diluted 1:200 in PBST. Then, cells were washed with and kept in PBS until embedded with Fluorescent mounting medium® (Dako Deutschland GmbH, Hamburg, Germany).

Data obtained by the Luxol fast blue cresyl-echt violet stain, Bielschowsky silver stain and immunohistochemistry were subjected to statistical analysis using the program “SPSS” for Windows, version 13.0 employing the Wilcoxon test as group-wise test. A *P* value of less than 0.05 was considered to be statistically significant. The correlation coefficient to compare p-NF and n-NF immunohistochemistry was calculated by using the non-parametric Spearman’s correlation test ($1 \geq \rho \geq -1$).

Electron microscopy was performed as described previously.¹⁰ Groups of six TMEV-infected and control mice were killed at 14, 42, 98, and 196 dpi and spinal cords were immersed in 5% glutaraldehyde/cacodylate buffer and subsequently in 1% osmium tetroxide. Then, sections were dehydrated and embedded in epoxy resin. Ultrathin sections (70nm) were stained with uranyl acetate and lead citrate and then analyzed by a Zeiss electron microscope EM 10 C (Zeiss, Oberkochen, Germany).

Confocal laser microscopy was performed as described previously²⁴ using the primary antibodies mentioned in Table 1. The labelled cells were imaged with an inverted microscope Leica DM IRE2 (Leica, Wetzlar, Germany) using an UV 405 (bis-benzimide), Ar-Ion (Cy2) 488 and HeNe 543 (Cy3) nm lasers.

Microarray analysis of transcriptional changes

RNA was isolated from frozen spinal cord specimens using the RNeasy Mini Kit (Qiagen, Hilden, Germany). Six biological replicates were used per group and time point, except for 5 TMEV-infected mice at 98 dpi. 250 ng total RNA of each sample was amplified and labeled with the MessageAmp II-Biotin Enhanced Kit (Ambion, Austin, TX) and hybridized to Affymetrix mouse genome 430 2.0 arrays (Affymetrix, Santa Clara, CA). MIME compliant data sets were obtained as described before²⁵ and are published in the ArrayExpress database (<http://www.ebi.ac.uk/microarray-as/ae/>). The probe sets corresponding to the axon-transport-

related proteins that were investigated in more detail by immunohistochemistry in the present study such as n-NF, p-NF, APP, Kif5A, Dync1h1, α -acetylated tubulin, β -tubulin III, Tau-1, Pp2ac and Pp2aa, ubiquitin-protein conjugates and Uchl-1, were manually extracted employing NetAffyx and are presented in Supplementary Table.

Results

TMEV-infected mice

Viral immunoreactivity and myelin loss

Virus immunoreactivity was detected in the spinal cord at 14 dpi in infected mice. The number of infected cells, predominantly glial cells and macrophages increased until 28dpi followed by a decline till 196dpi. TMEV-positive axons were infrequently found (Fig 1).

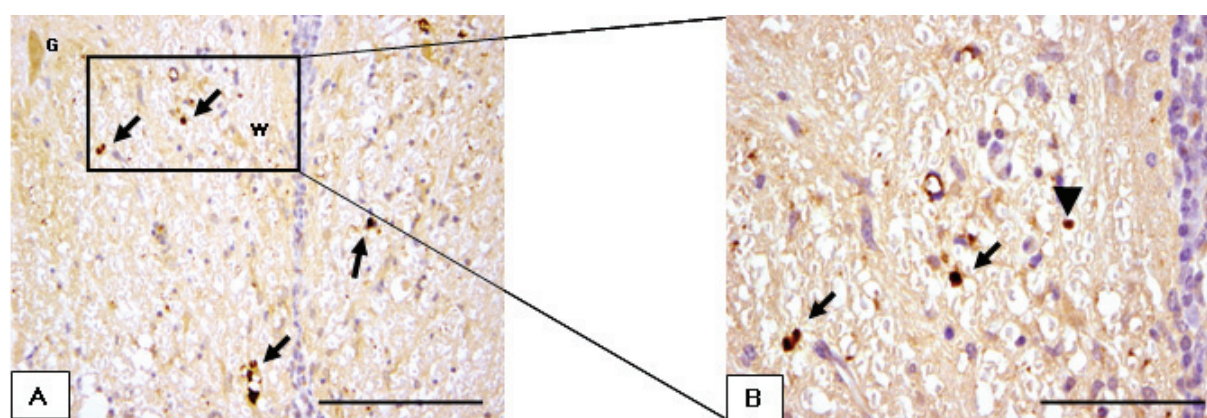


Figure 1. Theiler's murine encephalomyelitis virus spread in the spinal cord.

Figure 1A illustrates the distribution of TMEV-positive cells in the ventro-medial spinal cord at 28dpi. TMEV was found predominantly in microglia/macrophages (arrows). Scale bar = 200µm. Figure 1B is an inset of 1A which shows TMEV-positive microglia/macrophages cells (arrows) and a positive axon (arrowhead). Scale bar = 50µm. G=grey matter, W=white matter

First features of demyelination using the LFB stain were observed at 42dpi and loss of myelin continuously increased until 196 dpi and was most prominent in the ventro-medial and lateral spinal cord columns while dorsal columns were relatively spared (Fig 2).

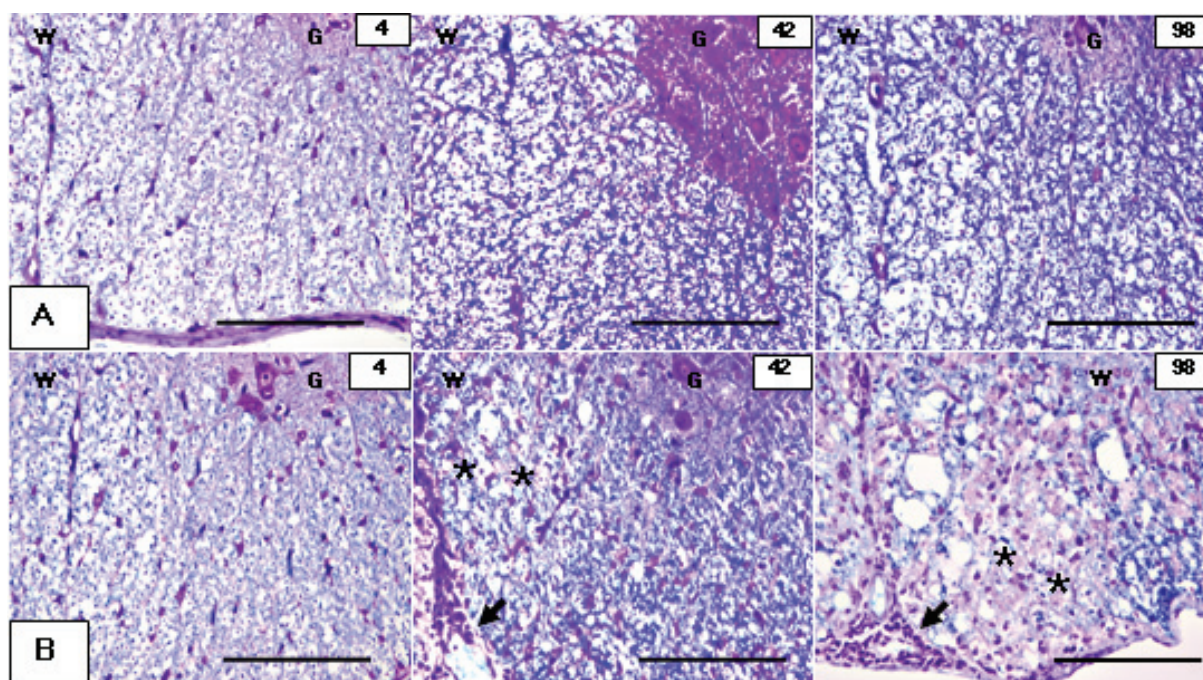


Figure 2. TMEV-induced demyelination.

Rows A and B illustrate the Luxol fast blue cresyl-echt violet stained ventro-medial spinal cord of control (A) and TMEV-infected mice (B) at 4, 42 and 98dpi. At 4dpi, the spinal cord of control and infected mice showed an uniformly Luxol fast blue stained white matter. At 42dpi, lymphohistiocytic (arrow) and mild demyelination of the white matter (asterisks) were present. At 98dpi, a diffuse parenchymal inflammatory reaction and lymphohistiocytic meningitis (arrows) and an increased area of demyelination can be observed (asterisks). Scale bar = 100 μ m. G=grey matter, W=white matter.

For a more detailed characterization of the demyelinating process electron microscopy was performed. In controls (Fig 3A), nerve fibers, enwrapped by myelin sheaths of various calibers were observed as expected. The earliest demyelinating changes in the spinal cord of infected mice were observed at 14dpi and were characterized by separation of the individual lamellae at the intraperiod line, formation of fluid-filled intramyelinic spaces and vesicles, and marked distention of the myelin sheaths (Fig 3B).

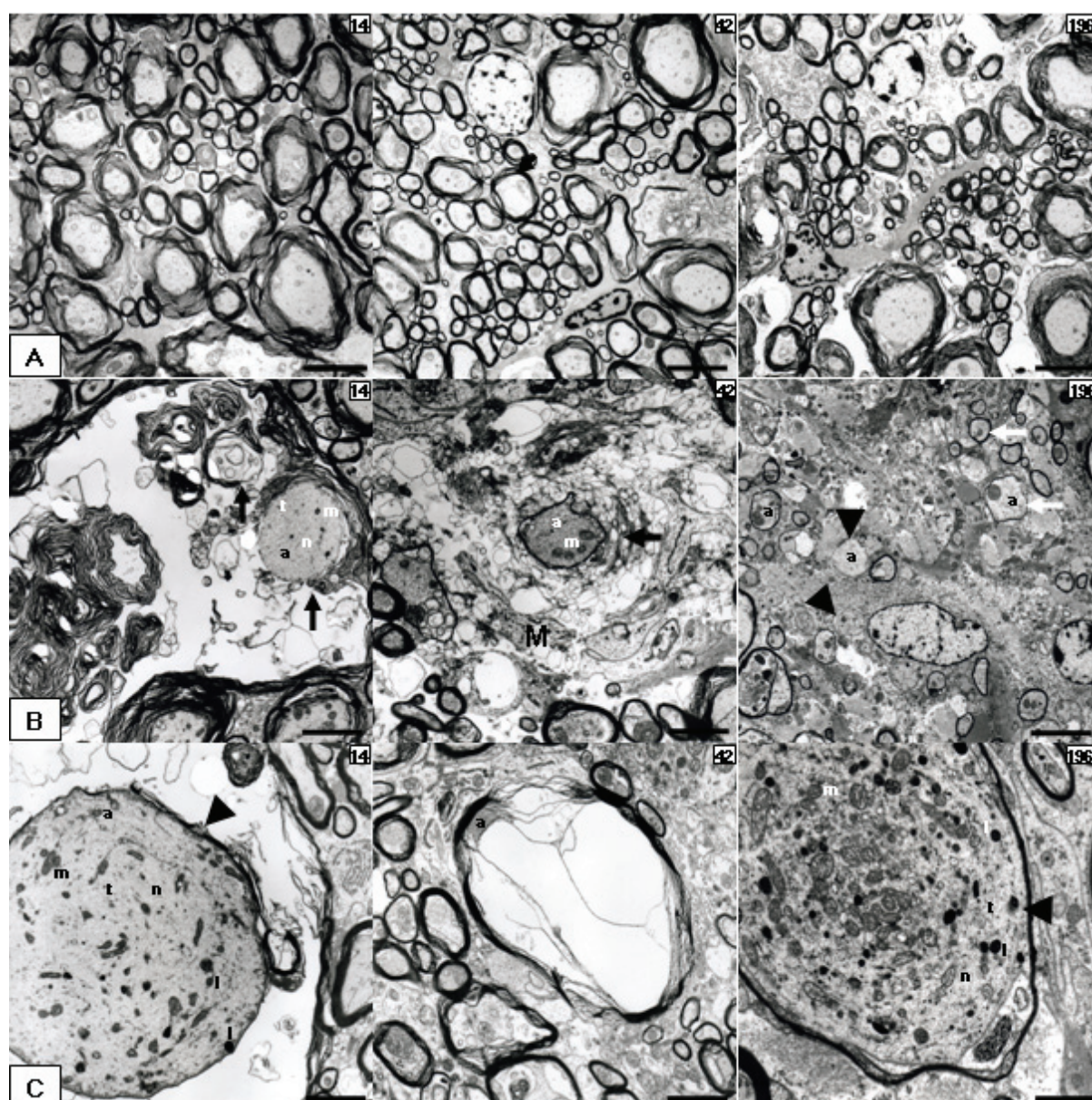


Figure 3. Electron microscopy features in TME.

Rows A, B and C illustrate electron micrographs obtained from spinal cords of placebo (A) and TMEV-infected mice (B, C) at 14, 42 and 98dpi. Row B shows specific features of myelin pathology including vesicular myelin degeneration (black arrows, 14 and 42dpi), naked axons (arrowheads, 196dpi) and remyelination (white arrows, 196dpi). Row C represents particularities of axonal pathology like distended axons (arrowheads) with accumulation of microtubule, neurofilaments and vesiculo-tubular structures containing mitochondria and lysosomes (14 and 196dpi) or compressed axon by myelin-sheath edema (42dpi); a=axon. t=microtubules, n=neurofilaments, m=mitochondria, l=lysosomes, M= microglia/macrophage cytoplasm. Row A and B196 scale bar = 4 μ m; B14, B42, C14 and C42 scale bar = 2 μ m; C196 scale bar = 1 μ m.

At 42dpi, morphologically altered myelin sheaths mostly displayed an invasion of their separated lamellae by interposed cellular processes containing a lysosome-rich cytoplasm, interpreted to be of macrophage/microglial origin. Furthermore, completely demyelinated axons surrounded by macrophage/microglia and Gitter cells with abundant whirls of lamellar and/or amorphous electron-dense debris in membrane-bound cytoplasmic vesicles as well as reactive microglial processes were detected between 42 and 196dpi. Notably, at 196dpi, axons surrounded by relatively thin myelin sheaths, interpreted as remyelination were present within the lesions.

Axonal pathology during TME progression

The Bielschowsky silver stain revealed normally stained nerve fibers characterized by an uniform distribution and similar caliber size in placebos (Fig 4A).

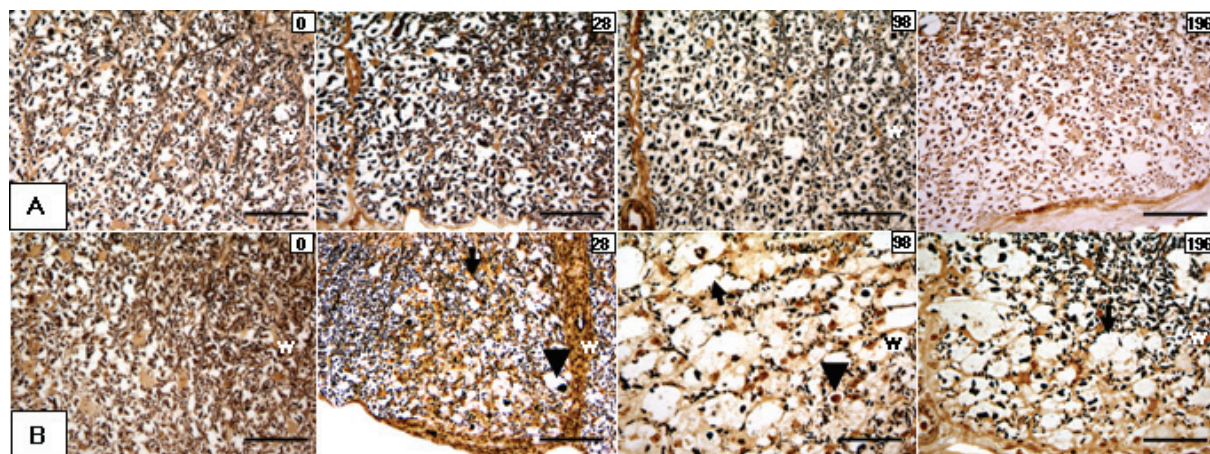


Figure 4. Axonal loss in TME.

Rows A and B illustrate results of Bielschowsky silver stain in the ventro-medial spinal cord of control (A) and TMEV-infected mice (B) at 0, 28, 98 and 196dpi. At 0dpi, normal staining of axons in the spinal cord of the control and TMEV- infected mice was seen. From 28 until 196dpi extensive pathology of the nerve fibers characterized by variation of axonal thickness, loss of axons (arrows) and presence of spheroids (arrowheads) was observed in TMEV-infected mice compared to controls. Scale bar= 100µm. W=white matter

In infected mice, a significant axonal loss and occurrence of swollen axons termed spheroids were observed between 28 and 196 dpi (Fig 4B and 5A).

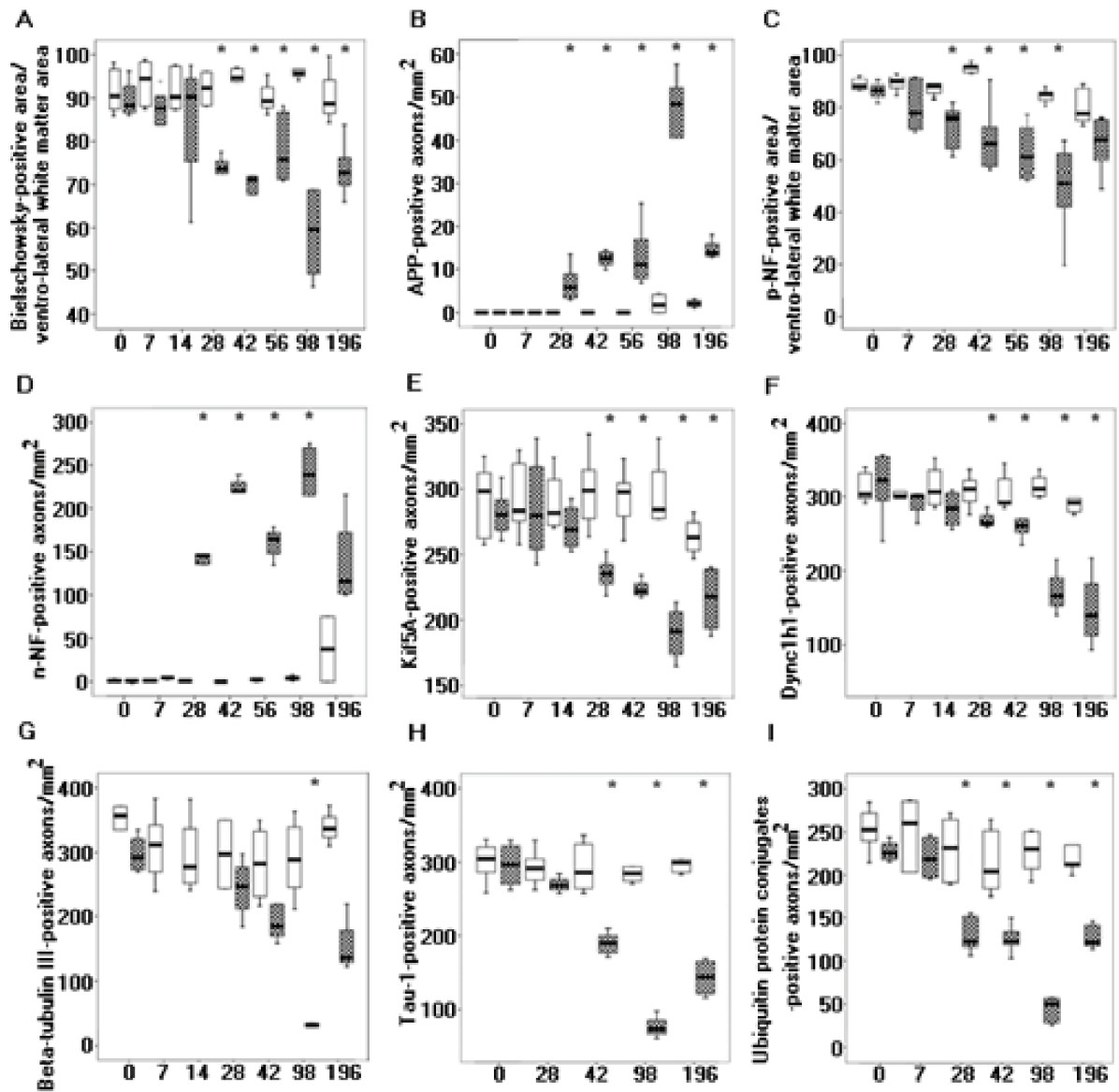


Figure 5. Kinetic of axonal pathology in TME.

The box and whisker plots illustrate, in a time-dependent manner, the loss of nerve fibers as detected by the Bielschowsky silver stain (A) and changed immunoreactivity of APP(B), p-NF (C), n-NF (D), Kif5A (E), Dync1h1 (F), β -tubulin III (G), Tau-1 (H) and ubiquitin-ligated proteins (I) following TMEV infection. Statistical significant differences ($p \leq 0.05$) were marked with asterisks (*). White box plots= controls; grey box plots=infected animals.

To better characterize the axonal pathology, electron microscopy was performed. A small amount of membranous organelles including few mitochondria and uniformly distributed axonal microtubules and neurofilaments were observed within the axoplasm of control animals (Fig 3A). In infected mice, axonal pathology was noticed between 14 and 196dpi (Fig 3C arrowheads). Altered axons were distended and filled with an accumulation of

microtubules, neurofilaments and vesiculotubular structures containing multiple mitochondria and lysosome-like dense-cored vesicles. A similar axonal pathology was observed in myelinated as well as demyelinated axons.

To identify axonal loss and subtle axonal changes the expression of APP, p-NF and n-NF was investigated. APP expression was confined to few glial cells in the white matter and to neuronal cell bodies in the gray matter in placebos (Fig 6A). In contrast, APP immunopositive axons were observed in the ventro-medial and lateral columns between 28 and 196dpi in TMEV infected mice in addition (Fig 6B).

p-NF expression was limited to axons and not found in neuronal perikarya in controls (Fig 6C). In infected mice, loss of p-NF expression of axons became evident at 14dpi. A statistical significant decrease beginning at 28dpi was observed (Fig 5C and 6D). In addition, few p-NF-positive spheroids were detected between 28 and 98dpi (Fig 6D).

n-NF expression characterized by positive neuronal perikarya and negative axons in controls was complementary to the p-NF immunoreactivity (Fig 6E). The first n-NF axonal accumulations were observed at 14dpi in TME mice. Thereafter, axonal expression of n-NF increased significantly and reached its maximum at 98dpi (Fig 5D and 6F). n-NF positive axons were often enlarged and contained densely accumulated NFs. Evaluation of the correlation coefficient showed a highly negative association between p-NF and n-NF (Spearman rank correlation $\rho = -0.824$, $p < 0.01$).

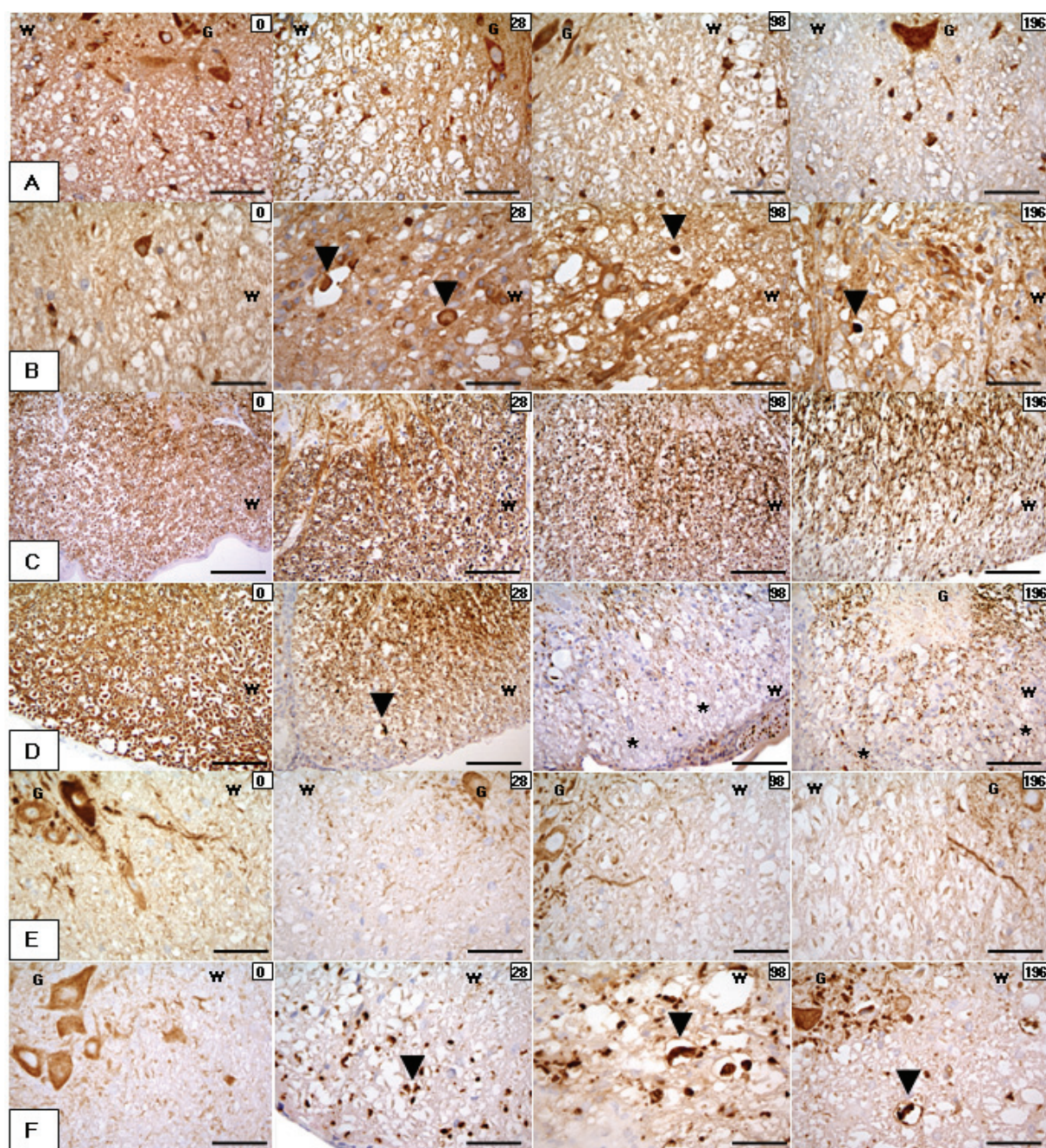


Figure 6. *APP, phosphorylated NF (p-NF), non-phosphorylated NF (n-NF) expression in TME.*

The rows illustrate APP (A, B), p-NF (C, D), n-NF (E, F) immunoreactivity in the ventro-medial spinal cord of controls (A, C, E) and TMEV-infected mice (B, D, F) at 0, 28, 98 and 196dpi. (A, B) At 0dpi, control and infected mice showed a similar pattern of APP expression in glial cells of the white matter and neurons of the grey matter. From 28 until 196dpi, APP-positive spheroids were observed in TMEV-infected mice (arrowheads). (C, D) At 0dpi, control and infected mice showed a similar pattern of p-NF expression with p-NF-positive axons in the white matter and p-NF-negative neurons in the grey matter. Between 28 and 196dpi a decreased p-NF expression was observed in TME. A p-NF-positive spheroid is marked with arrowhead and severe axonal loss with asterisks). (E, F) At 0dpi, control and infected mice showed the same pattern of n-NF expression with n-NF-negative axons in the white matter and n-NF-positive neurons in the grey matter. n-NF axonal expression, marked with an arrowhead, appeared at 28 until 196dpi in TMEV-infected mice only. Scale bar = 100µm. G=grey matter, W=white matter.

Transcriptional changes of axon-transport related genes

To identify possible candidate genes and to outline possible pathways causing abnormal axonal expression of p-NF and n-NF in TME mice, microarray experiments were performed. As described in detail recently, a total of 1210 probe sets were identified to be differentially expressed in the spinal cord over the study period at a false discovery rate of 1.0% in TMEV infected animals.²⁵ Furthermore, a machine learning approach of microarray data analysis revealed a group of genes functionally related to neurite morphogenesis and associated to demyelination in TME, providing evidence for an association between axonal changes and demyelination. In the present investigation, the expression data of 111 probe sets (Supplementary Table), identified on the Affymetrix mouse genome 430 2.0 array were further analyzed. Out of these 111 probe sets only 12 probe sets were differentially expressed in the spinal cord over the study period at a false discovery rate of 5.0% (Table 2).

Table 2. List of axon-related differentially expressed genes.

Probe Set ID	Gene Symbol	Gene Title	q-value	Fold change			
				14dpi	42dpi	98dpi	196dpi
1427442_a_at	App	amyloid beta (A4) precursor protein	0,015	1,056	-1,008	-1,029	-1,039
1429063_s_at	Kif16b	kinesin family member 16B	0,043	-1,191	1,040	1,083	1,102
1454107_a_at	Kif2a	kinesin family member 2A	0,041	1,200	1,185	-1,160	-1,473
1448946_at	Kif3c	kinesin family member 3C	0,006	1,063	-1,053	-1,070	-1,099
1434670_at	Kif5a	kinesin family member 5A	0,015	1,016	-1,101	-1,192	-1,178
1429715_at	Ppp2r2a	protein phosphatase 2 (formerly 2A), regulatory subunit B (PR 52), alpha isoform	0,017	1,039	-1,074	-1,214	-1,081
1438671_at	Ppp2r2c	protein phosphatase 2 (formerly 2A), regulatory subunit B (PR 52), gamma isoform	0,011	1,046	-1,118	-1,200	-1,230
1418884_x_at	Tuba1	tubulin, alpha 1	0,019	-1,047	-1,034	-1,022	-1,112
1417373_a_at	Tuba4	tubulin, alpha 4	0,006	-1,012	-1,052	-1,132	-1,126
1448232_x_at	Tuba6 /// EG626534	tubulin, alpha 6 /// predicted gene, EG626534	0,003	1,112	1,762	2,123	1,528
1423221_at	Tubb4	tubulin, beta 4	0,002	1,052	-1,003	-1,126	-1,238
1455719_at	Tubb5	tubulin, beta 5	0,001	1,062	1,276	1,488	1,334

Probe set ID = The probe set ID represents the unique probe set identifier of the Affymetrix mouse genome 430 2.0 array;

dpi= days post-infection; **q-value** = Significant differential gene expression between TMEV-infected and mock-infected mice in the time course of TME was determined employing the spline-based method embedded in extraction of differential gene expression (EDGE) software. A time course q-value of ≤ 0.05 was selected to designate significant changes in gene expression, and simultaneously limit the maximally allowed false discovery rate to 5.0%; **Fold change** = The fold change was calculated as the ratio of the inverse-transformed arithmetic means of the log2-transformed expression values of TMEV-infected versus mock-infected mice. Down-regulations are shown as negative reciprocal values.

There is a mild to moderate transcriptional down-regulation of kinesin family members (Kif2a, Kif3c, Kif5a; Fig 7A), and certain components of the protein phosphatase 2 complex (Ppp2r2a, Ppp2r2c) especially during the demyelinating phase of the disease between 42 and 196dpi. Furthermore, an up-regulation of tubulin alpha 6 (Tuba6), and tubulin beta 5 (Tubb5), and a down-regulation of tubulin alpha 1 (Tuba1), tubulin alpha 4 (Tuba4), and tubulin beta 4 (Tubb4) was observed. No significant or only minimal transcriptional changes ($-1.1 > \text{fold change} < 1.1$) were observed for APP, multiple components of the dynein complex (Fig 7B), Tau-1, neurofilament heavy chain (Nefh), neurofilament light chain (Nefl), neurofilament medium chain (Nefm) and Uchl1 (Supplementary Table).

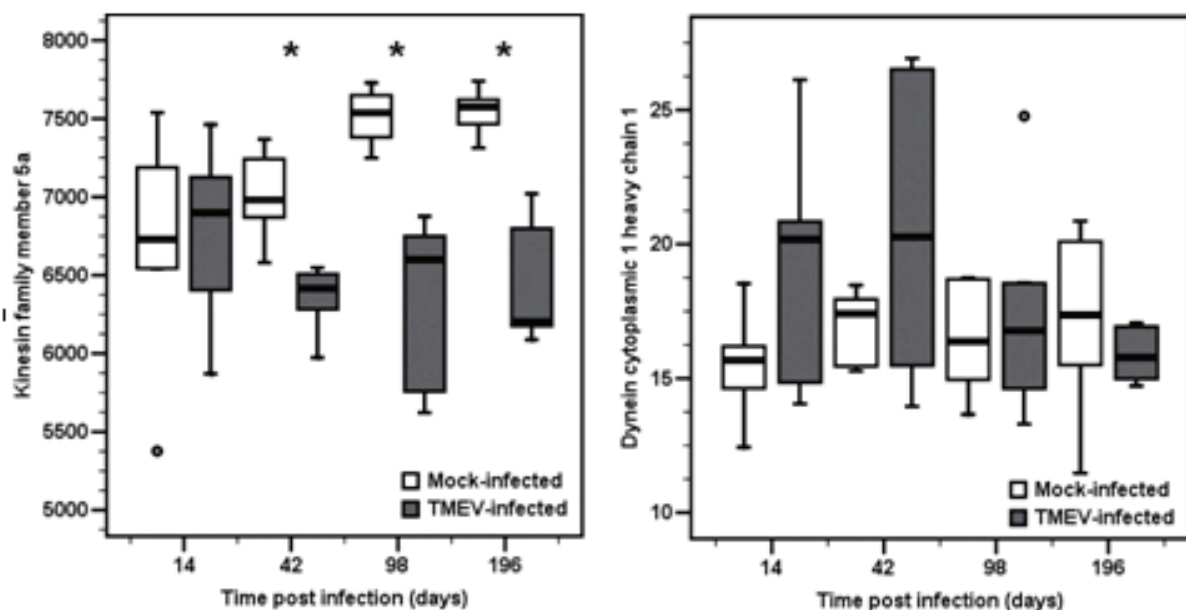


Figure 7: Direction-dependent transcriptional down-regulation of anterograde axonal transport proteins in TME.

The diagram displays the reduction of *Kif5A* following TMEV infection. In contrast, *Dync1h1* remained unchanged in both groups throughout the disease progression. Box and whisker plots show the median and quartiles of the arbitrary expression values of kinesin family member 5A (*Kif5A*) (A), and dynein cytoplasmic 1 heavy chain 1 (*Dync1h1*) (B) as detected by microarray analysis. Extreme values are shown as circles. Six mice were evaluated per group and time point, except for five TMEV-infected mice at 98 dpi. A significant difference between the groups as detected by the Mann–Whitney U-test is marked as follows: $*p \leq 0.05$.

Translational changes of axonal-transport-related proteins

To further substantiate the transcriptional changes immunohistochemistry of candidate genes was performed. *Kif5A* was expressed in neuronal cell bodies of the gray matter and axons of the white matter in controls (Fig 8A).

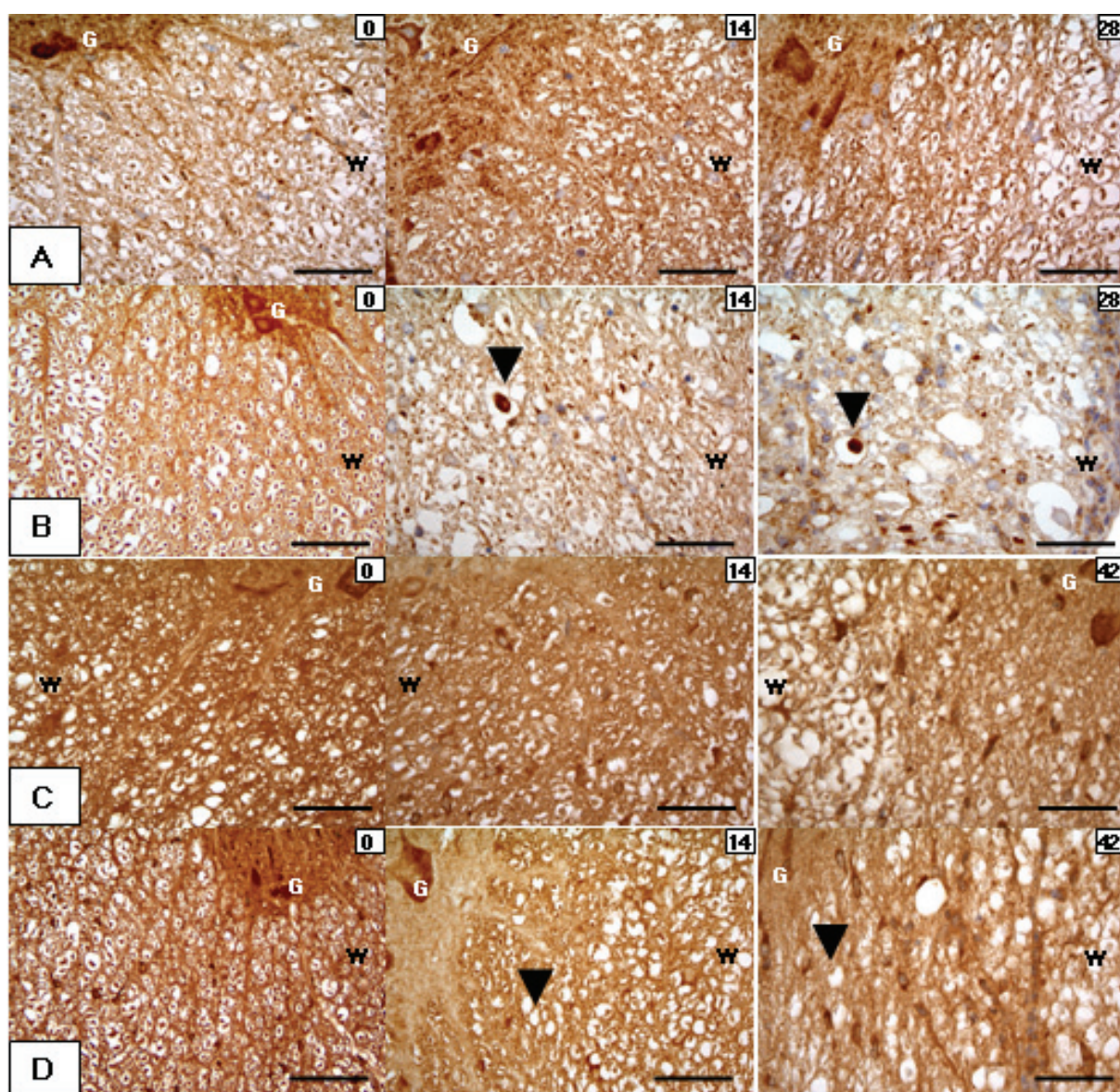


Figure 8. Expression of kinesin family member 5A (Kif5A) and dynein cytoplasmic heavy chain 1 (Dync1h1) in TME.

The rows illustrate Kif5A (A, B) and Dync1h1 (C, D) immunoreactivity in the ventro-medial and lateral spinal cord of control (A, C) and TMEV-infected mice (B, D) at 0, 14, and 28/42dpi (d). (A, B) At 0dpi control and infected mice showed the same pattern of Kif5A expression consisting of positive axons of the white matter and neurons in the grey matter. A decreased Kif5A expression and the appearance of Kif5A-positive spheroids (arrowheads) were observed in the TMEV-infected mice at 14 and 28dpi. (C, D) At 0dpi, axons in the white matter and neurons in grey matter were Dync1h1-positive in control and infected groups. A decrease in axonal Dync1h1 expression was seen in the TMEV-infected mice at 14 and 42dpi (arrowheads). Scale bar = 100µm. G=grey matter, W=white matter.

At day 14, Kif5A-positive immunoreactive spheroids appeared and axons showed an overall reduction of Kif5A expression in infected mice. At 98dpi, Kif5A reached a peak of decreased

expression when less than 50% of the axons showed Kif5A immunoreactivity (Fig 5E and 8B). Although *Dync1h1* showed no regulation at the transcriptional level (Fig. 7B), immunohistochemistry revealed a similar down-regulation at the translational level as observed for Kif5A (Fig 5F and 8D). However, no dynein-positive spheroids were detected (Fig 8D).

β -III and α -acetylated tubulin expression were analyzed to assess the stability of the axonal cytoskeleton. The latter is essential for the kinesin- and dynein-mediated transport of NF. In controls, β -tubulin III and α -acetylated tubulin (data not shown) followed the Kif5A expression pattern. In TME, their expression decreased significantly at 98dpi (Fig 5G).

Tau-1 was expressed in oligodendroglial cells of the gray and white matter and axons of the white the matter in controls. In TME mice, Tau-1 axonal expression was significantly reduced between 42 and 196dpi (Fig 5H). Furthermore, based on the diametrical axonal expression of p-NF and n-NF it was hypothesized that the excessive presence of axonal n-NF is the result of excessive p-NF dephosphorylation. To analyze abnormalities in the dephosphorylation processes, the expression of Pp2ac and Pp2aa was studied. However, these Pp2a subunits were similarly expressed in control and TME mice (data not shown).

To investigate whether the abnormalities in NF, Kif5A, *Dync1h1*, β -tubulin III and Tau-1 expression are the result of a dysregulated axonal protein degradation system, the axonal presence of ubiquitin-protein conjugates and Uchl-1 was studied. Both antibodies showed similar expression patterns characterized by positive neurons in the gray matter and glial cells and axons in the white matter of controls (Fig 9A and 9C). In TME mice, their expression dropped significantly at 28dpi and remained very low until 196dpi (Fig 5I and 9B, D).

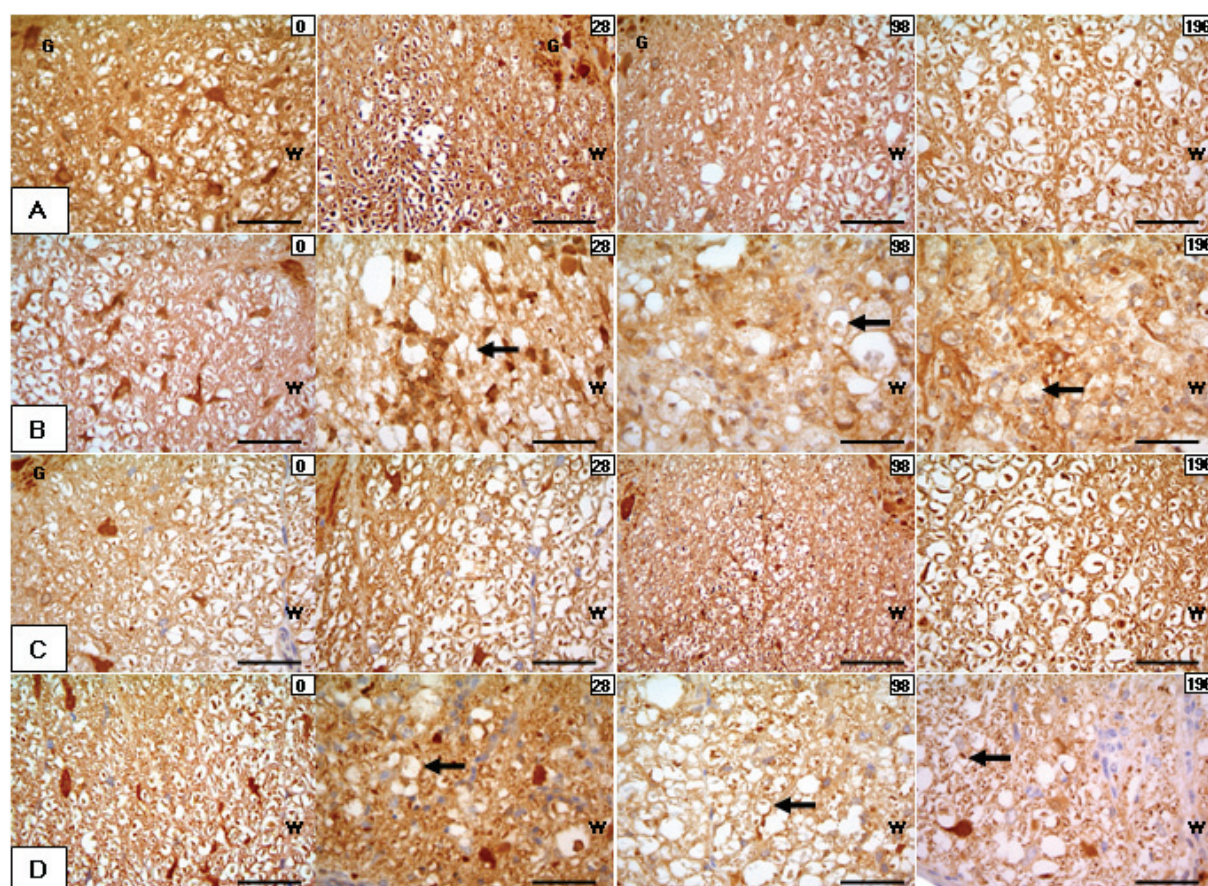


Figure 9. Expression of ubiquitin-ligated proteins and ubiquitin carboxy-terminal hydrolase ligase (Uchl-1) in TME.

The rows illustrate ubiquitin (A, B) and Uchl-1 (C, D) immunoreactivity in the ventro-medial spinal cord of control (A, C) and TMEV-infected mice (B, D) at 0, 28, 98 and 196dpi. (A, B) At 0dpi, axonal ubiquitin-ligated proteins were present in control and infected mice. At 28, 98 and 196dpi, a lower expression of ubiquitin-ligated proteins was seen in the TMEV-infected mice (arrows). (C, D) At 0dpi, axonal Uchl-1 was present in the spinal cord of both control and infected mice. At 28, 98 and 196dpi a lower expression of Uchl-1 was seen in the TMEV-infected mice (arrows). Scale bar = 100 μ m. G=grey matter, W=white matter

TMEV-infected N1E-115 cells

To answer the question whether TMEV alone or both the microenvironment and/or the pathogen may cause axonal changes, N1E-115 cells were analyzed after differentiation into neurons and following infection with the BeAn strain of TMEV. The differentiated N1E-115 cells displayed a neuron-like morphology while non-differentiated N1E-115 cells were round and compact (Fig 10).

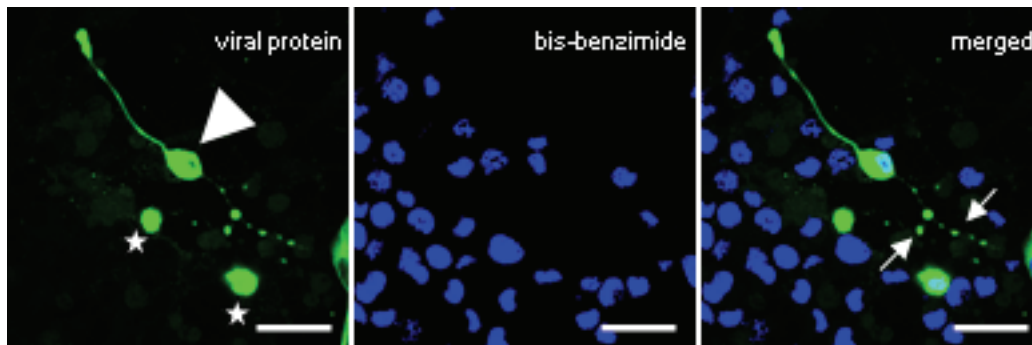


Figure 10. Axonal pathology in N1E-115 TMEV-infected cells.

The differentiated TMEV-infected cells showed tandem-repeated swellings along their axon-like processes. N1E-115 cells were stained with a polyclonal anti-capsid protein VP1-BeAn-TMEV specific antibody and Cy2-conjugated AffiniPure goat anti-rabbit serum (viral protein= green) and bis-benzimide (blue). Non-differentiated cells are marked with stars, differentiated cells with an arrowhead, the focal swelling with arrows.

Scale bars = 16 μ m

Approximately 80% of non-differentiated and 20% of differentiated cells were infected with TMEV-BeAn. The differentiated and infected N1E-115 cells showed an ubiquitous expression of the TMEV antigen and were characterized by a particular immunoreactivity of their processes which resembled the *in vivo* focal axonal swellings (Fig 10).

These focal swellings were further characterized with respect to n-NF and p-NF expression and revealed similarities with the *in vivo* situation. Thus, the axonal enlargements showed higher and lower levels of n-NF (Fig 11B) and p-NF (Fig 11D), resembling immunoreactivity of spheroids *in vivo*. In contrast, axonal-like structures of non-infected cells displayed a uniform expression of p-NF and a lack of n-NF immunoreactivity (Fig 11A, C).

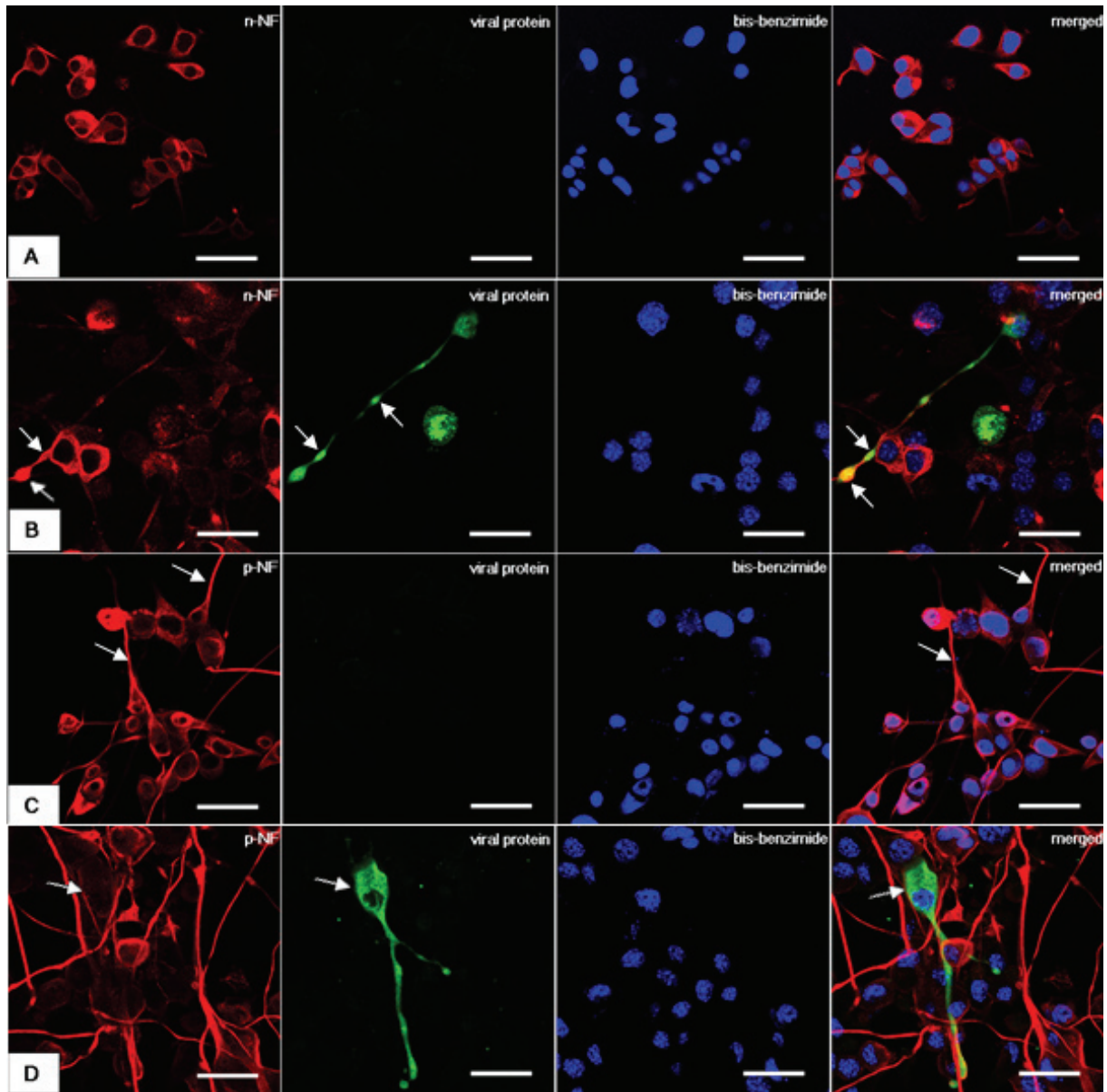


Figure 11. Expression of non-phosphorylated NF (n-NF) and phosphorylated NF (p-NF) in TMEV-infected N1E-115 cells.

The figures illustrate n-NF (A, B) and p-NF (C, D) immunofluorescence in controls (A, C) and TMEV-infected cells (B, D). (A) Non-infected cells showed a n-NF expression restricted to the cell body and lacking of TMEV expression. (B) Following infection with TMEV tandem-repeated swellings (arrows) with n-NF increased immunoreactivity can be recognized. Simultaneous expression of viral and n-NF proteins, especially of the swelling, can be observed in the merged picture as yellow discoloration. (C) p-NF shows a uniform expression (arrows) along the axon-like structures in non-infected cells. (D) Following TMEV expression a decrease in p-NF immunoreactivity can be observed (arrow) as demonstrated by weak focal yellow discolouration in the merged figure. N1E-115 cells were incubated with primary antibodies directed against: polyclonal anti-capsid protein VP1-BeAn-TMEV and anti-n-NF/p-NF and secondary antibodies: Cy2- conjugated AffiniPure goat anti-rabbit antibodies (green) and respectively, Cy3-conjugated AffiniPure goat anti-mouse (red) and with bis-benzimide (blue). Scale bars = 16µm

Discussion

In the present study, possible pathogenetic mechanisms involved in axonal accumulation of NF in TME were investigated using *in vivo* and *in vitro* experiments to elucidate molecular mechanisms responsible for initiation and development of axonopathies in this murine model of MS. Based on the hypothesis that the initiation and development of axonopathies are based on an impaired axonal transport of NFs, the aims were (i) to describe and characterize the degree of axonopathies and (ii) to investigate associated transcriptional and translational mechanisms.

A detailed description of the NF expression during the progression of TME revealed, in concordance with previous studies,¹ a decrease in p-NF levels and an increase in the number of n-NF-positive axons in the ventro-lateral white matter of the spinal cord of diseased animals. The onset of these alterations was noticed as early as 14dpi.¹⁰ Analysis of TMEV-infected N1E-115 neuroblastoma cells showed similar results, with n-NF accumulations at the level of axonal swellings after 7dpi. To further analyze the contributing pathogenetic mechanisms a variety of key factors that play directly (NF axonal transport, NF phosphorylation and NF degradation) or indirectly (viral persistence, demyelination) a crucial role in axon homeostasis were investigated at the transcriptional and translational level.

A low but consistent virus antigen expression of predominantly macrophages/microglial cells within the spinal cord was observed between 14 and 196 dpi. In contrast, only few virus positive axons were detected between 28 and 196 dpi. Similar results were obtained after infection with the DA strain of TMEV.³ Though, it is described that TMEV uses the axonal transport for its dissemination along the optical nerve,²⁶ virus spread along the axonal route seems to represent a rather rare phenomenon in the spinal cord. In addition, TMEV expression in macrophages/microglial cells indicated a pivotal role of cell-to-cell transmission for virus spread.²⁷ In contrast, the present *in vitro* experiments showed a prominent viral expression in the neuronal cell body and axon-like processes after TMEV-infection as observed in the early phase of TMEV-infection in the brain. Despite its low frequency, the role of axonal spread and its contribution to spinal cord disease initiation and progression remains to be determined. The present *in vitro* experiments showed a preferential infection of the non-differentiated N1E-115 neuroblastoma cells, whereas differentiated cells were infected to a lesser extent. Wada et al. (1993) obtained similar results.²⁶ Similarly, differentiated oligodendroglial precursor cells are more susceptible to TMEV infection than mature oligodendrocytes *in vitro*.²¹

To answer the question whether demyelination follows axonal injury or vice versa, kinetic phenotypic characterization of lesions was performed. Thus, the onset of demyelination was determined at 42dpi using LFB stain, while the first signs of axonal pathology appeared at 28dpi using the Bielschowsky silver stain. However, using transmission microscopy, a simultaneous onset for demyelination and axonal degeneration was observed at 14dpi. Similarly, degenerated axons within normal myelinated sheaths and degenerated myelin around normal axons were observed. These findings indicate that both primary and secondary myelin loss seemed to occur simultaneously indicating that both the inside-out as well as the outside-in model play an essential part during lesion development.²²

It was suggested that NF aggregates are the result of a defective NF axonal transport and/or phosphorylation in neurodegenerative disorders.²⁹ Microarray results of the present study revealed a transcriptional down-regulation for the members of the kinesin family and subunits of protein phosphatase 2 complex. Previous studies investigating NF phosphorylation by using mass spectrometry revealed no differences between ALS (amyotrophic lateral sclerosis) and control tissues.²⁹ This indicated that NF accumulation can be the result of their mislocation¹¹ as it has been shown for some transgenic models of ALS.^{30,31} A similar mechanism has been hypothesized for NF aggregation in MS.³² To obtain more detailed information about these processes, the expression of motor and cytoskeleton proteins involved in the axonal transport of NF was further studied by immunohistochemistry in the present investigation. Thus, the specific motor protein for the anterograde transport of NF,^{33,34} Kif5A, showed a reduced expression in the spinal cord, beginning at 14dpi. Though not regulated at the transcriptional levels, Dync1h1, involved in NF retrograde transport³³ and Tau-1, responsible for the MT stability, showed a similar translational down-regulation as Kif5A. In contrast to the motor proteins, the main components of the microtubules, α and β tubulins, showed a more stable expression at the translational levels.

An impaired axonal transport as observed in TMEV could have multiple possible consequences: (a) decrease of TMEV transport as shown before for vaccinia virus;³⁵ (b) impairment of APP and NF axonal function and (c) a reduction of axonal p-NF expression. APP, a sensitive indicator of early axonal injury,³⁶ was detected in small amounts in axons after TMEV-infection beginning at 28dpi. Kinesin light chains transport APP along the axons,³⁷ therefore a reduction in kinesin expression could trigger a lower APP accumulation compared to what was observed after TMEV-infection.

It still remains unclear how an impairment of the NF transport may result in increased expression of axonal n-NF. Beside differences in their neuronal localization and affinity for

motor proteins,^{13,14,33,38} there is a specific association between hypophosphorylated/phosphorylated-NF and other cytoskeleton components. Thus, unlike the extensively phosphorylated NF, only hypophosphorylated NF binds either MTs³⁹ or myosin with high affinity and translocates along actin in the axon.^{40,41} Moreover, the hypophosphorylated NF-MT association is regulated by the amount of Tau-1 fragments.¹⁷ A reduction in Tau-1 expression as observed in TME, could facilitate a hypophosphorylated-NF MT-dependent axonal transport. Thus, n-NF can be alternatively transported and can accumulate along the axons in the absence of motor proteins.

It is well known that axonal NF transport and phosphorylation are intimate processes.¹³ Although the amount of p-NF and n-NF was similar in control and ALS patients²⁹ active kinases like Cdk5 and p38 Map-kinase were found predominantly in perikarya and in proximal axons. The latter represent sub-cellular compartments with p-NF accumulations.²⁹ The complementary expression of both NF forms during TME led to the assumption that a local dephosphorylation process could be an additional mechanism responsible for the conversion of the preexisting p-NF into axonal n-NF. Pp2a represents the main enzyme exhibiting the most abundant endogenous phosphatase activity in spinal cord extracts.⁴² Interestingly, Ppp2r2a and Ppp2r2c expression was similar in control and infected mice. Though this indicated that a lack of phosphorylation might represent not a major pathogenetic mechanism, it can not exclude possible changes in protein phosphatase 2a activity or the participation of other phosphatases in the axonal NF dephosphorylation process.

Either transported from the neuronal cell bodies and/or locally produced in the axon, n-NF could represent a first step towards NF degradation. Previous studies reported that n-NF undergoes degradation,³¹ while p-NF was protected by phosphorylation.⁴³ The question arose why is n-NF degradation during TME not as efficient as in controls. Various proteases are involved in the NF degradation process.¹⁸ In addition, ubiquitination was described as an important mechanism of NF degradation.¹⁹ Ubiquitin-conjugated proteins are components of the intraneuronal inclusions and are found in several neurodegenerative diseases.³⁸ In the present study, in contrast to other neurodegenerative disorders, the expression of ubiquitin-protein conjugates and Uchl-1 was significantly reduced. Because ubiquitination is the first step in a non-lysosomal degradation pathway of proteins, it was concluded that a derangement of this proteolytic pathway may occur in infected mice. The presumed direct factors involved in the axonal accumulation of n-NF based on the present investigation are schematically summarized and displayed in figure 12.

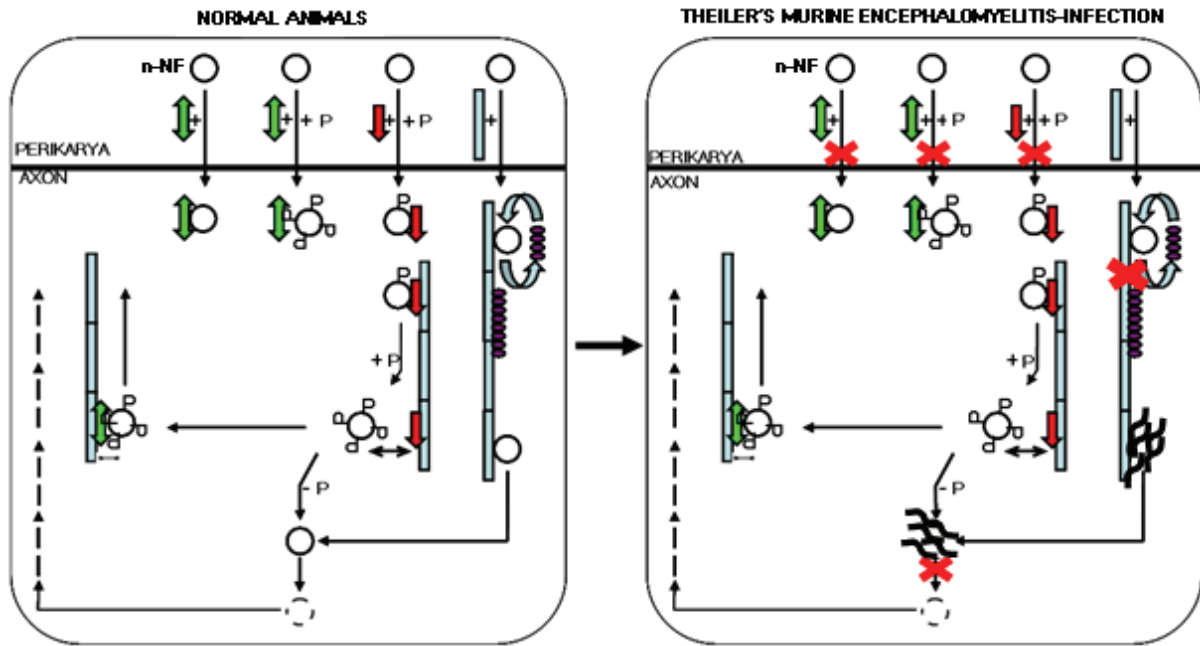


Figure 12. Schematic outline of the impact of the direct factors involved in alterations of NF metabolism during TME.

The figure shows perikaryon-axonal transport of neurofilaments and associated proteins. In normal animals, dynein is essential for the antero- and retrograde transport of non- and hyper-phosphorylated NFs whereas, kinesin is responsible for the anterograde transport of hypophosphorylated NF. There is a continuous exchange between Tau-1 and n-NF attached to microtubules. In axons, the hyper-phosphorylated NFs are dephosphorylated and then degraded. Following TMEV-infection, impairment of these processes (marked with red crosses) that give rise to NF axonal aggregations can be observed.

Non-phosphorylated neurofilaments (○); phosphorylated neurofilaments (○^P); kinesin (↓); dynein (↑); microtubules (▮); tau (●).

In conclusion, TMEV-associated axonopathy is characterized by neurofilament accumulations due to various impaired molecular interactions including mechanisms responsible for axonal transport, neurofilament-phosphorylation and protein metabolism. Thus, as shown by this study, neurofilament accumulation in TME seems to be the result of specific dysregulations in their axonal transport (Kif5A) and also the sequel of nonspecific impairments in the neuronal protein metabolism (ubiquitin-protein conjugates). Further studies are necessary to analyze the relationship between direct factors that are important for axonal transport and protein metabolism as well as indirect factors such as virus spread. The dissection of these various factors will contribute substantially to our understanding of their impact on disease initiation and development and will allow us to design new therapeutic strategies.

Acknowledgement

The authors would like to thank Petra Grünig, Bettina Buck, Danuta Waschke, Julia Schirrmeier, Kerstin Rohn, Claudia Hermann, Anuschka Unold, Martin Gamber, Thomas Feidl for their excellent technical support. The BeAn strain of TMEV was a generous gift of Dr. H.L. Lipton, Department of Microbiology-Immunology, University of Illinois, Chicago, IL, USA. Mihaela Kreutzer was supported by a Georg-Christoph-Lichtenberg scholarship provided by the Ministry for Science and Culture of Lower Saxony. Frauke Seehusen received a scholarship from Bayer HealthCare, Leverkusen. Reiner Ulrich and Robert Kreutzer received grants from the Centre for Systems Neuroscience, Hannover, Germany.

References

1. Noseworthy JH, Lucchinetti C, Rodriguez M, Weinshenker BG. Multiple sclerosis. *N Engl J Med* 2000;343:938-952.
2. Dziejczak T, Metz I, Dallenga T, et al. Wallerian degeneration: a major component of early axonal pathology in multiple sclerosis. *Brain Pathol* 2010;20:976-985.
3. Tsunoda I, Kuang LQ, Libbey JE, Fujinami RS. Axonal injury heralds virus-induced demyelination. *Am J Pathol* 2003;162:1259-1269.
4. Ferguson B, Matyszak MK, Esiri MM, Perry VH. Axonal damage in acute multiple sclerosis lesions. *Brain* 1997;120:393-399.
5. Trapp BD, Peterson J, Ransohoff RM, et al. Axonal transection in the lesions of multiple sclerosis. *N Engl J Med* 1998;338:278-285.
6. Seehusen F, Baumgärtner W. Axonal pathology and loss precede demyelination and accompany chronic lesions in a spontaneously occurring animal model of multiple sclerosis. *Brain Pathol* 2010;20:551-559.
7. Lee VM, Carden MJ, Schlaepfer WW, Trojanowski JQ. Monoclonal antibodies distinguish several differentially phosphorylated states of the two largest rat neurofilament subunits (NF-H and NF-M) and demonstrate their existence in the normal nervous system of adult rats. *J Neurosci* 1987;7:3474-3488.
8. Gentleman SM, Nash MJ, Sweeting CJ, et al. Beta-amyloid precursor protein (beta APP) as a marker for axonal injury after head injury. *Neurosci Lett* 1993;160:139-144.
9. Gehrmann J, Banati RB, Cuzner ML, et al. Amyloid precursor protein (APP) expression in multiple sclerosis lesions. *Glia* 1995;15:141-151.
10. Ulrich R, Seeliger F, Kreutzer M, et al. Limited remyelination in Theiler's murine encephalomyelitis due to insufficient oligodendroglial differentiation of nerve/glia antigen 2 (NG2)-positive putative oligodendroglial progenitor cells. *Neuropathol Appl Neurobiol* 2008;34:603-620.
11. Perrot R, Berges R, Bocquet A, Eyer J. Review of the multiple aspects of neurofilament functions, and their possible contribution to neurodegeneration. *Mol Neurobiol*. 2008;38:27-65.
12. Lew J, Winkfein RJ, Paudel HK, Wang JH. Brain proline-directed protein kinase is a neurofilament kinase which displays high sequence homology to p34cdc2. *J Biol Chem* 1992;267:25922-25926.

13. Veeranna, Shetty KT, Link WT, et al. Neuronal cyclin-dependent kinase-5 phosphorylation sites in neurofilament protein (NF-H) are dephosphorylated by protein phosphatase 2A. *J Neurochem* 1995;64:2681-2690.
14. Shea TB, Chan WK. Regulation of neurofilament dynamics by phosphorylation. *Eur J Neurosci* 2008;27:1893-1901.
15. Yabe JT, Pimenta A, Shea TB. Kinesin-mediated transport of neurofilament protein oligomers in growing axons. *J Cell Sci* 1999;112:3799-3814.
16. Motil J, Chan WK, Dubey M, et al. Dynein mediates retrograde neurofilament transport within axons and anterograde delivery of NFs from perikarya into axons: regulation by multiple phosphorylation events. *Cell Motil Cytoskeleton* 2006;63:266-286.
17. Weingarten MD, Lockwood AH, Hwo SY, Kirschner MW. A protein factor essential for microtubule assembly. *Proc Natl Acad Sci U S A* 1975;72:1858-1862.
18. Gotow T. Neurofilaments in health and disease. *Med Electron Microsc* 2000;33:173-199.
19. Schlaepfer WW, Zimmerman UJ. Mechanisms underlying the neuronal response to ischemic injury. Calcium-activated proteolysis of neurofilaments. *Prog Brain Res* 1985;63:185-196.
20. Masaki R, Saito T, Yamada K, Ohtani-Kaneko R. Accumulation of phosphorylated neurofilaments and increase in apoptosis-specific protein and phosphorylated c-Jun induced by proteasome inhibitors. *J Neurosci Res* 2000;62:75-83.
21. Pringproa K, Rohn K, Kummerfeld M, Wewetzer K, Baumgärtner W. Theiler's murine encephalomyelitis virus preferentially infects immature stages of the murine oligodendrocyte precursor cell line BO-1 and blocks oligodendrocytic differentiation in vitro. *Brain Res* 2010;1327:24-37.
22. Czasch P, Baumgärtner W. A comparison of immunohistochemical and silver staining methods for the detection of diffuse plaques in the aged canine brain. *Neurobiol Aging* 2006;27:293-305.
23. Kummerfeld M, Meens J, Haas L, Baumgärtner W, Beineke A. Generation and characterization of a polyclonal antibody for the detection of Theiler's murine encephalomyelitis virus by light and electron microscopy. *J Virol Methods* 2009;160:185-188.
24. Kreutzer R, Kreutzer M, Pröpsting MJ, Sewell AC, Naim HY, Leeb T, Baumgärtner W. *JCMM* 2008;12:1661-1671.
25. Ulrich R, Kalkuhl A, Deschl U, Baumgärtner W. Machine learning approach identifies new pathways associated with demyelination in a viral model of multiple sclerosis. *JCMM* 2010;14:434-448.
26. Wada Y, Fujinami RS. Viral infection and dissemination through the olfactory pathway and the limbic system by Theiler's virus. *Am J Pathol* 1993;143:221-229.
27. Lipton HL, Kumar AS, Trottier M. Theiler's virus persistence in the central nervous system of mice is associated with continuous viral replication and a difference in outcome of infection of infiltrating macrophages versus oligodendrocytes. *Virus Res* 2005;111:214-223.
28. Conforti L, Adalbert R, Coleman MP. Neuronal death: where does the end begin? *Trends Neurosci* 2007;30:159-166.
29. Bajaj NP, al-Sarraj ST, Leigh PN, et al. Cyclin dependent kinase-5 (CDK-5) phosphorylates neurofilament heavy (NF-H) chain to generate epitopes for antibodies that label neurofilament accumulations in amyotrophic lateral sclerosis (ALS) and is present in affected motor neurones in ALS. *Prog Neuropsychopharmacol Biol Psychiatry* 1999;23:833-850.

30. Collard JF, Cote F, Julien JP. Defective axonal transport in a transgenic mouse model of amyotrophic lateral sclerosis. *Nature* 1995;375:61-64.
31. Millicamps S, Robertson J, Lariviere R, et al. Defective axonal transport of neurofilament proteins in neurons overexpressing peripherin. *J Neurochem* 2006;98:926-938.
32. Petzold A, Gveric D, Groves M, et al. Phosphorylation and compactness of neurofilaments in multiple sclerosis: indicators of axonal pathology. *Exp Neurol* 2008;213:326-335.
33. Shah JV, Flanagan LA, Janmey PA, Leterrier JF. Bidirectional translocation of neurofilaments along microtubules mediated in part by dynein/dynactin. *Mol Biol Cell* 2000;11:3495-3508.
34. Xia CH, Roberts EA, Her LS, et al. Abnormal neurofilament transport caused by targeted disruption of neuronal kinesin heavy chain KIF5A. *J Cell Biol* 2003;161:55-66.
35. Rietdorf J, Ploubidou A, Reckmann I, et al. Kinesin-dependent movement on microtubules precedes actin-based motility of vaccinia virus. *Nat Cell Biol* 2001;3:992-1000.
36. Mancardi G, Hart B, Roccatagliata L, et al. Demyelination and axonal damage in a non-human primate model of multiple sclerosis. *J Neurol Sci* 2001;184:41-49.
37. Kamal A, Almenar-Queralt A, LeBlanc JF, et al. Kinesin-mediated axonal transport of a membrane compartment containing beta-secretase and presenilin-1 requires APP. *Nature* 2001;414:643-648.
38. Miller CC, Ackerley S, Brownlees J, et al. Axonal transport of neurofilaments in normal and disease states. *Cell Mol Life Sci* 2002;59:323-330.
39. Hisanaga S, Hirokawa N. Dephosphorylation-induced interactions of neurofilaments with microtubules. *J Biol Chem* 1990;265:21852-21858.
40. Ahmad FJ, Echeverri CJ, Vallee RB, Baas PW. Cytoplasmic dynein and dynactin are required for the transport of microtubules into the axon. *J Cell Biol* 1998;140:391-401.
41. Jung C, Chylinski TM, Pimenta A, et al. Neurofilament transport is dependent on actin and myosin. *J Neurosci* 2004;24:9486-9496.
42. Strack S, Westphal RS, Colbran RJ, et al. Protein serine/threonine phosphatase 1 and 2A associate with and dephosphorylate neurofilaments. *Brain Res Mol Brain Res* 1997;49:15-28.
43. Goldstein ME, Sternberger NH, Sternberger LA. Phosphorylation protects neurofilaments against proteolysis. *J Neuroimmunol* 1987;14:149-160.
44. Coleman M. Axon degeneration mechanisms: commonality amid diversity. *Nat Rev Neurosci* 2005;6:889-898.

Supplementary Table: Transcriptional regulation of the axon-transport-related proteins

ProbeSetID	GeneSymbol	GeneTitle	PValue	QValue	FC14	FC42
1453524_at	5530401D11Rik	RIKEN cDNA 5530401D11 gene amyloid beta (A4) precursor	0,4573588	0,5213196	1,13503464	1,15230623
1427442_a_at	App	protein ankyrin repeat and SOCS box-	0,00070841	0,01506691	1,0565717	-1,00823993
1449547_at	Asb14	containing protein 14	0,741737	0,6123669	1,08194413	-1,10612672
1436560_at	AW124694	expressed sequence AW124694	0,04148356	0,1919766	1,05687567	-1,04096243
1434594_at	Dnahc1	dynein, axonemal, heavy chain 1	0,09882929	0,2884179	1,04862039	-1,12326799
1421544_at	Dnahc11	dynein, axonemal, heavy chain 11 Dynein, axonemal, heavy chain	0,7481765	0,6141095	1,02090538	1,0107773
1443060_at	Dnahc17	17	0,2069413	0,3896411	-1,12380379	-1,00873356
	Dnahc2 ///	dynein, axonemal, heavy chain 2				
1438763_at	Dnhd3	/// dynein heavy chain domain 3	0,5738806	0,5631051	-1,17653317	-1,16927005
1421434_at	Dnahc5	dynein, axonemal, heavy chain 5	0,1514483	0,3455057	-1,00347233	1,08394746
1442894_at	Dnahc6	dynein, axonemal, heavy chain 6	0,4991606	0,5375985	1,02969947	-1,08068333
1440456_at	Dnahc7	dynein, axonemal, heavy chain 7	0,7500146	0,6146038	-1,13333262	-1,10566896
1446424_at	Dnahc7c	dynein, axonemal, heavy chain 7c	0,5246853	0,545998	-1,04694053	-1,14214105
	Dnahc7c ///	dynein, axonemal, heavy chain 7c				
	Dnahc7b ///	/// dynein, axonemal, heavy chain				
1438466_at	LOC433299	7b /// dynein heavy chain-related	0,2069768	0,3896411	1,18737447	-1,11378814
1425692_a_at	Dnahc8	dynein, axonemal, heavy chain 8	0,4934802	0,5357711	-1,05679655	1,00929704
1457401_at	Dnahc9	dynein, axonemal, heavy chain 9 dynein, axonemal, intermediate	0,4970411	0,5371487	-1,03346725	-1,06254443
1437094_x_at	Dnaic1	chain 1 dynein, axonemal, intermediate	0,6338004	0,5818294	-1,13010409	-1,10355778
1445408_at	Dnaic2	chain 2	0,4088426	0,4992992	-1,07415374	1,00136204
1455630_at	Dnalc1	dynein, axonemal, light chain 1	0,1040292	0,2953793	-1,02055033	-1,13265723
1416870_at	Dnalc4	dynein, axonemal, light chain 4 dynein, axonemal, light	0,4653464	0,5248562	1,00213428	-1,13383968
1455379_at	Dnali1	intermediate polypeptide 1	0,04746192	0,2043088	1,13802599	-1,00679491

Supplementary Table-continued

1430753_at	Dnhd1	dynein heavy chain domain 1	0,826693	0,6344841	1,01786684	-1,03216217
1454103_at	Dnhd3	dynein heavy chain domain 3	0,5016538	0,5381788	-1,04595129	-1,15393463
		dynein cytoplasmic 1 heavy chain				
1439950_at	Dync1h1	1	0,1523563	0,3463051	1,22887925	1,17482198
		dynein cytoplasmic 1				
1416361_a_at	Dync1i1	intermediate chain 1	0,01394515	0,1061065	-1,10286332	-1,08108416
		dynein cytoplasmic 1				
1415841_at	Dync1i2	intermediate chain 2	0,452176	0,5191465	1,01334481	-1,03892715
		dynein cytoplasmic 1 light				
1424947_at	Dync1li1	intermediate chain 1	0,5914015	0,5691298	-1,11046031	-1,09145615
		dynein, cytoplasmic 1 light				
1433926_at	Dync1li2	intermediate chain 2	0,2504565	0,4172732	1,00976448	-1,01179405
		dynein cytoplasmic 2 heavy chain				
1429250_at	Dync2h1	1	0,00771956	0,07444488	1,1046195	-1,14782471
		dynein cytoplasmic 2 light				
1428446_at	Dync2li1	intermediate chain 1	0,6808514	0,5960763	-1,10776895	-1,10012427
1448682_at	Dynll1	dynein light chain LC8-type 1	0,1446551	0,3390002	-1,01762651	-1,09267334
		dynein light chain LC8-type 1 ///				
	Dynll1 ///	predicted gene, EG627788 ///				
	EG627788 ///	similar to dynein, cytoplasmic,				
	LOC637840 ///	light peptide /// similar to dynein,				
1417339_a_at	LOC672375	cytoplasmic, light peptide	0,4969014	0,5371487	-1,11848791	-1,1372716
1418258_s_at	Dynll2	dynein light chain LC8-type 2	0,00797322	0,07599947	1,03151788	-1,00180415
		dynein light chain roadblock-type				
1428257_s_at	Dynlrb1	1	0,8027778	0,628522	-1,08852245	-1,10845625
		dynein light chain roadblock-type				
1428987_at	Dynlrb2	2	0,05769828	0,2262129	-1,14845076	-1,18438709
1428116_a_at	Dynlt1	dynein light chain Tctex-type 1	0,2870542	0,4386391	1,07261525	1,1112914

Supplementary Table-continued

		dynein light chain Tctex-type 1 ///				
		similar to Cytoplasmic dynein				
	Dynlt1 ///	light chain (T-complex testis-				
1453473_a_at	LOC671261	specific protein 1) (TCTEX-1)	0,2742921	0,4315075	1,08156285	1,05582032
1459854_s_at	Dynlt3	dynein light chain Tctex-type 3	0,1663178	0,3583839	-1,13209759	-1,0883737
1435306_a_at	Kif11	kinesin family member 11	0,08305536	0,2667171	-1,11480033	1,16572851
1424910_at	Kif12	kinesin family member 12	0,299986	0,4463414	-1,00872552	1,06081531
1451890_at	Kif13a	kinesin family member 13A	0,02164209	0,1372773	1,03394731	-1,13816483
1453276_at	Kif13b	kinesin family member 13B	0,1539241	0,3474812	-1,14448416	1,04545454
1431718_at	Kif15	kinesin family member 15	0,2745735	0,4316061	1,04338927	-1,08678081
1429063_s_at	Kif16b	kinesin family member 16B	0,00322232	0,04262579	-1,19100062	1,04044461
1419827_s_at	Kif17	kinesin family member 17	0,04656016	0,2025265	1,06319336	-1,06721684
1424107_at	Kif18a	kinesin family member 18A	0,00687878	0,06939296	-1,07487682	-1,02624391
1450108_at	Kif1a	kinesin family member 1A	0,413582	0,5015954	1,05284216	-1,15123724
1455182_at	Kif1b	kinesin family member 1B	0,00750516	0,07311498	-1,09370652	-1,28008875
1426325_at	Kif1c	kinesin family member 1C	0,0564881	0,2239467	1,07328384	1,09635955
1449207_a_at	Kif20a	kinesin family member 20A	0,06540498	0,2394466	-1,12463395	1,12795747
1450738_at	Kif21a	kinesin family member 21A	0,05186515	0,2141079	1,03969413	-1,04475102
1435772_at	Kif21b	kinesin family member 21B	0,04199774	0,1930248	1,20818287	1,10367903
1437716_x_at	Kif22	kinesin family member 22	0,04730693	0,2039963	-1,00815013	1,0531234
1455990_at	Kif23	kinesin family member 23	0,00650008	0,06695296	-1,16238944	1,21370642
1431937_at	Kif24	kinesin family member 24	0,2839234	0,4368623	-1,04863032	-1,13839271
1445404_at	Kif27	kinesin family member 27	0,175166	0,3660033	1,06083994	-1,11331988
1454107_a_at	Kif2a	kinesin family member 2A	0,00301812	0,0410812	1,20014288	1,1853951
1429333_at	Kif2b	kinesin family member 2B	0,04571429	0,2006248	-1,12645134	-1,08984125
1432392_at	Kif2c	kinesin family member 2C	0,01452651	0,1085024	-1,13444343	1,03746764
		kinesin family member 2C ///				
	Kif2c ///	similar to Kinesin-like protein				
1449060_at	LOC631653	KIF2C (Mitotic centromere-associated kinesin) (MCAK)	0,0255746	0,1502071	-1,15618439	1,18481283

Supplementary Table-continued

1420375_at	Kif3a	kinesin family member 3A	0,4450334	0,5158341	1,09441469	-1,0561059
1450074_at	Kif3b	kinesin family member 3B	0,549951	0,5551938	-1,09212652	1,04639835
1448946_at	Kif3c	kinesin family member 3C	0,00021596	0,00635055	1,06304709	-1,05344853
1450692_at	Kif4	kinesin family member 4	0,8242895	0,6338207	1,00681736	1,00675502
1434670_at	Kif5a	kinesin family member 5A	0,00070908	0,01507053	1,01626173	-1,10149733
		kinesin family member 5A ///				
1450249_s_at	Kif5a /// Kif5c	kinesin family member 5C	0,05905368	0,2283603	-1,16115065	-1,03928476
1418431_at	Kif5b	kinesin family member 5B	0,09567925	0,2841275	1,02613817	-1,093153
1422945_a_at	Kif5c	kinesin family member 5C	0,05805237	0,2268388	-1,02866163	-1,04003951
1439637_at	Kif7	kinesin family member 7	0,8861258	0,6486819	-1,03862738	-1,0627352
1420395_a_at	Kif9	kinesin family member 9	0,7418678	0,6124246	-1,01310919	-1,01778488
1451783_a_at	Kifap3	kinesin-associated protein 3	0,03756835	0,1824123	-1,03913205	-1,08039036
1456136_at	Kifc1	Kinesin family member C1	0,2098353	0,3915648	1,03576413	1,07683261
		kinesin family member C1 ///				
		similar to kinesin family member				
	Kifc1 ///	C1 isoform 2 /// similar to kinesin				
	LOC638962 ///	family member C1 isoform 2 ///				
	LOC671944 ///	similar to kinesin family member				
1449877_s_at	LOC676980	C1 isoform 2	0,320612	0,4576688	-1,04626526	1,09486551
1421312_a_at	Kifc2	kinesin family member C2	0,06718077	0,2425186	1,07852678	1,03655045
1416199_at	Kifc3	kinesin family member C3	0,2423392	0,4118292	1,08317149	1,00202916
1418214_at	Klc2	kinesin light chain 2	0,270276	0,4291393	-1,03676661	-1,08607357
1417108_at	Klc4	kinesin light chain 4	0,8779916	0,6465884	1,03074431	1,01838354
1417005_at	Kns2	kinesin 2	0,08192812	0,2645133	-1,03532197	-1,03320629
		microtubule-associated protein				
1424719_a_at	Mapt	tau	0,00573602	0,06177564	1,05208335	-1,06774021
1424847_at	Nefh	neurofilament, heavy polypeptide	0,07081794	0,2484007	-1,00549204	-1,06861512
1426255_at	Nefl	neurofilament, light polypeptide	0,1455041	0,3396283	-1,03372612	-1,01642904
1422520_at	Nefm	neurofilament, medium polypeptide	0,3947957	0,4933285	-1,02963429	-1,04547375

Supplementary Table-continued

		protein phosphatase 2 (formerly 2A), catalytic subunit, alpha				
1417367_at	Ppp2ca	isoform	0,07403716	0,2532994	-1,03000607	-1,07300242
		protein phosphatase 2 (formerly 2A), catalytic subunit, beta				
1421823_a_at	Ppp2cb	isoform	0,2431002	0,4124503	-1,03002665	-1,11600514
		protein phosphatase 2 (formerly 2A), regulatory subunit A (PR				
1438383_x_at	Ppp2r1a	65), alpha isoform	0,00456154	0,05317209	1,02128133	1,01638184
		Protein phosphatase 2 (formerly 2A), regulatory subunit A (PR				
1419871_at	Ppp2r1b	65), beta isoform	0,2611037	0,4235808	-1,01483159	1,06116831
		protein phosphatase 2 (formerly 2A), regulatory subunit B (PR				
1429715_at	Ppp2r2a	52), alpha isoform	0,00082903	0,01682349	1,03910756	-1,07419023
		protein phosphatase 2 (formerly 2A), regulatory subunit B (PR				
1426621_a_at	Ppp2r2b	52), beta isoform	0,3587136	0,4761271	-1,08853151	-1,05095945
		protein phosphatase 2 (formerly 2A), regulatory subunit B (PR				
1438671_at	Ppp2r2c	52), gamma isoform	0,00045631	0,01108376	1,04677703	-1,11887601
		protein phosphatase 2 (formerly 2A), regulatory subunit B, alpha				
1455198_a_at	Ppp2r3a	protein phosphatase 2A,	0,6022554	0,5724982	-1,09313052	-1,14949936
		regulatory subunit B (PR 53)				
1439383_x_at	Ppp2r4	protein phosphatase 2, regulatory	0,2178814	0,396254	1,05592803	-1,01215904
		subunit B (B56), epsilon isoform				
1428462_at	Ppp2r5e		0,1068841	0,2986015	-1,00774177	-1,13400657
1446507_at	Prnp	Prion protein	0,1246476	0,3184771	1,067241	1,07527562
1418650_at	Spata6	spermatogenesis associated 6	0,06403206	0,2367398	-1,06752967	1,02258339

Supplementary Table-continued

1428117_x_at	Tmem181	Transmembrane protein 181	0,09130529	0,278632	1,18437395	-1,03859979
1418884_x_at	Tuba1	tubulin, alpha 1	0,00099798	0,0191755	-1,04715947	-1,03436605
	Tuba1 ///	tubulin, alpha 1 /// similar to				
1433584_at	LOC544863	tubulin, alpha 1	0,6771848	0,5950742	-1,13985633	1,04362314
1423846_x_at	Tuba2	tubulin, alpha 2	0,07024545	0,2472522	-1,00880966	-1,00493475
1448296_x_at	Tuba3	tubulin, alpha 3	0,8366353	0,63677	-1,10431863	-1,13014796
	Tuba3 /// Tuba7	tubulin, alpha 3 /// tubulin, alpha				
1416311_s_at	/// LOC384954	7 /// similar to tubulin, alpha 1	0,7934121	0,626154	-1,1405957	-1,16079443
1417373_a_at	Tuba4	tubulin, alpha 4	0,00019334	0,0058378	-1,01276375	-1,05298362
	Tuba6 ///	tubulin, alpha 6 /// predicted gene,				
1448232_x_at	EG626534	EG626534	8,9577E-05	0,00319239	1,11265989	1,76294158
1419518_at	Tuba8	tubulin, alpha 8	0,05261746	0,2159431	1,02524237	-1,01280306
1427838_at	Tubb2a	tubulin, beta 2a	0,5846573	0,5668955	-1,0202231	-1,04000142
	Tubb2a ///					
	Tubb2b ///	tubulin, beta 2a /// tubulin, beta				
	LOC665524 ///	2b /// similar to tubulin, beta 3 ///				
1427347_s_at	LOC671656	similar to tubulin, beta 3	0,1750963	0,3659855	-1,07145741	-1,05392193
1452679_at	Tubb2b	tubulin, beta 2b	0,00850979	0,07920456	-1,1015663	-1,02549385
1456470_x_at	Tubb2c	tubulin, beta 2c	0,139486	0,3333776	-1,06590165	-1,0004555
1415978_at	Tubb3	tubulin, beta 3	0,2414148	0,411405	-1,08205225	-1,09090427
1423221_at	Tubb4	tubulin, beta 4	5,787E-05	0,00226098	1,05226689	-1,00358756
1455719_at	Tubb5	tubulin, beta 5	1,8625E-05	0,00092322	1,0621636	1,27632022
1416431_at	Tubb6	tubulin, beta 6	0,00684641	0,06915809	-1,03424931	1,25820093
		ubiquitin carboxy-terminal				
1448260_at	Uchl1	hydrolase L1	0,2277566	0,4027033	-1,1067065	-1,09065627

Chapter 4: General discussions

4.1 Hypothesis and aims

For many neurodegenerative diseases, like MS and TMEV-ID, a viral mouse model of MS, beside demyelinating and inflammatory processes, axonal damages represents an essential aspect of their pathogenesis. Pathologically, either the primary lesion is represented by the demyelination and axonal injuries develop secondary (Tsunoda and Fujinami, 2002) or the primary target is the axon and the demyelination is a secondary process (Ferguson *et al.*, 1997; Trapp *et al.*, 1998; Bitsch *et al.*, 2000). Either primary or secondary, axonal damages seemed to contribute substantially to the observed neurological deficits (Filippi and Rocca, 2005; Neumann *et al.*, 2003; Herrero-Herranz *et al.*, 2008). Therefore, the goal of any therapeutic approach should include the maintenance of fully functional axons.

Axons are responsible for a continuous flow of information among pre- and post-synaptic compartments codified as electrical impulses and chemical signals. The speed and the quality of these processes are dependent on axonal myelination and axonal transport mechanisms. MS and TMEV-ID are characterized by a delayed and incomplete remyelination and by a significant axonal loss and dysfunction (Charcot, 1868; Pittock *et al.*, 2007; Tsunoda *et al.*, 2003; Bjartmar *et al.*, 2000). Regarding these characteristics, the following two aspects of TMEV-ID pathogenesis were investigated in the present study:

- a possible dysregulation of oligodendroglial progenitor cells (OPCs) differentiation which could be responsible for insufficient regeneration;
- modifications in axonal transport and protein degradation which could cause non-phosphorylated neurofilaments accumulation during axonopathy.

4.2 Myelin pathology

For most MS models including anti-MOG antibody-augmented experimental autoimmune encephalomyelitis (EAE) in Lewis rats (Di Bello *et al.*, 1999), cuprizone toxicity in C57BL6 mice (Mason *et al.*, 2000; Morell *et al.*, 1998) lysolecithin-induced demyelination in the caudal cerebellar peduncle of Sprague Dawley rats (Woodruff *et al.*, 1999) and murine hepatitis virus (MHV) A-59 strain infection of C57BL6 mice (Redwine and Armstrong, 1998; Jordan *et al.*, 1989) a fast and complete remyelination is reported.

In contrast, demyelination is followed by a weak and delayed in the TMEV-ID model and MS. Causes for this insufficient remyelination in chronic progressive MS and TMEV-ID include the inability of oligodendroglial progenitor cells (OPCs) to proliferate and differentiate, axonal loss or the inability of chronically injured axons to be remyelinated (Franklin, 2002; Mason *et al.*, 2004). These morphological deficiency are mirrored in the clinical progression.

In the present study, footprint analysis of the TMEV-infected mice revealed a shortened, irregular, sometimes sliding gait, and a progressively declining stride length. At 196dpi, the stride length was reduced to 62.3% of the baseline measurement from 0dpi. Furthermore, it was observed that demyelination was a progressive process during TMEV-ID. Thus, minimal changes characterized by focal dilated myelin sheaths, infiltrated with microglia/macrophages were observed at 14dpi. Later, at 42dpi, multiple demyelinated foci, mainly in the ventral and lateral funiculi were identified. At 98 and 147dpi, lesioned areas further enlarged. In addition, at 147dpi few remyelinated axons were present, while at 196dpi, mild to moderate remyelination and a severe astrogliosis was present. The remyelinated areas displayed a similar extent of oligodendrocytes (OGs) and Schwann cell type of remyelination.

Regarding the presence of NG2-positive cells, immunohistochemistry investigations showed moderately increased numbers of intralésional NG2-positive cells with a pronounced immunoreactivity at 28, 42 and 98dpi. Most of these cells displayed a moderately enlarged bi- or oligo-polar phenotype resembling OPCs. At 98 and 196dpi, an increased fraction of the NG2-positive cells in the lesion centres displayed a stellate-shaped phenotype, interpreted as pre-OGs. In contrast, enlarged bi- or oligo-polar NG2-positive cells resembling OPCs were still present at the lesion border at 196dpi. Moreover, the relative mRNA expression of two OPC marker proteins, PDGFa-R and NG2, was only temporarily increased at 7, 14, 56dpi and 14, 56 and 98dpi, respectively in TMEV-infected mice.

To further analyze the differentiation status of OPC into OGs, CNPase immunoreactivity was followed during TMEV-ID progression. Thus, at 28dpi, small foci with vacuolated myelin sheaths and a mildly reduced density of CNPase-positive cells were detected. At later time points, the density of intralesional CNPase-positive cells continuously declined. At 196dpi, large areas in the lesion centres lacked CNPase immunoreactivity. At the mRNA levels, the transcripts of mature myelin proteins, such as CNPase and MBP, remained either unchanged or exhibited a decrease in the TMEV-infected mice. Simultaneously, the expression of the exon 2 containing variants of MBP mRNA was reduced at 7, 56, 98 and 196dpi.

Furthermore, a possible alternative differentiation of the OPCs towards glial fibrillary acidic protein (GFAP)-positive astrocytes which leads to the formation of an astroglial scar was also studied. Thus, although the number of intralesional GFAP-positive cells remained unchanged at 28dpi, astrocytes appeared hypertrophic and exhibited thickened processes. At later time points, both the amount of GFAP-positive processes and the number of intralesional GFAP positive cells progressively increased. The relative expression of GFAP mRNA progressively increased in the TMEV-infected mice during the observation period.

Several studies showed that the proliferation and differentiation of oligodendroglial progenitor cells is a prerequisite for remyelination and functional recovery, whereas surviving oligodendrocytes are relatively quiescent and do not participate in remyelination (Godfraind *et al.*, 1989; Gensert and Goldman, 1997). In TMEV-infected mice, the number of intralesional NG2-positive cells was transiently elevated between 28 and 98dpi, indicating that a proliferating cell population that possesses the intrinsic capacity to initiate remyelination can be found at least during the first months during lesion development. Similar cellular morphologies and proliferative properties of OPCs were found in MS (Chang *et al.*, 2000), EAE (Reynolds *et al.*, 2002; Di Bello *et al.*, 1999; Kuhlmann *et al.*, 2006), cuprizone toxicity (Mason *et al.*, 2000; Mason *et al.*, 2004), MHV-induced demyelination (Redwine and Armstrong, 1998) and traumatic brain injuries (Alonso, 2005; Tang *et al.*, 2003) ethidium bromide-induced lesions (Kotter *et al.*, 2006), anti-GalC antibodies/complement-induced lesions (Keirstead *et al.*, 1998). Thus, a depletion of the OPCs seems not to be the main cause of deficient demyelination in TMEV-ID.

Subsequently, the hypothesis of an inhibited oligodendroglial differentiation was formulated. This hypothesis was supported by either the unchanged or mildly decreased gene expression of the myelin proteins CNPase and MBP, and the reduction of the exon 2 containing splice variants of MBP compared with total MBP mRNA, in TMEV-ID. Similar to the presented results, SJL/J mice infected with the DA strain of TMEV demonstrated a down-

regulation of PLP and MBP mRNA as shown by in situ hybridization (Yamada *et al.*, 1990). In contrast, an increase of the exon 2 containing variants of MBP has been described in association with rapid and efficient remyelination in passive EAE in mice (Nagasato *et al.*, 1997) and MHV-induced demyelination (Jordan *et al.*, 1990).

Interestingly, a low significant positive linear correlation was detected between NG2-positive cells and GFAP mRNA. This seems to further support the hypothesis of an astrocytic differentiation of, at least, some NG2-positive OPCs. In vitro, about 80% of NG2-positive OPCs develop into GFAP-positive astrocytes after incubation with a serum-enriched medium (Levine *et al.*, 1993; Pringproa *et al.*, 2008).

4.3 Axonal pathology

In the last decades, new research tools were possible after discovery of specific markers for axonal injury, like neurofilaments (NFs) and amyloid precursor protein (APP) accumulation (Lee *et al.*, 1986; Lee *et al.*, 1987; Adams *et al.*, 1991; Gentleman *et al.*, 1993; Sherriff *et al.*, 1994; Karlsson *et al.*, 1991; Meller *et al.*, 1993; Dunn-Meynell *et al.*, 1997). Beside their marker particularities, p-NF, n-NF and APP seemed to be active participants in disease pathogenesis (Miller *et al.*, 2002; Hirai *et al.*, 1999; Collard *et al.*, 1995; Zhang *et al.*, 1997; Williamson *et al.*, 1999) and the elucidation of their metabolism could reveal more information about disease pathogenesis.

Therefore, the pattern of NFs aggregation and different steps of NF-metabolism during the evolution of TMEV-ID were studied. Thus, besides different aspects of TMEV-ID specific axonal pathology, NF axonal transport and NF post-translational modifications, disease-related conditions like virus persistence, virus-induced demyelination and *in vitro* behaviour of selected antigens were investigated.

To analyze *in vivo* general aspects of axonal pathology, Bielschowsky staining and electron microscopy analyses were done. A significant axonal loss and occurrence of swollen axons termed spheroids were observed between 14 and 196dpi. Immunohistochemistry results revealed APP immunopositive axons in the ventro-medial and lateral columns between 28 and 196dpi. In addition, loss of axonal p-NF expression and n-NF axonal accumulations became evident at 14dpi in TMEV infected mice.

Analysis of the transcriptional status of axon transport-related genes revealed a mild to moderate transcriptional down-regulation of kinesin family members (Kif2a, Kif3c, Kif5a) and certain components of the protein phosphatase 2 complex (Ppp2r2a, Ppp2r2c) especially

during the demyelinating phase of the disease between 42 and 196dpi. Furthermore, an up-regulation of tubulin alpha 6 and tubulin beta 5 and a down-regulation of tubulin alpha 1, tubulin alpha 4, and tubulin beta 4 was observed. No significant or only minimal transcriptional changes were observed for APP, multiple components of the dynein complex, Tau-1, neurofilament heavy chain, neurofilament light chain, neurofilament medium chain and Uchl1.

The translational status of these genes was further investigated. Thus, already at 14dpi kinesin family member 5A (Kif5A)-positive immunoreactive spheroids appeared and axons showed an overall reduction of Kif5A expression in infected mice. At 98dpi, Kif5A reached a peak of decreased expression when less than 50% of the axons showed Kif5A. Dynein cytoplasmic heavy chain 1 (Dync1h1) immunoreactivity revealed a Kif5A similar down-regulation at the translational level. In addition, β -tubulin III and α -acetylated tubulin significantly decreased expression at 98dpi similar to KifA. Tau-1 axonal expression was significantly reduced at 42dpi, while ubiquitin-protein conjugates and Uchl-1 expression dropped significantly already at 28dpi. In contrast, Pp2a subunits were similarly expressed in control and TMEV-infected mice at all time points.

The *in vitro* studies performed on the differentiated N1E-115 cells showed an ubiquitous expression of the TMEV antigen after infection with TMEV-BeAn strain. The infected differentiated cells were characterized by a particular immunoreactivity of their processes which resembled the *in vivo* focal axonal swellings. Thus, these enlargements showed, similar with the *in vivo* situation, higher and lower levels of n-NF and p-NF, respectively. In contrast, axonal-like structures of non-infected cells displayed a uniform expression of p-NF and a lack of n-NF immunoreactivity.

Previous studies found an earlier onset of axonal pathology compared to demyelination (Tsunoda *et al.*, 2003). Though only few axons were TMEV-positive, a direct relationship between the virus spread and myelin/ axonal pathology cannot be ruled out (Tsunoda *et al.*, 2002; Tsunoda *et al.*, 2003). To investigate whether or how these modifications are an indirect consequence of virus presence, additional studies based on kinetic analyses of both brain and spinal cord lesions are necessary.

In TMEV-ID, axonal pathological changes are detected early in disease progression. Thus, at 14dpi, accumulation of the non-phosphorylated NF is accompanied by a down-regulation of its transporter molecules Kif5A and Dync1h1, while a reduction of the expression of the cytoskeleton proteins such as Beta-tubulin III and Tau-1 was found later at 28dpi. These observations suggest a sequential progression of the pathological lesions at the axonal level.

Thus, the cargoes-carriers are firstly affected and then the “rails” on which these cargoes are transported. Therefore, the modification of the specific axonal transport of neurofilaments (Kif5A) is accompanied by the alteration of other axonal transport compartments. While an impaired axonal transport could result in a decrease of TMEV transport (Rietdorf *et al.*, 2001) and a low APP accumulation (Kamal *et al.*, 2001), the specific pattern of the axonal p-NF and n-NF expression after TMEV-infection is substantiated by their specific association with the cytoskeleton elements (Hisanaga and Hirokawa, 1990; Hisanaga *et al.*, 1993).

The complementary expression of the NF forms further suggested a local dephosphorylation process, however no change in PP2AC and PP2AA expression in control and TMEV-infected mice was observed. This result, though indicated no lack in phosphorylation, can not exclude possible changes in PP2A activity or the participation of other phosphatases in the axonal NF dephosphorylation.

Either transported from the neuronal cell bodies and/or locally produced in the axon, accumulated n-NFs could represent a first step towards NF degradation. In several other neurodegenerative diseases like ALS (Lowe *et al.*, 1988; Manetto *et al.*, 1988), Alzheimer’s (Mori *et al.*, 1987), Parkinson’s (Galloway *et al.*, 1988), ubiquitin-conjugated proteins are components of the intraneuronal inclusions. Thus, ubiquitination is described as an important mechanism involved in NF degradation (Gou and Leterrier, 1995; Balastik *et al.*, 2008). The present analysis revealed a significant reduction of the ubiquitin-protein conjugates and UCHL-1 expression during TMEV-ID evolution which suggest a derangement of the proteolytic pathway in TMEV-infected mice.

















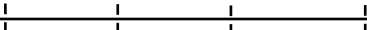


In conclusion, multiple molecular mechanisms are involved in the neurofilaments axonal accumulation in TMEV-ID. To analyze whether the alterations described above have a direct consequence on motoneurons degeneration in TMEV-ID, additional studies are necessary. The present *in vitro* experiments suggest an affirmative answer while frequent morphological manifestations of the axonal degeneration observed as tandem-repeated swellings (called spheroids; Coleman, 2005) where observed after infection of the neuroblastoma N1E-115 cells with TMEV.




4.4 Glial-axonal interaction

One of the most important unsolved problem regarding MS and TMEV-ID pathology remains the identification of the initiating mechanism which is further responsible for the dramatic progression observed during these diseases. Changes where observed both at the glial but also

at the axonal level in the present study. Thus, subsidiary modifications at both cellular compartments, glial and axonal, could together be the reason of the further lesion development. The present work investigated both the glial and the axonal cellular compartments and an overview of the lesions observed at the spinal cord is given in table 4.

Table 4. Overview of the investigated factors and their kinetic during TMEV-ID.

TMEV-ID pathology	0	7	14	28	42	98	196	Methods
Footprint analysis								Stride length
Virus presence								IHC
Demyelination								ELMI LFB
Remyelination								ELMI
Oligodendrocyte precursor cells								NG2
Oligodendrocytes								CNP-ase
Axonal loss								Bielschowsky
Axonal injury			   					n-NF p-NF APP ELMI
Neurofilament dephosphorylation						 		PP2AC PP2AA
Neurofilament axonal transport			   					Kif5A Dync1h1 Beta-tubulin III Tau-1
Neurofilament degradation				 				Ub-conj prot UCHL1
	days post-infection (dpi)							

Down-regulated=  ; up-regulated=  ; up- and down-regulated or unchanged antigens =  ; IHC= immunohistochemistry, ELMI= electron microscopy; LFB= luxol fast blue; NG2= nerve/glial antigen 2; CNP-ase= 2',3'-cyclic nucleotide 3'-phosphodiesterase; n-NF= non-phosphorylated neurofilaments; p-NF= phosphorylated neurofilaments; APP= amyloid precursor protein; PP2AC= protein phosphatase 2A catalytic subunit; PP2AA= protein phosphatase 2A regulatory subunit; Kif5A= kinesin family member 5A; Dync1h1= dynein cytoplasmic heavy chain 1; Ub-conj proteins= ubiquitin conjugated proteins; UCHL1= ubiquitin carboxy-terminal hydrolase L1.

While the virus was detected beginning with 14dpi until 196dpi, the first clinical manifestations revealed by footprint analysis showed a significant decreased stride length at 147 and 196dpi. Pathologically, the glial compartment (demyelination, NG2) as well as the axonal compartment (n-NF, Kif5A, Dync1h1) showed both alterations starting at day 14pi. An abnormal expression of additional markers like CNP-ase (OGs), p-NF, APP, Beta-tubulin III, Tau-1, UCHL1 and Ub-conjugates proteins (axons) was observed. The protein phosphatase 2 subunits were similarly expressed in control and infected mice. Functionally, these modifications are responsible for a dysregulated OPC differentiation and an impaired axonal transport and protein metabolism.

During TMEV-ID progression, a damaged axon could be a triggering signal for the dysregulation of OPC differentiation that may cause additional axonal injuries and a delayed and incomplete remyelination. Axonal injuries like n-NF accumulations seemed to be the result of specific alterations in their axonal transport e.g. by Kif5A and also the sequel of nonspecific impairments in the neuronal protein metabolism including ubiquitin-protein conjugates. A delayed and incomplete remyelination associated with axonal loss and axonal injuries could be responsible for the clinical manifestations of TMEV-ID.

The priorities of future studies will be the functional analysis of these interdependences and the identification of elements that could be delay where disease progression.

4.5 References

1. Adams JH, Graham DI, Gennarelli TA, Maxwell WL. Diffuse axonal injury in non-missile head injury. *J. Neurol. Neurosurg. Psychiatry.* 54:481-483, 1991.
2. Alonso G. NG2 proteoglycan-expressing cells of the adult rat brain: possible involvement in the formation of glial scar astrocytes following stab wound. *Glia* 49: 318–338, 2005.
3. Balastik M, Ferraguti F, Pires-da Silva A, Lee TH, Alvarez-Bolado G, Lu KP. Deficiency in ubiquitin ligase TRIM2 causes accumulation of neurofilament light chain and neurodegeneration. *Proc. Natl. Acad. Sci. U S A.* 105:12016-12021, 2008.
4. Bitsch A, Schuchardt J, Bunkowski S, Kuhlmann T, Bruck W. Acute axonal injury in multiple sclerosis. Correlation with demyelination and inflammation. *Brain.* 123:1174-1183, 2000.

5. Bjartmar C, Kidd G, Mörk S, Rudick R, Trapp BD. Neurological disability correlates with spinal cord axonal loss and reduced N-acetyl aspartate in chronic multiple sclerosis patients. *Ann. Neurol.* 48:893-901, 2000.
6. Chang A, Nishiyama A, Peterson J, Prineas J, Trapp BD. NG2-positive oligodendrocyte progenitor cells in adult human brain and multiple sclerosis lesions. *J. Neurosci.* 20:6404–6412, 2000.
7. Coleman M. Axon degeneration mechanisms: commonality amid diversity. *Nat. Rev. Neurosci.* 6:889-898, 2005.
8. Collard JF, Cote F, Julien JP. Defective axonal transport in a transgenic mouse model of amyotrophic lateral sclerosis. *Nature.* 375:61-64, 1995.
9. Di Bello IC, Dawson MRL, Levine JM, Reynolds R. Generation of oligodendroglial progenitors in acute inflammatory demyelinating lesions of the rat brain stem is associated with demyelination rather than inflammation. *J. Neurocytol.* 28:365–381, 1999.
10. Dunn-Meynell AA, Levin BE. Histological markers of neuronal, axonal and astrocytic changes after lateral rigid impact traumatic brain injury. *Brain Res.* 761:25-41, 1997.
11. Ferguson B, Matyszak MK, Esiri MM, Perry VH. Axonal damage in acute multiple sclerosis lesions. *Brain.* 120:393-399, 1997.
12. Filippi M, Rocca MA. MRI evidence for multiple sclerosis as a diffuse disease of the central nervous system. *J. Neurol.* 252:16-24, 2005.
13. Franklin RJM. Why does remyelination fail in multiple sclerosis? *Nat. Rev. Neurosci.* 3: 705–714, 2002.
14. Galloway PG, Grundke-Iqbal I, Iqbal K, Perry G. Lewy bodies contain epitopes both shared and distinct from Alzheimer neurofibrillary tangles. *J. Neuropathol. Exp. Neurol.* 47:654-663, 1988.
15. Gensert JM, Goldman JE. Endogenous progenitors remyelinate demyelinated axons in the adult CNS. *Neuron.* 19: 197–203, 1997.
16. Gentleman SM, Nash MJ, Sweeting CJ, Graham DI, Roberts GW. Beta-amyloid precursor protein (beta APP) as a marker for axonal injury after head injury. *Neurosci. Lett.* 160:139-144, 1993.
17. Godfraind C, Friedrich VL, Holmes KV, Dubois-Dalcq M. In vivo analysis of glial-cell phenotypes during a viral demyelinating disease in mice. *J. Cell. Biol.* 109: 2405–2416, 1989.

18. Gou JP, Leterrier JF. Possible involvement of ubiquitination in neurofilament degradation. *Biochem. Biophys. Res. Commun.* 217:529-538, 1995.
19. Herrero-Herranz E, Pardo LA, Gold R, Linker RA. Pattern of axonal injury in murine myelin oligodendrocyte glycoprotein induced experimental autoimmune encephalomyelitis: implications for multiple sclerosis. *Neurobiol. Dis.* 30:162-173, 2008.
20. Hirai T, Mizutani M, Ochiai K, Umemura T, Itakura C. Distal axonopathy does not occur without neurofilament accumulation in gamma-diketone neuropathy: comparative studies of normal and neurofilament-deficient quail. *Acta Neuropathol.* 97:552-556, 1999.
21. Hisanaga S, Hirokawa N. Dephosphorylation-induced interactions of neurofilaments with microtubules. *J. Biol. Chem.* 265:21852-21858, 1990.
22. Hisanaga S, Yasugawa S, Yamakawa T, Miyamoto E, Ikebe M, Uchiyama M. Dephosphorylation of microtubule-binding sites at the neurofilament-H tail domain by alkaline, acid, and protein phosphatases. *J. Biochem.* 113:705-709, 1993.
23. Jordan C, Friedrich V, Dubois-Dalcq M. In situ hybridization analysis of myelin gene transcripts in developing mouse spinal-cord. *J. Neurosci.* 9:248-257, 1989.
24. Jordan CA, Friedrich VL, Deferra F, Weismiller DG, Holmes KV, Dubois-Dalcq M. Differential exon expression in myelin basic-protein transcripts during central-nervous-system (CNS) Remyelination. *Cell. Mol. Neurobiol.* 10:3-17, 1990.
25. Kamal A, Almenar-Queralt A, LeBlanc JF, Roberts EA, Goldstein LS. Kinesin-mediated axonal transport of a membrane compartment containing beta-secretase and presenilin-1 requires APP. *Nature.* 414:643-648, 2001.
26. Karlsson JE, Rosengren LE, Haglid KG. Quantitative and qualitative alterations of neuronal and glial intermediate filaments in rat nervous system after exposure to 2,5-hexanedione. *J. Neurochem.* 57:1437-1444, 1991.
27. Keirstead HS, Levine JM, Blakemore WF. Response of the oligodendrocyte progenitor cell population (defined by NG2 labelling) to demyelination of the adult spinal cord. *Glia* 22:161-170, 1998.
28. Kotter MR, Li WW, Zhao C, Franklin RJM. Myelin impairs CNS remyelination by inhibiting oligodendrocyte precursor cell differentiation. *J. Neurosci.* 26:328-332, 2006.

29. Kuhlmann T, Remington L, Cognet I, Bourbonniere L, Zehntner S, Guilhot F, Herman A, Guay-Giroux A, Antel JP, Owens T, Gauchat JF. Continued administration of ciliary neurotrophic factor protects mice from inflammatory pathology in experimental autoimmune encephalomyelitis. *Am. J. Pathol.* 169: 584–598, 2006.
30. Lee VM, Carden MJ, Schlaepfer WW. Structural similarities and differences between neurofilament proteins from five different species as revealed using monoclonal antibodies. *J. Neurosci.* 6:2179-2186, 1986.
31. Lee VM, Carden MJ, Schlaepfer WW, Trojanowski JQ. Monoclonal antibodies distinguish several differentially phosphorylated states of the two largest rat neurofilament subunits (NF-H and NF-M) and demonstrate their existence in the normal nervous system of adult rats. *J. Neurosci.* 7:3474-488, 1987.
32. Lowe J, Lennox G, Jefferson D, Morrell K, McQuire D, Gray T. A filamentous inclusion body within anterior horn neurones in motor neurone disease defined by immunocytochemical localisation of ubiquitin. *Neurosci. Lett.* 94:203-210, 1988.
33. Manetto V, Perry G, Tabaton M, Mulvihill P, Fried VA, Smith HT. Ubiquitin is associated with abnormal cytoplasmic filaments characteristic of neurodegenerative diseases. *Proc. Natl. Acad. Sci. U S A.* 85:4501-4505, 1988.
34. Mason JL, Jones JJ, Taniike M, Morell P, Suzuki K, Matsushima GK. Mature oligodendrocyte apoptosis precedes IGF-1 production and oligodendrocyte progenitor accumulation and differentiation during demyelination/remyelination. *J. Neurosci. Res.* 61:251–262, 2000.
35. Mason JL, Toews A, Hostettler JD, Morell P, Suzuki K, Goldman JE, Matsushima GK. Oligodendrocytes and progenitors become progressively depleted within chronically demyelinated lesions. *Am. J. Pathol.* 164:1673–1682, 2004.
36. Meller D, Bellander BM, Schmidt-Kastner R, Ingvar M. Immunohistochemical studies with antibodies to neurofilament proteins on axonal damage in experimental focal lesions in rat. *J Neurol Sci.* 117:164-174, 1993.
37. Miller CC, Ackerley S, Brownlees J, Grierson AJ, Jacobsen NJ, Thornhill P. Axonal transport of neurofilaments in normal and disease states. *Cell. Mol. Life Sci.* 59:323-330, 2002.
38. Morell P, Barrett CV, Mason JL, Toews AD, Hostettler JD, Knapp GW, Matsushima GK. Gene expression in brain during Cuprizone-induced demyelination and remyelination. *Mol. Cell. Neurosci.* 12:220–227, 1998.

39. Mori H, Kondo J, Ihara Y. Ubiquitin is a component of paired helical filaments in Alzheimer's disease. *Science*. 235:1641-1644, 1987.
40. Nagasato K, Farris RW, DuboisDalcq M, Voskuhl RR. Exon 2 containing myelin basic protein (MBP) transcripts are expressed in lesions of experimental allergic encephalomyelitis (EAE). *J. Neuroimmunol.* 72:21–25, 1997.
41. Neumann H. Molecular mechanisms of axonal damage in inflammatory central nervous system diseases. *Curr. Opin. Neurol.* 16:267-273, 2003.
42. Pittock SJ, Lucchinetti CF. The pathology of MS: new insights and potential clinical applications. *Neurologist.* 13:45-56, 2007.
43. Pringproa K, Kumnok J, Ulrich R, Baumgärtner W, Wewetzer K. In vitro characterization of a murine oligodendrocyte precursor cell line (BO-1) following spontaneous immortalization. *Int. J. Dev. Neurosci.* 26:283–291, 2008.
44. Yamada M, Zurbriggen A, Fujinami RS. The relationship between viral-RNA, myelin-specific messenger-RNAs, and demyelination in central-nervous-system disease during Theiler's virus-infection. *Am. J. Pathol.* 137:1467–1479, 1990.
45. Redwine JM, Armstrong RC. In vivo proliferation of oligodendrocyte progenitors expressing PDGF alpha R during early remyelination. *J. Neurobiol.* 37: 413–428, 1998.
46. Reynolds R, Dawson M, Papadopoulos D, Polito A, Di Bello IC, Pham-Dinh D, Levine J. The response of NG2-expressing oligodendrocyte progenitors to demyelination in MOG-EAE and MS. *J. Neurocytol.* 31:523–536, 2002.
47. Rietdorf J, Ploubidou A, Reckmann I, Holmstrom A, Frischknecht F, Zettl M. Kinesin-dependent movement on microtubules precedes actin-based motility of vaccinia virus. *Nat. Cell. Biol.* 3:992-1000, 2001.
48. Sherriff FE, Bridges LR, Gentleman SM, Sivaloganathan S, Wilson S. Markers of axonal injury in post mortem human brain. *Acta Neuropathol.* 88:433-439, 1994.
49. Tang XF, Davies JE, Davies SJA. Changes in distribution, cell associations, and protein expression levels of NG2, neurocan, phosphacan, brevican, versican V2, and tenascin-C during acute to chronic maturation of spinal cord scar tissue. *J. Neurosci. Res.* 71:427–444, 2003.
50. Tsunoda I, Fujinami RS. Inside-Out versus Outside-In models for virus induced demyelination: axonal damage triggering demyelination. *Springer Semin. Immunopathol.* 24:105-125, 2002.

51. Tsunoda I, Kuang LQ, Libbey JE, Fujinami RS. Axonal injury heralds virus-induced demyelination. *Am. J. Pathol.* 162:1259-1269, 2003.
52. Trapp BD, Peterson J, Ransohoff RM, Rudick R, Mork S, Bo L. Axonal transection in the lesions of multiple sclerosis. *N. Engl. J. Med.* 338:278-298, 1998.
53. Williamson TL, Cleveland DW. Slowing of axonal transport is a very early event in the toxicity of ALS-linked SOD1 mutants to motor neurons. *Nat. Neurosci.* 2:50-56, 1999.
54. Woodruff RH, Franklin RJM. The expression of myelin protein mRNAs during remyelination of lysolecithin-induced demyelination. *Neuropathol. Appl. Neurobiol.* 25: 226–235, 1999.
55. Zhang B, Tu P, Abtahian F, Trojanowski JQ, Lee VM. Neurofilaments and orthograde transport are reduced in ventral root axons of transgenic mice that express human SOD1 with a G93A mutation. *J. Cell. Biol.* 139:1307-1315, 1997.

Molecular and cellular mechanisms of axonal pathology in Theiler's murine encephalomyelitis virus-induced demyelination

Mihaela Kreutzer

SUMMARY

Theiler's murine encephalomyelitis virus-induced demyelination (TMEV-ID) is, beside canine distemper virus encephalitis, one of the best known viral murine models of multiple sclerosis (MS), a human immune-mediated demyelinating disease of the central nervous system affecting over 2.5 million individuals. MS and TMEV-ID share common pathological features characterized by a delayed and incomplete remyelination and prominent axonal pathology. The axonal damage correlates with the observed neurological deficits and is responsible for the irreversible clinical outcome. Therefore the goal of any therapeutic approach should include maintenance of physiologic-like conditions inside and outside the axons.

The following two aspects of TMEV-ID pathogenesis were investigated in the present study: (i) a possible dysregulation of oligodendroglial progenitor cells (OPCs) differentiation which could be responsible for insufficient regeneration and (ii) modifications in the axonal transport and protein degradation which could cause non-phosphorylated neurofilaments accumulation and a progressive axonopathy.

The aim of the first part of the thesis was based on the hypothesis that a dysregulation of differentiation of OPCs represents the main cause of insufficient regeneration in TMEV-ID.

Clinically, footprint analysis revealed a significantly decreased stride length at 147 and 196dpi. Pathologically, a progressive demyelination was observed beginning with 14dpi until 196dpi. A mild amount of remyelination was detected at 147 and 196dpi. Early onset axonal injury was detected from 14dpi on. Intralésional nerve/glia antigen 2 (NG2)-positive OPCs were temporarily increased between 28 and 98dpi. Similarly, a transient upregulation of NG2 and platelet-derived growth factor α -receptor mRNA was noticed. In contrast, intralésional CNPase-positive oligodendrocytes were decreased between 56 and 196dpi. Although CNPase mRNA remained unchanged, myelin basic protein mRNA and especially its exon 2 containing splice variants were decreased. GFAP-positive astrocytes and GFAP mRNA were increased in the late phase of TME. A mildly increased colocalization of both NG2/CNPase and NG2/GFAP was revealed at 196dpi. Thus, findings indicated that a dysregulation of OPC

differentiation by unknown directly or indirectly TMEV-related factors seems to represent a dominating pathogenetic mechanism causing delayed and limited remyelination in TMEV-ID. For the second part of the thesis the underlying hypothesis was that the initiation and development of TMEV-induced axonopathy are based on an impaired axonal transport of NFs.

Therefore, molecular processes involved in axonal accumulation of non-phosphorylated neurofilament in TMEV-ID, were analyzed in detail.

The accumulation of non-phosphorylated neurofilaments showed a temporal development due to sequential impairments of the bidirectional axonal traffic consisting of the down-regulation of kinesin family member 5A, dynein cytoplasmic heavy chain 1, tau-1 and β -tubulin III expression. In addition, alterations of the neuronal protein metabolism, including down-regulation of ubiquitin-protein conjugates and ubiquitin carboxy-terminal hydrolase L1, causing diminished degradation of non-phosphorylated neurofilament, were noticed. In addition, *in vitro* experiments showed a direct role of the virus for these modifications and the morphological manifestation of the axonal degeneration expressed as tandem-repeated swellings in neuroblastoma N1E-115 cell line after infection with TMEV.

Thus, neurofilament accumulation in TMEV-ID seems to be the result of specific dysregulations in the axonal transport mediated by Kif5A and also the sequel of nonspecific impairments in the neuronal protein metabolism including the ubiquitin-protein conjugates.

During TMEV-ID progression, a damaged axon could be a triggering signal for the dysregulation of OPC differentiation that may cause additional axonal injuries and a delayed and incomplete remyelination.

The presented findings may have important implications for our understanding of molecular mechanisms responsible for initiation and development of axonopathies in neurodegenerative disorders.

Molekulare und zelluläre Mechanismen der axonalen Pathologie in Theiler's murine Encephalomyelitis Virus induzierten Entmarkung

Mihaela Kreutzer

Zusammenfassung

Die durch das murine Theiler-Encephalomyelitis-Virus induzierte Demyelinisierung (*Theiler's murine encephalomyelitis virus-induced demyelination* [TMEV-ID]) ist neben der kaninen Staupeenzephalitis eines der am Besten bekannten viralen Tiermodelle für die Multiple Sklerose (MS) des Menschen. Bei der MS handelt es sich um eine immunvermittelte demyelinisierende Erkrankung des zentralen Nervensystems, welche weltweit ca. 2,5 Millionen Menschen betrifft. MS und TMEV-ID zeigen gleichartige pathologische Merkmale, die durch eine verzögerte und unzureichende Remyelinsierung sowie prominente Axonschädigungen charakterisiert sind. Die Alterationen bzw. der Verlust von Axonen bedingt in großem Maße die Symptomatik sowie den irreversiblen klinischen Verlauf. Aus diesem Grund sollte das Ziel möglicher therapeutischer Ansätze die Aufrechterhaltung der physiologischen Konditionen der Axonstruktur als auch des axonalen Umfelds beinhalten.

Die folgenden zwei Aspekte der Pathogenese der TMEV-ID wurden in der vorliegenden Studie untersucht: i) die mögliche Dysregulation der Differenzierung oligodendroglialer Vorläuferzellen (*oligodendroglial progenitor cells* [OPCs]), welche für die unzureichende Regeneration verantwortlich sein kann sowie ii) Veränderungen im axonalen Transport und Proteindegradation, welche zu einer Ablagerung von nicht-phosphorilierten Neurofilamenten und somit zu progressiven Axonopathien beitragen können.

Zur Klärung der ersten Fragestellung, nämlich inwiefern die Dysregulation der Differenzierung der OPCs eine Ursache der mangelhaften Remyelinsierung darstellt, wurden sowohl molekularbiologische als auch pathomorphologische bzw. immunhistologische Untersuchungen an TMEV-infizierten Mäusen sowie Placebo-Tieren durchgeführt. Zusätzlich fand eine klinische Untersuchung der Tiere in Form einer Schrittlängenmessung statt. Hierbei zeigte sich eine signifikant verringerte Schrittlänge der TMEV-infizierten Tiere gegenüber den Placebo-Tieren 147 und 196 Tage *post infectionem* (dpi). Morphologisch war in den Rückenmärkern eine progressive Demyelinisierung in der Zeitspanne von 14 bis 196 dpi zu detektieren. Eine geringgradige Remyelinsierung war zum Zeitpunkt 147 und 196 dpi aufzufinden. Eine Axonschädigung zeigte sich bereits ab 14 dpi. Ein vermehrtes

intraläsionales Auffinden von „*nerve/glial antigen 2*“ (NG2)-positiven OPCs war zwischen 28 und 98 dpi nachzuweisen. Weiterhin zeigte sich eine transiente Aufregulierung von NG2- und „*platelet-derived growth factor α -receptor*“-mRNS. Im Gegensatz dazu war die intraläsionale Anzahl CNPase-positiver Oligodendrozyten im Zeitraum zwischen 56 und 196 dpi vermindert. Obwohl der Gehalt von CNPase-mRNS unverändert blieb, war die Menge an mRNA des basischen Myelinproteins und insbesondere seiner Exon 2-Splicevariante vermindert. Weiterhin zeigte sich ein Anstieg von GFAP-positiven Astrozyten sowie GFAP-mRNA in der Spätphase der TMEV-Infektion. Eine geringgradige vermehrte Kolo-kalisation von NG2/CNPase sowie NG2/GFAP wurde zum Zeitpunkt 196 dpi festgestellt. Diese Ergebnisse deuten auf eine Dysregulation der Differenzierung der OPCs und damit auf eine konsekutive verzögerte und unzureichende Remyelinisierung hin. Ursächlich müssen hierfür direkte als auch indirekte TMEV-abhängige Faktoren in Betracht gezogen werden.

Im zweiten Teil der Arbeit wurde die Hypothese untersucht, inwiefern die durch die TMEV-Infektion induzierten Axonschädigungen auf einem gestörten axonalen Transport von Neurofilamenten basieren. Die Akkumulation von nicht-phosphorilierten Neurofilamenten entwickelte sich über die Zeit des Versuchs wahrscheinlich durch eine Beeinträchtigung des bidirektionalen axonalen Transports. Diese zeichnete sich durch eine verminderte Expression von Kinesin 5 A, der zytoplasmatischen schweren Kette 1 des Dyneins, Tau-1 und β -Tubulin III aus. Zusätzlich waren Alterationen des Proteinabbaus in Form einer verminderten Expression von Ubiquitin-Protein-Konjugaten sowie der Ubiquitin-Carboxy-terminalen Hydrolase L1 sichtbar. Infolgedessen ist eine verringerte Degradation der nicht-phosphorilierten Neurofilamente wahrscheinlich. Zusätzlich konnte durch *in vitro*-Experimente eine direkte Rolle des TMEV für die morphologische Ausprägung des Axonschadens aufgezeigt werden. Dieser manifestierte sich als sogenannte „tandem repeats“ in Zellen der Neuroblastoma N1E-115 Zelllinie nach Infektion mit TMEV.

Abschließend lässt sich aus pathogenetischer Sicht vermuten, dass während der TMEV-Infektion ein geschädigtes Axon möglicherweise die Dysregulation der Differenzierung der OPCs induziert, welche konsekutiv weitere Axonopathien nach sich zieht und auch für die verspätete und unzureichende Remyelinisierung verantwortlich ist.

Die Ergebnisse der vorliegenden Untersuchungen geben erste Einblicke in molekulare und zelluläre Mechanismen, welche für die Pathogenese von axonalen Schäden verantwortlich sind.

ACKNOWLEDGEMENTS

First of all I want to express my gratitude to my supervisor Prof. Dr. Wolfgang Baumgärtner, Ph.D. for all the help and support during the preparation and accomplishment of the present work, including constant opportunity for critical discussion and advices.

I kindly thank to Prof. Dr. Claudia Grothe and PD Dr. Claus Krampfl from my tutorial group for thoughtful discussions and comments.

I thank to Dr. Frauke Seehusen, Dr. Reiner Ulrich, Ph.D. and all the actual and former colleagues from the Department of Pathology, Hannover for the excellent working atmosphere.

I would like to thank to Petra Grünig, Bettina Buck, Danuta Waschke, Kerstin Rohn, Kerstin Schöne, Claudia Hermann, Julia Schirrmeier and Brigitte Behrens for their excellent technical support.

I also thank to Dr. Dagmar Esser and Nadja Borsum from the Coordination Office of Center for Systems Neuroscience, Hannover for their dedication to the Ph.D. program.

Many thanks to the Ministry for Science and Culture of Lower Saxony for awarding me the Georg-Christoph-Lichtenberg scholarship which makes this work possible.

A very special thank to Vanessa and Florian for their help in every situations and for the nice atmosphere that they created around me.

Last but not least, a huge thank to my family for encouraging me and supporting me all the time.